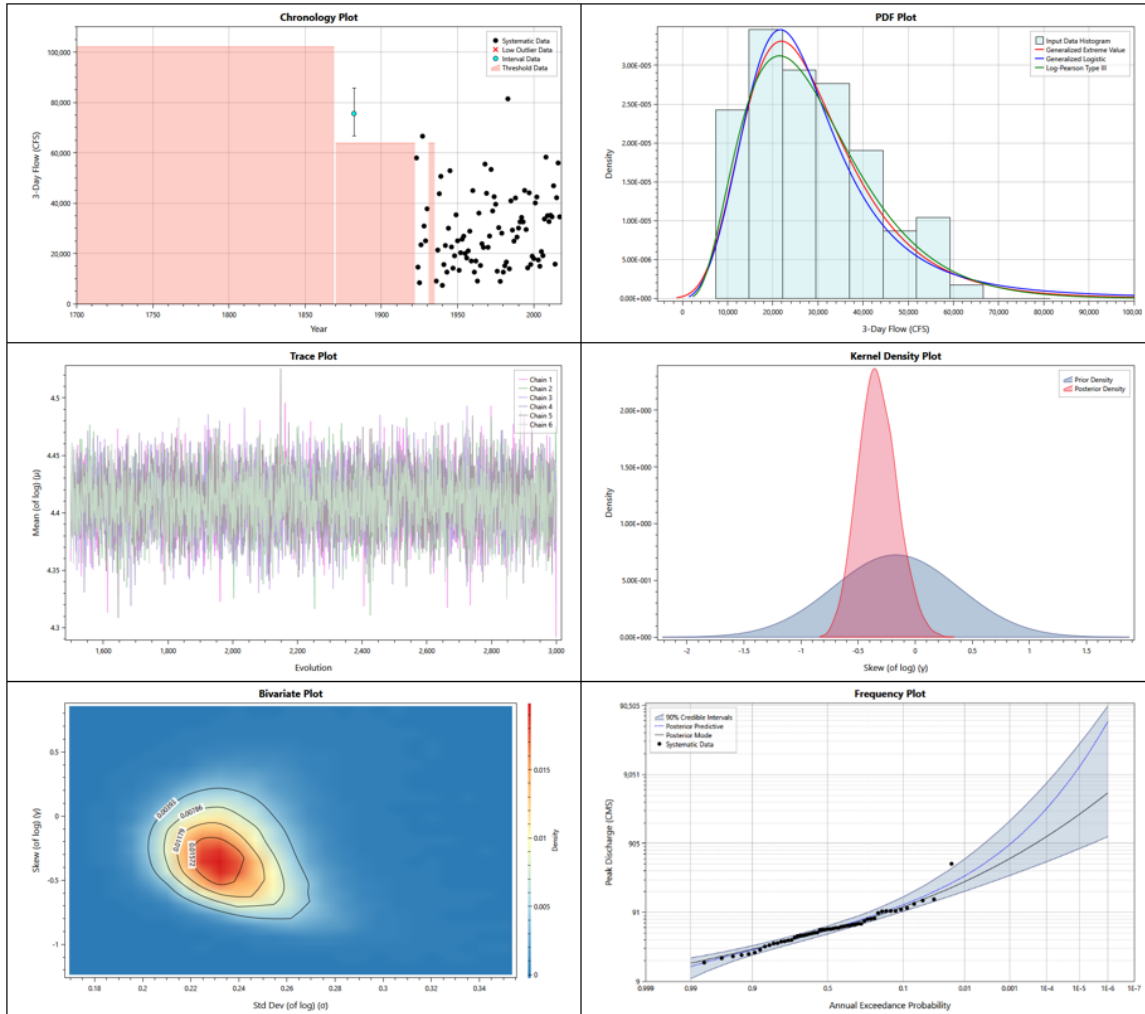


Verification of the Bayesian Estimation and Fitting Software (RMC-BestFit)

RMC-TR-2020-02



REPORT DOCUMENTATION PAGE

*Form Approved
OMB No. 0704-0188*

The public reporting burden for this collection of information is estimated to average 1 hour per response, including the time for reviewing instructions, searching existing data sources, gathering and maintaining the data needed, and completing and reviewing the collection of information. Send comments regarding this burden estimate or any other aspect of this collection of information, including suggestions for reducing the burden, to Department of Defense, Washington Headquarters Services, Directorate for Information Operations and Reports (0704-0188), 1215 Jefferson Davis Highway, Suite 1204, Arlington, VA 22202-4302. Respondents should be aware that notwithstanding any other provision of law, no person shall be subject to any penalty for failing to comply with a collection of information if it does not display a currently valid OMB control number.

PLEASE DO NOT RETURN YOUR FORM TO THE ABOVE ADDRESS.

1. REPORT DATE (DD-MM-YYYY) 06-16-2020	2. REPORT TYPE Technical Report	3. DATES COVERED (From - To)
--	---	-------------------------------------

4. TITLE AND SUBTITLE Verification of the Bayesian Estimation and Fitting Software (RMC-BestFit)	5a. CONTRACT NUMBER
	5b. GRANT NUMBER
	5c. PROGRAM ELEMENT NUMBER

6. AUTHOR(S) Haden Smith, Risk Management Center, U.S. Army Corps of Engineers	5d. PROJECT NUMBER
	5e. TASK NUMBER
	5f. WORK UNIT NUMBER

7. PERFORMING ORGANIZATION NAME(S) AND ADDRESS(ES) Risk Management Center 12596 West Bayaud Ave. Suite 400 Lakewood, CO 80228	8. PERFORMING ORGANIZATION REPORT NUMBER RMC-TR-2020-02
---	---

9. SPONSORING/MONITORING AGENCY NAME(S) AND ADDRESS(ES)	10. SPONSOR/MONITOR'S ACRONYM(S)
	11. SPONSOR/MONITOR'S REPORT NUMBER(S) RMC-TR-2020-02

12. DISTRIBUTION/AVAILABILITY STATEMENT
Approved for public release; distribution is unlimited.

13. SUPPLEMENTARY NOTES

14. ABSTRACT

The purpose of this document is to provide verification of critical RMC-BestFit computations. Software verification involves comparison of the numerical solution generated by the code with one or more analytical solutions, or with other numerical solutions. Verification ensures that the software accurately solves the equations that constitute the mathematical model. RMC-BestFit has three functional components: 1) Input data; 2) Distribution fitting analysis; and 3) Bayesian estimation analysis. The numerical components were verified against theoretical solutions, academic literature, as well as several prominent software in industry. In all cases, the computations within RMC-BestFit performed as intended.

15. SUBJECT TERMS

Software, verification, Bayesian estimation, distribution fitting, frequency analysis, probability distributions, uncertainty

16. SECURITY CLASSIFICATION OF:			17. LIMITATION OF ABSTRACT UU	18. NUMBER OF PAGES 87	19a. NAME OF RESPONSIBLE PERSON
a. REPORT U	b. ABSTRACT U	c. THIS PAGE U			19b. TELEPHONE NUMBER (Include area code)

Verification of the Bayesian Estimation and Fitting Software (RMC-BestFit)

June 2020

*U.S. Army Corps of Engineers
Institute for Water Resources
Risk Management Center
12596 West Bayaud Ave. Suite 400
Lakewood, CO 80228*

Author(s)

Haden Smith, USACE Risk Management Center

Contents

Purpose and Scope	1
Input Data	2
Multiple Grubbs-Beck Test	2
Hirsch-Stedinger Plotting Positions	2
Nonparametric Summary Statistics	8
Distribution Fitting Analysis	11
Maximum Likelihood Estimation (MLE)	11
Probability Distributions	14
Goodness-of-Fit Measures	30
Bayesian Estimation	31
Bayesian Analysis Framework	31
Theoretical Verification	32
Comparison with R-Stan	49
Comparison with Viglione et al. (2013)	57
Comparison with Evdbayes	61
Comparison with Flike	66
Comparison with EMA	70
Conclusion	75
References	76

Figures

Figure 1 – Example of Input Data Chronology Plot	3
Figure 2 – Example of Input Data Frequency Plot	3
Figure 3 – Chronology Plot of the Arkansas River at Pueblo State Park (Example #4 from Bulletin 17C (U.S. Geological Survey, 2018)).	6
Figure 4 – Chronology Plot of the America River at Fair Oaks (Example #7 from Bulletin 17C (U.S. Geological Survey, 2018)).	6
Figure 5 – Comparison of RMC-BestFit with HEC-SSP for the Hirsch-Stedinger Plotting Positions for Example #4 in Bulletin 17C (U.S. Geological Survey, 2018).	7
Figure 6 – Comparison of RMC-BestFit with HEC-SSP for the Hirsch-Stedinger Plotting Positions for Example #7 in Bulletin 17C (U.S. Geological Survey, 2018).	7
Figure 7 – Summary Statistics for Input Data (USGS 01562000) in RMC-BestFit.	8
Figure 8 – Real-space Summary Statistics for Input Data (USGS 01562000) in Palisade's @Risk.	9
Figure 9 – Log10-space Summary Statistics for Input Data (USGS 01562000) in Palisade's @Risk.	10
Figure 10 – Nelder-Mead Verification in MS Excel.	12
Figure 11 – Unit Test for the Nelder-Mead algorithm contained in Numerics.dll.	13
Figure 12 – Unit Test output for the Nelder-Mead algorithm.	13
Figure 13 – Example code for R-Stan with the Normal Distribution.	15
Figure 14 – Distribution Fitting Analysis for the Wabash River at Lafayette, Indiana dataset.	19
Figure 15 – Distribution Fitting Analysis for the Synthetic dataset.	19
Figure 16 – Diagram Illustrating the Basic Steps in Bayesian Analysis (adapted from (Meylan, 2012), which was originally taken (Perreault, 2000)).	32
Figure 17 – Comparison of RMC-BestFit with Default Flat Priors with the Theoretical Distribution for Mean (N = 30).	33
Figure 18 – Comparison of RMC-BestFit with Default Flat Priors with the Theoretical Distribution for Standard Deviation (N = 30).	34

Figure 19 – Comparison of RMC-BestFit Frequency Curve with Default Flat Priors with the Theoretical Distribution (N = 30)..... 34

Figure 20 – Comparison of RMC-BestFit with Default Flat Priors with the Theoretical Distribution for Mean (N = 100). 35

Figure 21 – Comparison of RMC-BestFit with Default Flat Priors with the Theoretical Distribution for Standard Deviation (N = 100). 35

Figure 22 – Comparison of RMC-BestFit Frequency Curve with Default Flat Priors with the Theoretical Distribution (N = 100). 36

Figure 23 – Comparison of RMC-BestFit with Default Flat Priors with the Theoretical Distribution for Mean (N = 500). 36

Figure 24 – Comparison of RMC-BestFit with Default Flat Priors with the Theoretical Distribution for Standard Deviation (N = 500). 37

Figure 25 – Comparison of RMC-BestFit Frequency Curve with Default Flat Priors with the Theoretical Distribution (N = 500). 37

Figure 26 – Comparison of RMC-BestFit with Jeffreys' Prior with the Theoretical Distribution for Mean (N = 30). 38

Figure 27 – Comparison of RMC-BestFit with Jeffreys' Prior with the Theoretical Distribution for Standard Deviation (N = 30). 39

Figure 28 – Comparison of RMC-BestFit Frequency Curve with Jeffreys' Prior with the Theoretical Distribution (N = 30). 39

Figure 29 – Default Flat Prior and Posterior for the Mean Parameter in RMC-BestFit..... 40

Figure 30 – Exponential Prior and Posterior Distributions for the Standard Deviation Parameter in RMC-BestFit. 41

Figure 31 – Comparison of RMC-BestFit with an Exponential Prior with the Theoretical Distribution for Standard Deviation (N = 30). 41

Figure 32 – Ln-Normal Prior and Posterior Distributions for the Standard Deviation Parameter in RMC-BestFit. 42

Figure 33 – Comparison of RMC-BestFit with a Ln-Normal Prior with the Theoretical Distribution for Standard Deviation (N = 30). 42

Figure 34 – Normal Prior and Posterior for the Mean Parameter in RMC-BestFit. 43

Figure 35 – Gamma Prior and Posterior Distributions for the Standard Deviation Parameter in RMC-BestFit. 44

Figure 36 – Comparison of RMC-BestFit with a Gamma Prior with the Theoretical Distribution for Standard Deviation (N = 30). 44

Figure 37 – Marginal Distribution of Skew in RMC-BestFit for Systematic Data Only..... 46

Figure 38 – Marginal Distribution of Skew in RMC-BestFit for Systematic and Historical Data. 47

Figure 39 – Marginal Distribution of Skew in RMC-BestFit for Systematic, Historical and Paleoflood Data. 48

Figure 40 – Comparison of RMC-BestFit with R-Stan for the Gumbel Distribution Location Parameter. 50

Figure 41 – Comparison of RMC-BestFit with R-Stan for the Gumbel Distribution Scale Parameter. 50

Figure 42 – Comparison of RMC-BestFit with R-Stan for the Logistic Distribution Location Parameter..... 51

Figure 43 – Comparison of RMC-BestFit with R-Stan for the Logistic Distribution Scale Parameter. 52

Figure 44 – Comparison of RMC-BestFit with R-Stan for the Normal Distribution Mean Parameter..... 53

Figure 45 – Comparison of RMC-BestFit with R-Stan for the Normal Distribution Std. Deviation Parameter..... 53

Figure 46 – Comparison of RMC-BestFit with R-Stan for the Weibull Distribution Scale Parameter..... 54

Figure 47 – Comparison of RMC-BestFit with R-Stan for the Weibull Distribution Shape Parameter. 55

Figure 48 – Example code for R-Stan for MCMC Sampling with the Normal Distribution..... 56

Figure 49 – Distributions of Quantile Q_{500} in RMC-BestFit for MCMC Simulation #5..... 59

Figure 50 – Distributions of Quantile Q_{500} in RMC-BestFit for MCMC Simulation #7..... 60

Figure 51 – Example code for evdbayes with uninformative priors. 62

Figure 52 – Comparison of RMC-BestFit with Evdbayes with Uninformative Priors. 63

Figure 53 – Comparison of RMC-BestFit with Evdbayes with Informative Priors on Quantiles. 64

Figure 54 – Example code for evdbayes with Informative Priors on Quantiles. 65

Figure 55 – Comparison of RMC-BestFit and Flike for Example #3..... 66

Figure 56 – Comparison of RMC-BestFit and Flike for Example #4..... 67

Figure 57 – Comparison of RMC-BestFit and Flike for Example #5..... 68

Figure 58 – Comparison of RMC-BestFit and Flike for Example #6a..... 68

Figure 59 – Comparison of RMC-BestFit and Flike for Example #6b..... 69

Figure 60 – Comparison of RMC-BestFit and EMA for USGS 01439500 Bush Kill at Shoemaker, PA..... 71

Figure 61 – RMC-BestFit Results for USGS 11274500 Orestimba Creek near Newman, CA..... 72

Figure 62 – Comparison of RMC-BestFit and EMA for USGS 11274500 Orestimba Creek near Newman, CA. 72

Figure 63 – Comparison of RMC-BestFit Posterior Predictive with the EMA Expected Probability Curve for USGS 11274500 Orestimba Creek near Newman, CA. 73

Figure 64 – Comparison of RMC-BestFit and EMA for USGS 11446500 American River at Fair Oaks, CA..... 74

Tables

Table 1 – Comparison between HEC-SSP and RMC-BestFit for MGBT Results and Hirsch-Stedinger Plotting Positions.	4
Table 2 – Nonparametric Summary Statistics Results	9
Table 3 – Tippecanoe River near Delphi, Indiana dataset (Rao & Hamed, 2000).	14
Table 4 – Normal Distribution Method of Moments (MOM) Results.	15
Table 5 – Normal Distribution Maximum Likelihood Estimation (MLE) Results.	15
Table 6 – Normal Distribution MLE Results Compared to R-Stan.	15
Table 7 – Normal Distribution Quantile Results.	16
Table 8 – Normal Distribution Quantile Standard Error.	16
Table 9 – Comparison of Summary Statistics for the Wabash River at Lafayette, Indiana dataset (Rao & Hamed, 2000).	16
Table 10 – Summary Statistics for the Wabash River at Lafayette, Indiana dataset (Rao & Hamed, 2000).	17
Table 11 – Wabash River at Lafayette, Indiana dataset (Rao & Hamed, 2000).	17
Table 12 – Log-Normal Distribution MOM Results.	17
Table 13 – Log-Normal Distribution MLE Results.	17
Table 14 – Log-Normal Distribution MLE Results Compared to R-Stan.	17
Table 15 – Log-Normal Distribution Quantile Results.	18
Table 16 – Log-Normal Distribution Quantile Standard Error.	18
Table 17 – Exponential Distribution MOM Results.	18
Table 18 – Exponential Distribution MLE Results.	18
Table 19 – Exponential Distribution MLE Results for Synthetic Dataset.	18
Table 20 – Exponential Distribution Quantile Results.	18
Table 21 – Exponential Distribution Quantile Standard Error.	19
Table 22 – Harricana River at Amos (Quebec, Canada) (Bobee & Ashkar, 1991).	20
Table 23 – Gamma Distribution MOM Results.	20
Table 24 – Gamma Distribution MLE Results.	20
Table 25 – Gamma Distribution MLE Results Compared to R-Stan.	21
Table 26 – Gamma Distribution Quantile Results.	21
Table 27 – Gamma Distribution Quantile Standard Error.	21
Table 28 – Pearson Type III Distribution MOM Results.	21
Table 29 – Pearson Type III Distribution MLE Results.	21
Table 30 – Pearson Type III Distribution Quantile Results.	22
Table 31 – Pearson Type III Distribution Quantile Standard Error.	22
Table 32 – Log-Pearson Type III Distribution MOM Results.	22
Table 33 – Log-Pearson Type III Distribution MLE Results.	22
Table 34 – Log-Pearson Type III Distribution Quantile Results.	22
Table 35 – Log-Pearson Type III Distribution Quantile Standard Error.	23
Table 36 – Sugar Creek at Crawfordsville, Indiana dataset (Rao & Hamed, 2000).	23
Table 37 – Gumbel Distribution MOM Results.	23
Table 38 – Gumbel Distribution MLE Results.	23
Table 39 – Gumbel Distribution MLE Results Compared to R-Stan.	24
Table 40 – Gumbel Distribution Quantile Results.	24
Table 41 – Gumbel Distribution Quantile Standard Error.	24
Table 42 – Weibull Distribution MLE Results Compared to R-Stan.	24
Table 43 – Weibull Distribution MLE Results Compared to Palisade’s @Risk.	24
Table 44 – Weibull Distribution Quantile Results.	24
Table 45 – Generalized Extreme Value Distribution MOM Results.	24
Table 46 – White River near Nora, Indiana dataset (Rao & Hamed, 2000).	25
Table 47 – Generalized Extreme Value MLE Results.	25
Table 48 – Generalized Extreme Value Distribution Quantile Results.	25
Table 49 – Generalized Extreme Value Distribution Quantile Standard Error.	25
Table 50 – White River Flows at Mt. Carmel, Indiana dataset (Threshold = 50,000 cfs) (Rao & Hamed, 2000).	26
Table 51 – Generalized Pareto Distribution MOM Results.	27

Table 52 – Generalized Pareto Distribution MLE Results.	27
Table 53 – Generalized Pareto Distribution Quantile Results.	27
Table 54 – Generalized Pareto Distribution Quantile Standard Error.	27
Table 55 – Logistic Distribution MOM Results.	27
Table 56 – Logistic Distribution MLE Results.	27
Table 57 – Logistic Distribution MLE Results Compared to R-Stan.	27
Table 58 – Logistic Distribution Quantile Results.	28
Table 59 – Logistic Distribution Quantile Standard Error.	28
Table 60 – East Fork White River at Seymour, Indiana dataset (Rao & Hamed, 2000).	28
Table 61 – Summary statistics for the East Fork White River at Seymour, Indiana dataset (Rao & Hamed, 2000).	28
Table 62 – Generalized Logistic Distribution MOM Results Using Book Summary Statistics.	29
Table 63 – Generalized Logistic Distribution MOM Results Using Actual Dataset.	29
Table 64 – Generalized Logistic Distribution MLE Results Using Actual Dataset.	29
Table 65 – Generalized Logistic Distribution Quantile Results.	29
Table 66 – Generalized Logistic Distribution Partial Derivatives.	29
Table 67 – Verification of Goodness-of-Fit Measures with Palisade’s @Risk.	30
Table 68 – Summary Statistics for the At-Site Skew Parameter for Each Dataset at Blakely Mountain Dam.	46
Table 69 – Posterior Skew Statistics in RMC-BestFit Compared to the Theoretical Solution for Systematic Data Only.	46
Table 70 – Posterior Skew Statistics in RMC-BestFit Compared to the Theoretical Solution for Systematic and Historical Data.	47
Table 71 – Posterior Skew Statistics in RMC-BestFit Compared to the Theoretical Solution for Systematic, Historical and Paleoflood Data.	48
Table 72 – Parameter Summary Statistics for the Gumbel Distribution from R-Stan.	49
Table 73 – Parameter Summary Statistics for the Gumbel Distribution from RMC-BestFit.	49
Table 74 – Parameter Summary Statistics for the Logistic Distribution from R-Stan.	51
Table 75 – Parameter Summary Statistics for the Logistic Distribution from RMC-BestFit.	51
Table 76 – Parameter Summary Statistics for the Normal Distribution from R-Stan.	52
Table 77 – Parameter Summary Statistics for the Normal Distribution from RMC-BestFit.	52
Table 78 – Parameter Summary Statistics for the Weibull Distribution from R-Stan.	54
Table 79 – Parameter Summary Statistics for the Weibull Distribution from RMC-BestFit.	54
Table 80 – Summary of the Eight Distinct MCMC Simulation (Skahill, Viglione, & Byrd, 2016).	57
Table 81 – Comparison RMC-BestFit with (Skahill, Viglione, & Byrd, 2016) for Posterior Mode Parameters for the GEV Distribution.	58
Table 82 – Comparison RMC-BestFit with (Skahill, Viglione, & Byrd, 2016) for the 100-yr Quantile.	58
Table 83 – Comparison RMC-BestFit with (Skahill, Viglione, & Byrd, 2016) for the 1,000-yr Quantile.	58
Table 84 – Summary Statistics for the At-Site 500-Year Quantile for Kamp at Zwettl.	59
Table 85 – Posterior Quantile Statistics in RMC-BestFit Compared to the Theoretical Solution for MCMC Simulation #5.	60
Table 86 – Posterior Quantile Statistics in RMC-BestFit Compared to the Theoretical Solution for MCMC Simulation #7.	60
Table 87 – Parameter Summary Statistics from Evdbayes with Uninformative Priors.	61
Table 88 – Parameter Summary Statistics from RMC-BestFit with Uninformative Priors.	61
Table 89 – Summary of Prior Distributions on Quantiles.	63
Table 90 – Parameter Summary Statistics from Evdbayes with Informative Priors on Quantiles.	63
Table 91 – Parameter Summary Statistics from RMC-BestFit with Informative Priors on Quantiles.	64
Table 92 – Comparison of RMC-BestFit and EMA parameters for USGS 01439500 Bush Kill at Shoemaker, PA.	70

This page blank intentionally

Purpose and Scope

The U.S. Army Corps of Engineers (USACE) Risk Management Center (RMC), in collaboration with the Engineer Research and Development Center (ERDC) Coastal and Hydraulics Laboratory (CHL), developed the Bayesian estimation and fitting software (RMC-BestFit) to enhance and expedite flood hazard assessments within the Flood Risk Management, Planning, and Dam and Levee Safety communities of practice.

RMC-BestFit is designed for interactive use in a multi-tasking environment. The software features a fully integrated modeling platform, including a modern graphical user interface, data entry capabilities, distribution fitting analysis, Bayesian estimation analysis, and report quality charts. RMC-BestFit is a menu-driven software package, which performs distribution fitting and Bayesian estimation from a choice of thirteen probability distributions. Input data is entered as a block annual maxima series, and the software supports the use of interval and threshold censored data.

The purpose of this document is to provide verification of critical RMC-BestFit computations. Software verification involves comparison of the numerical solution generated by the code with one or more analytical solutions, or other numerical solutions. Verification ensures that the software accurately solves the equations that constitute the mathematical model.

The RMC-BestFit software uses two dynamic link libraries (dll) for performing numerical analyses: *Numerics.dll* and *RMC.BestFit.dll*. *Numerics* is a numerical library for .NET, which provides methods and algorithms for numerical computations in science and engineering. *Numerics* includes routines for special functions, interpolation, statistics, random numbers, probability distributions, uncertainty analysis, optimization, root finding, and more. *RMC.BestFit* is a model library for the RMC-BestFit software, written in the .NET framework, which contains all remaining necessary functionality for input data, distribution fitting, and Bayesian estimation. Both of these libraries were developed internally by the RMC and, as such, the numerical methods contained within need to be verified.

RMC-BestFit has three functional components: 1) Input data; 2) Distribution fitting analysis; and 3) Bayesian estimation analysis. Numerical verification for each component is detailed in this report and organized as follows:

- **Input Data:** The multiple Grubbs-Beck test and Hirsch-Stedinger plotting positions were verified using the 82 test sites developed for Bulletin 17C (U.S. Geological Survey, 2018) and compared against results from *HEC-SSP*¹. Two additional examples from Bulletin 17C, which incorporate multiple thresholds, were used for further verification of the Hirsch-Stedinger plotting positions. Nonparametric summary statistics were verified using the *Palisade's @Risk* software².
- **Distribution Fitting Analysis:** The Nelder-Mead optimization method was verified using Microsoft (MS) Excel's Solver add-in, and implicitly confirmed through verification of the Maximum Likelihood Estimation (MLE) results for each distribution. The thirteen probability distributions used within RMC-BestFit were verified using textbook solutions found in (Bobee & Ashkar, 1991) and (Rao & Hamed, 2000), and results from *R-Stan*³ for select distributions. The Akaike and Bayesian Information Criteria (AIC and BIC) were verified using *Palisade's @Risk* software, and root-mean-squared-error (RMSE) calculations were verified using MS Excel.
- **Bayesian Estimation:** The Bayesian estimation methods used in RMC-BestFit were verified using known theoretical solutions for the Normal (Gaussian) distribution, and with other widely used Bayesian software packages, such as *R-Stan*, *evdbayes*⁴, and *Flike*⁵. Finally, a comparison was made with flood frequency results from the Expected Moments Algorithm (EMA) (Cohn, Lane, & Baier, 1997) provided in the *HEC-SSP* software.

¹ <https://www.hec.usace.army.mil/software/hec-ssp/>

² <https://www.palisade.com/risk/default.asp>

³ <https://mc-stan.org/users/interfaces/rstan>

⁴ <https://cran.r-project.org/web/packages/evdbayes/index.html>

⁵ <https://flike.tuflow.com/>

Input Data

RMC-BestFit allows the user to enter block annual maxima data, which is assumed to be independent and identically distributed. RMC-BestFit supports three different data types:

1. **Systematic Data:** Data that are collected at regular, prescribed intervals under a defined protocol. In a maximum likelihood context, these values are treated as exact measurements.
2. **Interval Data:** Data whose magnitudes are not known exactly, but are known to fall within a range or interval. In a maximum likelihood context, these values are treated as interval-censored.
3. **Perception Thresholds:** Data points that occurred during a period of years and have magnitudes that are below a threshold value, but unknown by how much. In a maximum likelihood context, these values are treated as left-censored.

The Distribution Fitting Analysis chapter provides greater detail on how these data types are treated in a likelihood context.

Multiple Grubbs-Beck Test

For the distribution fitting or Bayesian estimation to be theoretically valid, the input data must be independent and identically distributed. As a means to ensure homogeneity, RMC-BestFit provides the Multiple Grubbs-Beck test (MGBT) (Cohn, et al., 2013) for low outliers, which is consistent with the Bulletin 17C guidelines (U.S. Geological Survey, 2018). Other hypothesis tests are planned for future versions of the software.

The code for MGBT was modified from the Fortran source code for PeakfqSA⁶. The original Fortran source code used a globally adaptive Gauss-Kronrod integration method; whereas, in *Numerics* the definite integral is solved using the trapezoidal rule with 1,000 steps. Results for the MGBT implementation in RMC-BestFit were compared against results from *HEC-SSP* for 82 USGS gage sites (see Table 1). In all cases, RMC-BestFit produces the same results as *HEC-SSP*.

In RMC-BestFit, the MGBT is only applied to systematic data, which are considered exact measurements. Interval- and threshold-censored data are not included in the test. Likewise, in *HEC-SSP*, only systematic data are included in the MGBT. However, in *HEC-SSP*, data labeled as "Historical" are not included in MGBT, even if those historical data points are exact values. This design choice between the two software can lead to significant differences in MGBT results.

Hirsch-Stedinger Plotting Positions

In RMC-BestFit, the input data can be plotted as a chronology plot, as shown in Figure 1, or a nonparametric frequency plot, as shown in Figure 2. The nonparametric analysis is based on the Hirsch-Stedinger (H-S) plotting position formula (Hirsch & Stedinger, 1987) (U.S. Geological Survey, 2018). The H-S plotting positions are used to visually and quantitatively assess the goodness-of-fit of the fitted distributions (see the Goodness-of-Fit Measures section for more detail). The programmatic subroutine for the H-S plotting positions was written based on the description of the method found in (U.S. Geological Survey, 2018). The H-S plotting positions computed in RMC-BestFit were compared with results from *HEC-SSP* for 82 USGS gage sites (see Table 1). The only scenarios where the results do not match are in cases where there are low outliers.

The low outlier threshold value identified by the MGBT is automatically treated as a left-censored threshold in the fitting analysis for both RMC-BestFit and *HEC-SSP*. For example, if the MGBT threshold value is 8,000 and there are eight data points below the threshold identified as low outliers, then this is treated equivalent to a left-censored threshold with eight values below and zero above. However, RMC-BestFit does not include the MGBT threshold in the H-S plotting position routine; whereas, *HEC-SSP* does include the threshold. This is a software design choice rather than a numerical difference. Conceptually, the MGBT removes exact data points and replaces them with a threshold-censored value. This represents a loss in information. However, if this MGBT threshold is included in the H-S routine,

⁶ <https://sites.google.com/a/alumni.colostate.edu/jengland/resources>

then it will make the plotting positions rarer, signaling an increase in information. This is counterintuitive, and for this reason RMC-BestFit does not include the MGBT threshold in the H-S plotting position routine.

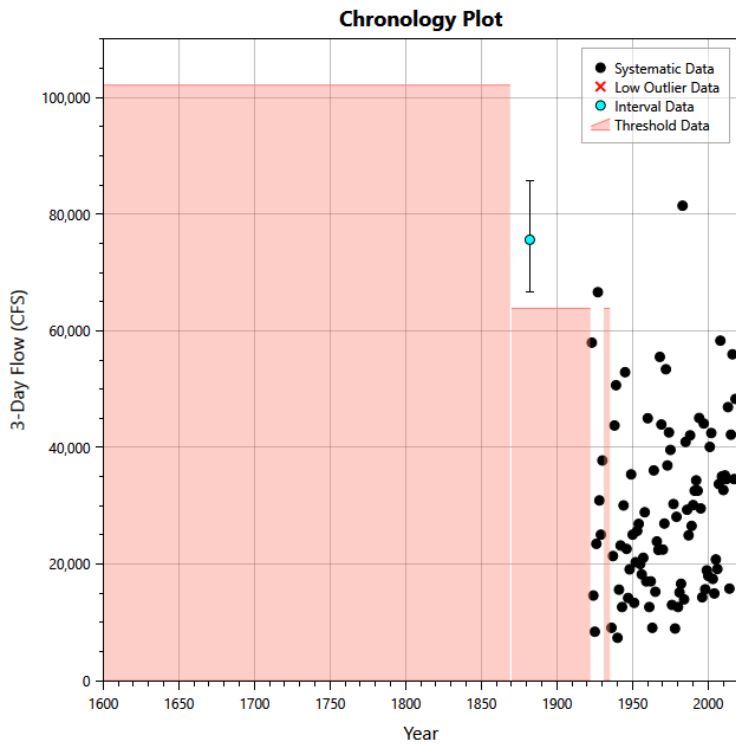


Figure 1 – Example of Input Data Chronology Plot

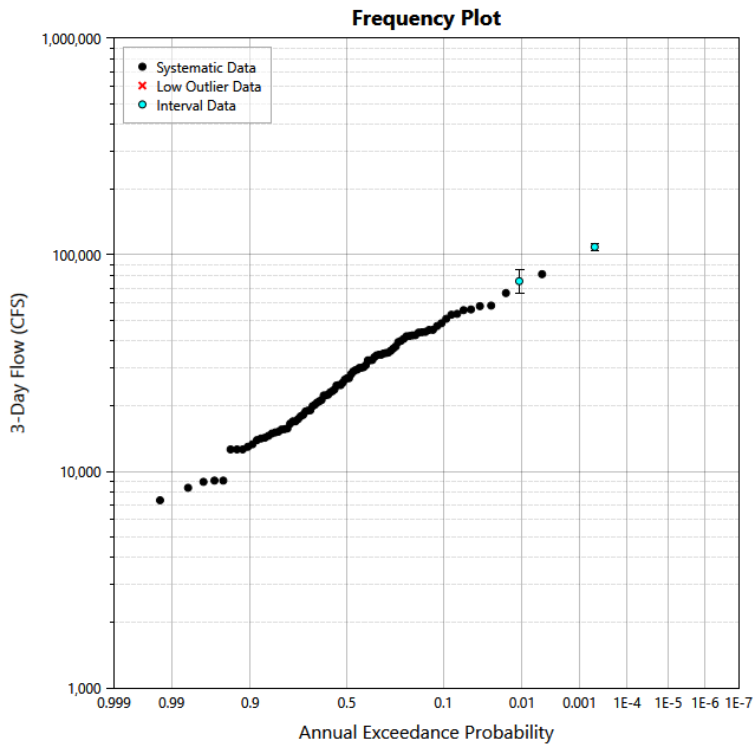


Figure 2 – Example of Input Data Frequency Plot.

Another key difference between RMC-BestFit and *HEC-SSP* is that *HEC-SSP* uses different plotting position coefficients for low outliers and non-outliers. In *HEC-SSP*, non-outliers use the Weibull coefficient ($\alpha = 0$), and low outliers use the Median coefficient ($\alpha = 0.3175$). RMC-BestFit uses the same coefficient throughout, and the user can choose from the following coefficients:

- Weibull ($\alpha = 0.0$)
- Median ($\alpha = 0.3175$)
- Blom ($\alpha = 0.375$)
- Cunnane ($\alpha = 0.40$)
- Gringorten ($\alpha = 0.44$)
- Hazen ($\alpha = 0.50$)

Again, the differences in H-S plotting positions are based on alternative software design choices rather than numerical differences.

Table 1 – Comparison between *HEC-SSP* and RMC-BestFit for MGBT Results and Hirsch-Stedinger Plotting Positions.

Site No.	No. of Events	No. of Low Outliers		MGBT Threshold		H-S Plotting Positions
		HEC-SSP	RMC-BestFit	HEC-SSP	RMC-BestFit	Max % Difference
01076500	106	-	-	-	-	0.00%
01350000	99	-	-	-	-	0.00%
01439500	102	-	-	-	-	0.00%
01555500	81	-	-	-	-	0.00%
01562000	98	-	-	-	-	0.00%
01635500	78	-	-	-	-	0.00%
01636500	97	-	-	-	-	0.00%
01668000	100	2	2	9,220	9,220	0.30%
02037500	75	-	-	-	-	0.00%
02138500	88	-	-	-	-	0.00%
02256500	79	-	-	-	-	0.00%
03011020	107	-	-	-	-	0.00%
03051000	103	-	-	-	-	0.00%
03159500	78	-	-	-	-	0.00%
03183500	115	-	-	-	-	0.00%
03289500	72	5	5	6,220	6,220	0.45%
03345500	99	34	34	11,600	11,600	1.01%
03550000	101	-	-	-	-	0.00%
03558000	85	-	-	-	-	0.00%
03606500	69	-	-	-	-	0.00%
04293500	92	-	-	-	-	0.00%
05270500	75	1	1	275	275	0.39%
05291000	83	29	29	950	950	0.84%
05464500	109	5	5	8,100	8,100	0.35%
05572000	101	1	1	1,370	1,370	0.29%
05586500	44	-	-	-	-	0.00%
06062500	94	2	2	41	41	0.32%
06176500	37	7	7	39	39	0.78%
06216500	49	-	-	-	-	0.00%
06406000	61	-	-	-	-	0.00%
06600500	76	-	-	-	-	0.00%
06710500	98	-	-	-	-	0.00%
06897000	53	3	3	925	925	0.56%
06898000	80	-	-	-	-	0.00%
06933500	91	-	-	-	-	0.00%
07067000	99	-	-	-	-	0.00%
07138600	39	12	12	36	36	1.21%
07203000	76	6	6	317	317	0.39%
07208500	86	-	-	-	-	0.00%
07382000	72	-	-	-	-	0.00%
08133500	65	23	23	634	634	1.32%

Verification of the Bayesian Estimation and Fitting Software (RMC-BestFit)

Site No.	No. of Events	No. of Low Outliers		MGBT Threshold		H-S Plotting Positions
		HEC-SSP	RMC-BestFit	HEC-SSP	RMC-BestFit	Max % Difference
08150000	91	16	16	1,610	1,610	0.92%
08164000	73	1	1	1,480	1,480	0.11%
08167000	76	-	-	-	-	0.00%
08171000	84	27	27	4,260	4,260	2.41%
08189500	71	12	12	2,150	2,150	0.72%
08378500	87	-	-	-	-	0.00%
08380500	93	-	-	-	-	0.00%
08387000	56	-	-	-	-	0.00%
09241000	78	22	22	2,300	2,300	0.79%
09361500	102	2	2	2,230	2,230	0.30%
09471000	95	3	3	1,490	1,490	0.32%
09480000	62	8	8	380	380	0.63%
09482500	94	-	-	-	-	0.00%
10128500	105	-	-	-	-	0.00%
10234500	97	45	45	364	364	0.99%
11028500	71	13	13	10	10	0.72%
11152000	105	46	46	6,580	6,580	1.06%
11176000	57	19	19	106	106	1.19%
11266500	94	-	-	-	-	0.00%
11274500	79	29	29	782	782	0.80%
11383500	94	1	1	939	939	0.31%
11464500	39	15	15	6,780	6,780	1.79%
11522500	86	1	1	3,210	3,210	0.34%
12039500	97	47	47	23,200	23,200	0.97%
12134500	82	-	-	-	-	0.00%
12307500	53	12	12	5,380	5,380	0.55%
12413000	74	-	-	-	-	0.00%
12414500	92	-	-	-	-	0.00%
12437950	21	-	-	-	-	0.00%
12451000	89	-	-	-	-	0.00%
13185000	102	1	1	2,420	2,420	0.30%
13302500	96	42	42	8,420	8,420	0.98%
13343660	20	3	3	10	10	1.39%
14021000	57	-	-	-	-	0.00%
14048000	105	-	-	-	-	0.00%
14137000	99	-	-	-	-	0.00%
14321000	104	9	9	51,000	51,000	0.35%
15072000	91	-	-	-	-	0.00%
16068000	95	5	5	964	964	0.32%
16518000	90	-	-	-	-	0.00%
16587000	98	-	-	-	-	0.00%

Two additional examples from Bulletin 17C, which incorporate multiple thresholds with varying magnitudes, were used for further verification of the H-S plotting positions. Example #4 from Appendix 10 of Bulletin 17C (U.S. Geological Survey, 2018) incorporates a historical record with several large floods and paleoflood information for the Arkansas River at Pueblo Dam near Pueblo, Colorado. Example #7 from Bulletin 17C incorporates several large, historical floods and detailed paleoflood data for Reclamation's Folsom Dam. The chronology plots for these two examples are shown in Figure 3 and Figure 4. These complex datasets provided a means of stress testing the H-S plotting position routine in RMC-BestFit. Results are provided in Figure 5 and Figure 6. RMC-BestFit produces the exact same results as HEC-SSP for these two examples.

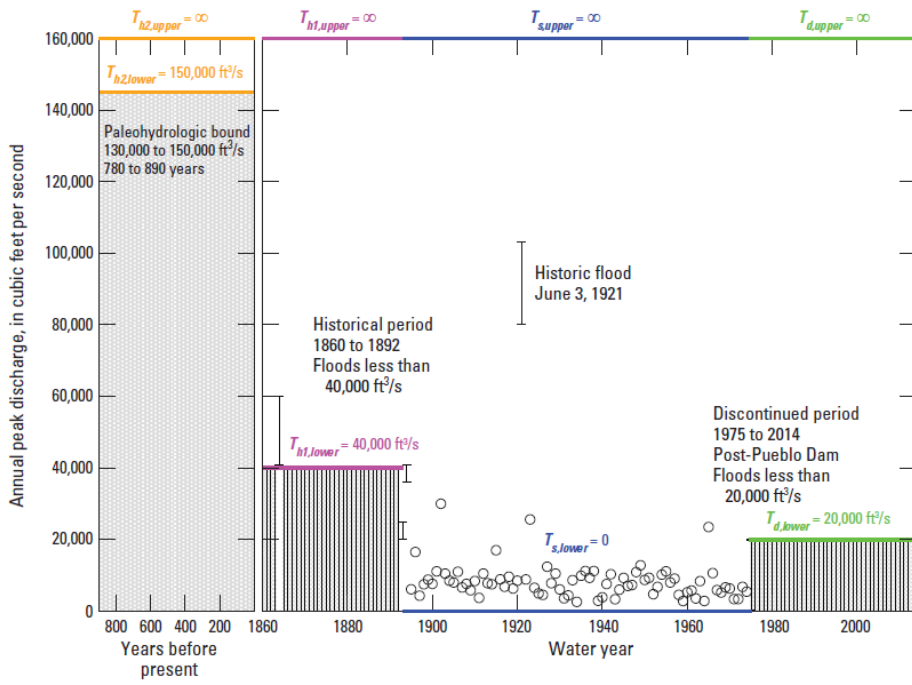


Figure 3 – Chronology Plot of the Arkansas River at Pueblo State Park (Example #4 from Bulletin 17C (U.S. Geological Survey, 2018)).

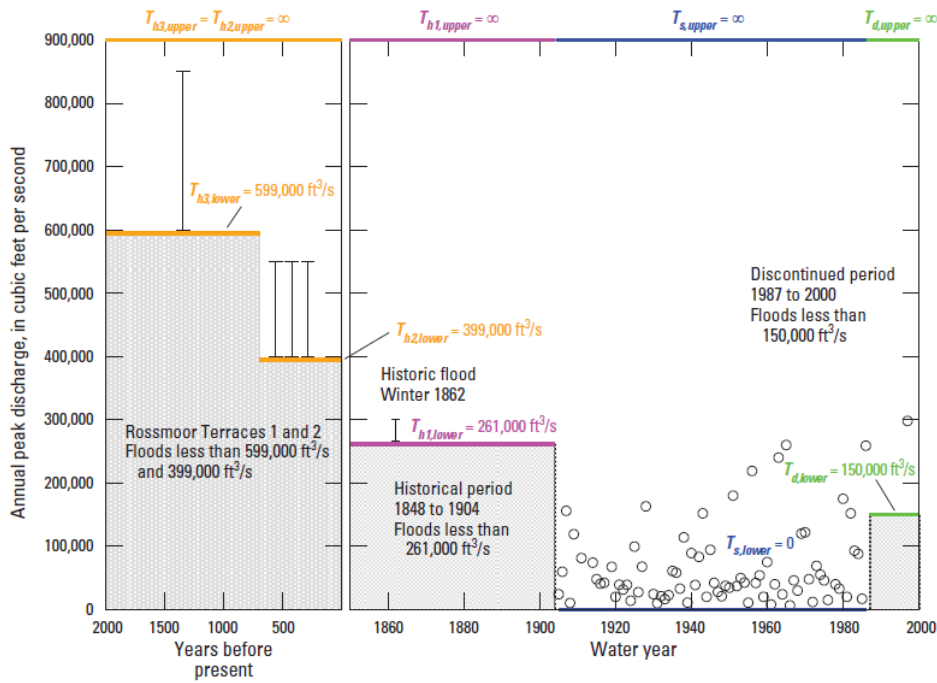


Figure 4 – Chronology Plot of the America River at Fair Oaks (Example #7 from Bulletin 17C (U.S. Geological Survey, 2018)).

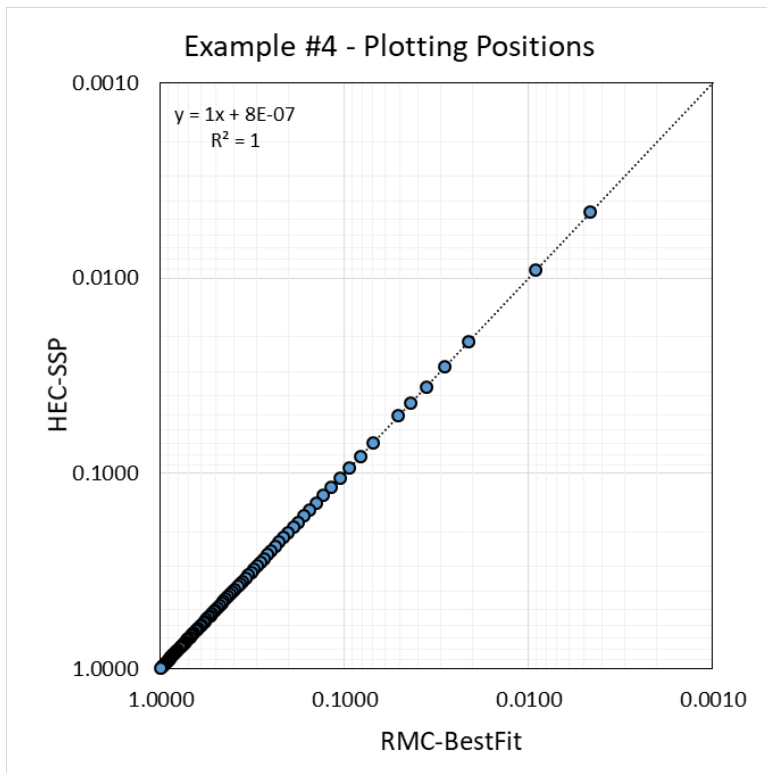


Figure 5 – Comparison of RMC-BestFit with HEC-SSP for the Hirsch-Stedinger Plotting Positions for Example #4 in Bulletin 17C (U.S. Geological Survey, 2018).

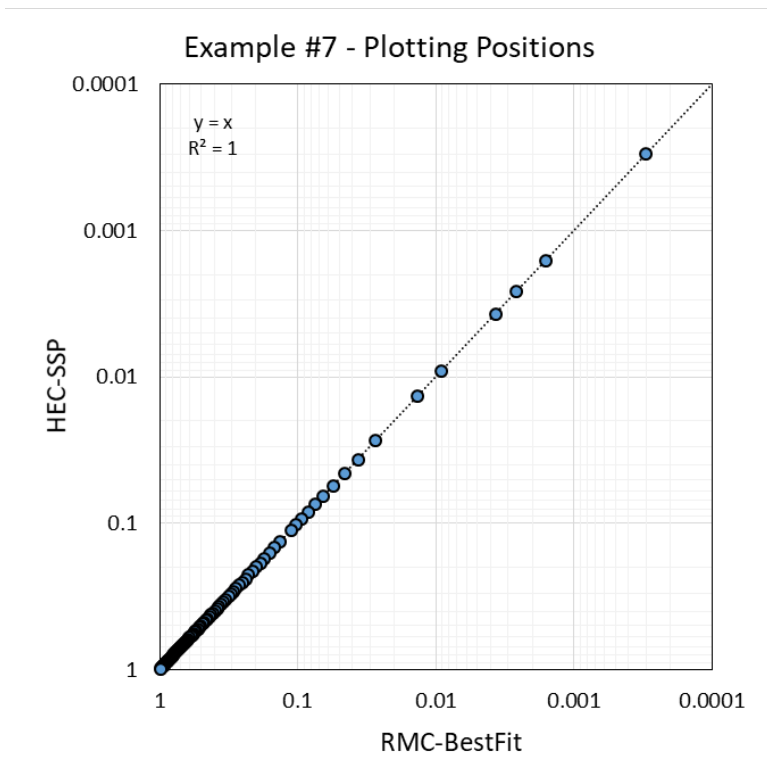


Figure 6 – Comparison of RMC-BestFit with HEC-SSP for the Hirsch-Stedinger Plotting Positions for Example #7 in Bulletin 17C (U.S. Geological Survey, 2018).

Nonparametric Summary Statistics

RMC-BestFit provides summary statistics for the systematic data and for all of the data, including low outliers, intervals, and perception thresholds (see Figure 7). Summary statistics for the systematic data use standard moment and percentile estimates, while summary statistics for all data are based on the nonparametric H-S plotting positions. The central moments of the nonparametric distribution are estimated using numerical integration; specifically, the trapezoidal rule is used with 1,000 integration steps. The nonparametric distribution functions are provided in Equation 1 to Equation 3. Percentiles are estimated using the inverse cumulative distribution function as shown in Equation 3.

$$f(x) = \frac{p_{i+1} - p_i}{x_{i+1} - x_i}, \tag{Equation 1}$$

where $f(x)$ is the probability density function (PDF) of the variable X ; there is an array of continuous values $\{x\} = \{x_1, x_2, \dots, x_n\}$ for $x_i \leq x < x_{i+1}$ with non-exceedance probabilities $\{p\} = \{p_1, p_2, \dots, p_n\}$ with $0 \leq p_i \leq 1$.

$$F(x) = p_i + (p_{i+1} - p_i) \left(\frac{x - x_i}{x_{i+1} - x_i} \right) \tag{Equation 2}$$

$$F^{-1}(p) = x_i + (x_{i+1} - x_i) \left(\frac{p - p_i}{p_{i+1} - p_i} \right) \tag{Equation 3}$$

where $F(x)$ is the cumulative distribution function (CDF) of the variable X ; $F^{-1}(p)$ is the inverse CDF; and there is an array of continuous values $\{x\} = \{x_1, x_2, \dots, x_n\}$ for $x_i \leq x \leq x_{i+1}$ with non-exceedance probabilities $\{p\} = \{p_1, p_2, \dots, p_n\}$ with $0 \leq p_i \leq 1$ and $p_i \leq p \leq p_{i+1}$.

The nonparametric summary statistics were verified using *Palisade's @Risk*. Results are shown in Table 2 and Figure 8 and Figure 9. The minor differences in results are likely caused by different choices in integration methods and the number of integrations steps.

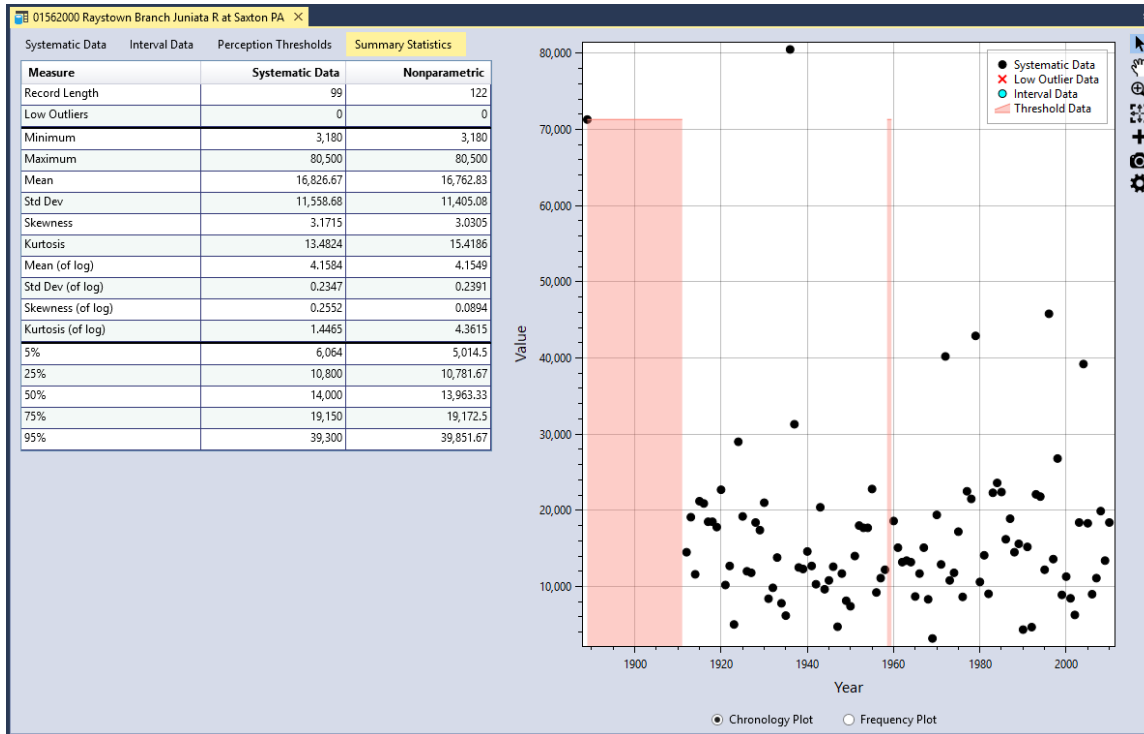


Figure 7 – Summary Statistics for Input Data (USGS 01562000) in RMC-BestFit.

Table 2 – Nonparametric Summary Statistics Results

Parameter	@Risk	RMC-BestFit	% Difference
Mean	16,763.82	16,762.83	0.01%
Std. Deviation	11,405.12	11,405.08	0.00%
Skewness	3.0303	3.0305	0.01%
Kurtosis	15.4169	15.4186	0.01%
Mean (of log)	4.1548	4.1549	0.00%
Std. Dev (of log)	0.2391	0.2391	0.00%
Skewness (of log)	0.0894	0.0894	0.00%
Kurtosis (of log)	4.3626	4.3615	0.03%
5%	5,014.50	5,014.50	0.00%
25%	10,781.67	10,781.67	0.00%
50%	13,963.33	13,963.33	0.00%
75%	19,172.50	19,172.50	0.00%
95%	39,851.67	39,851.67	0.00%

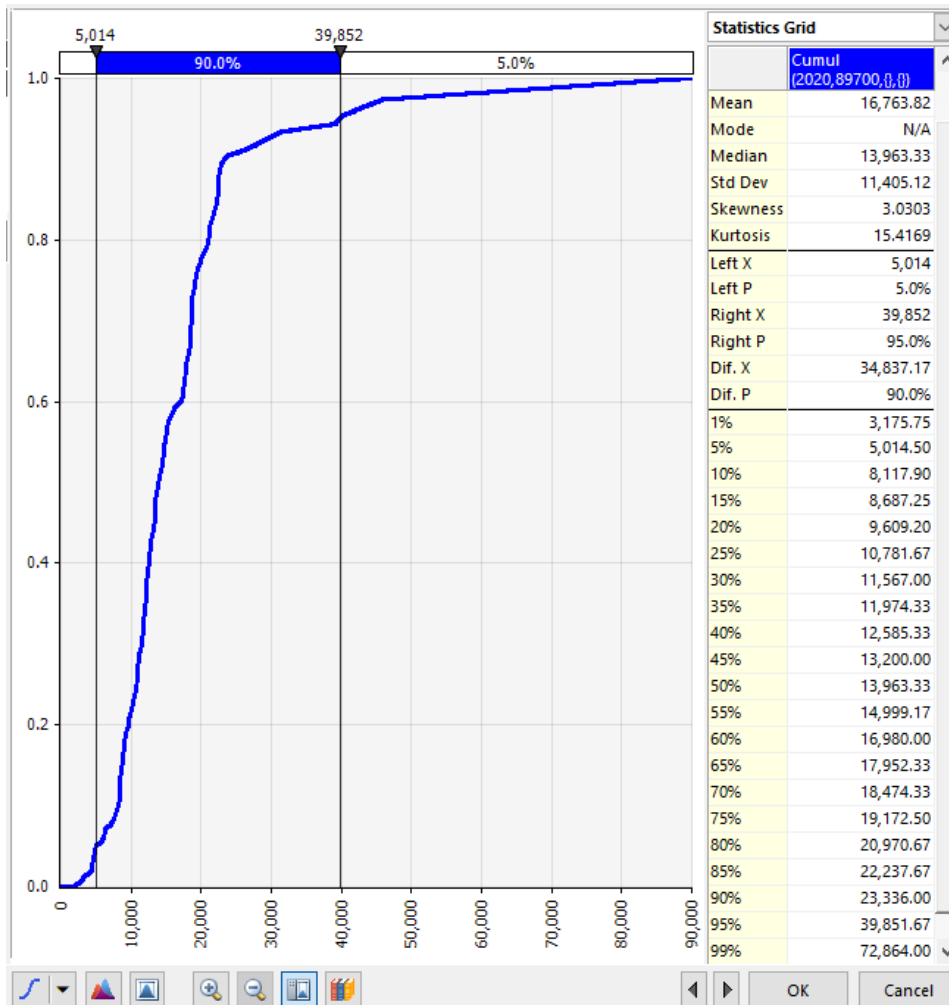


Figure 8 – Real-space Summary Statistics for Input Data (USGS 01562000) in Palisade’s @Risk.

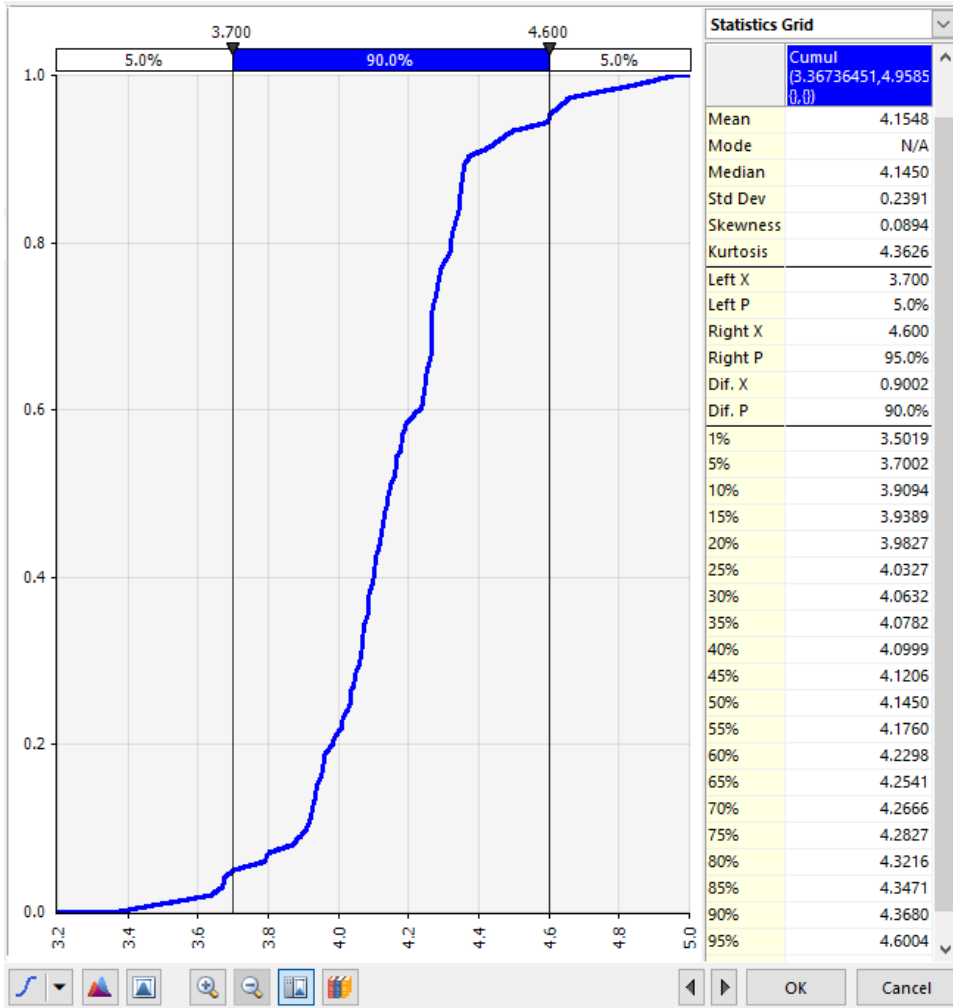


Figure 9 – Log10-space Summary Statistics for Input Data (USGS 01562000) in Palisade's @Risk.

Distribution Fitting Analysis

A distribution fitting analysis can be performed in RMC-BestFit, where univariate probability distributions are fit to the specified input data using the method of Maximum Likelihood Estimation (MLE). The distribution fitting analysis can be used to inform model selection for use in the Bayesian estimation analysis. For each fitted distribution, RMC-BestFit provides three goodness-of-fit measures: the Akaike Information Criteria (AIC), the Bayesian Information Criteria (BIC), and Root-Mean Squared Error (RMSE). These measures indicate how well the distribution fits the input data, with a smaller value representing a better fit.

RMC-BestFit uses the *Numerics* library, which was developed by the RMC, for performing a significant portion of the computations for the distribution fitting analysis. *Numerics* is a numerical library for .NET, which provides methods and algorithms for numerical computations in science and engineering. Numerics.dll includes routines for special functions, interpolation, statistics, random numbers, probability distributions, uncertainty analysis, optimization, root finding, and more.

The Nelder-Mead optimization method used to perform MLE was verified using Microsoft (MS) Excel's Solver add-in, and implicitly verified through verification of the MLE results for each distribution. The thirteen probability distributions used within RMC-BestFit were verified using textbook solutions found in (Bobee & Ashkar, 1991) and (Rao & Hamed, 2000), and results from *R-Stan* for select distributions. The AIC and BIC were verified using *Palisade's @Risk* software, and RMSE calculations were verified using MS Excel.

The following sections describe the numerical methods used for the distribution fitting analysis in RMC-BestFit, and numerical verification is provided therein.

Maximum Likelihood Estimation (MLE)

In the distribution fitting analysis, parameters are estimated using the MLE method. The MLE method formulates a likelihood function using sample data $D = (X_1, \dots, X_n)$ and the parameters θ of the probability distribution, and solves for the value of the parameters that maximize the likelihood function (Rao & Hamed, 2000) (Jongejan, 2018). The likelihood function gives the probability of the data conditional on the distribution parameters (Equation 4).

$$L_S(D|\theta) = \prod_{i=1}^{n_S} f(X_i|\theta) \quad \text{Equation 4}$$

where D is the sample of systematically recorded annual discharge maxima (X_1, \dots, X_{n_S}) ; and $f(\cdot)$ is the probability density function (PDF) of the variable X . Censored data can be incorporated into the MLE method by augmenting the likelihood function. Left-censored threshold data has the following likelihood function:

$$L_L(D|\theta) = \prod_{i=1}^{n_L} \binom{h}{k} F(X_0|\theta)^{(h-k)} \quad \text{Equation 5}$$

where X_0 is the threshold; h is the threshold period; k is the number of observations that exceeded the threshold during the period; $\binom{h}{k}$ is the binomial coefficient; and $F(\cdot)$ is the cumulative distribution function (CDF) of the variable X_0 . The binomial coefficient can be dropped from Equation 5 because it will be held constant as θ is varied. Interval-censored data has the following likelihood function:

$$L_I(D|\theta) = \prod_{i=1}^{n_I} [F(X_{U_i}|\theta) - F(X_{L_i}|\theta)] \quad \text{Equation 6}$$

where there are n_I observations known to lie between upper and lower bounds, X_U and X_L . The overall likelihood function is then constructed by multiplying the components:

$$L(D|\theta) = L_S(D|\theta) \cdot L_L(D|\theta) \cdot L_I(D|\theta) \tag{Equation 7}$$

These likelihood formulations for censored data are consistent with those presented in (Stedinger & Cohn, 1986), (Kuczera G. , 1999), and (O'Connell, Ostenaar, Levish, & Klinger, 2002). RMC-BestFit uses the Nelder-Mead method (also commonly called the downhill simplex method or amoeba method) to perform MLE for every distribution.

Nelder-Mead (Downhill Simplex)

The Nelder-Mead method is an optimization method that requires only function evaluations, not derivatives (Press, Teukolsky, Vetterling, & Flannery, 2017). The Nelder-Mead algorithm contained in *Numerics* was translated from Press et al. (2017) and augmented to include constraints on parameters.

The Microsoft (MS) Excel solver was used to verify the Nelder-Mead algorithm contained in *Numerics*. Equation 8 was used to perform numerical verification on the Nelder-Mead algorithm. The initial guess for the parameters x, y, and z were 0.5, 0.5, and 0.5, respectively. The lower bounds for each parameter were set to 0 and the upper bound was set to 1.

$$f(x,y,z) = (4x - 0.5)^2 + (3y - 0.6)^2 + (2z - 0.7)^2 \tag{Equation 8}$$

The objective function seeks to find the parameters that minimizes $f(x,y,z)$. The problem was solved in MS Excel as shown in Figure 10.

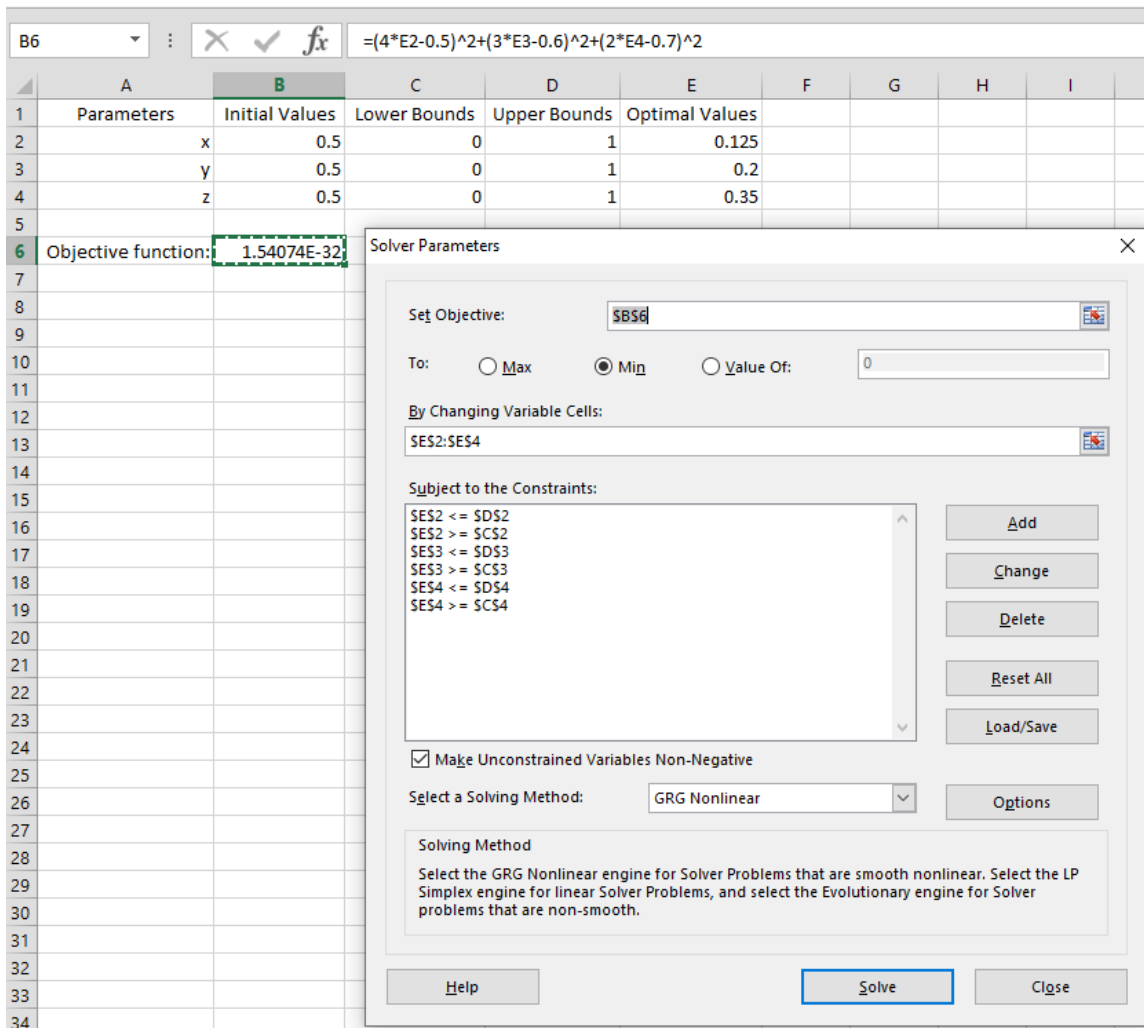


Figure 10 – Nelder-Mead Verification in MS Excel.

A unit test for the Nelder-Mead method was set up as shown in Figure 11, and unit test output is shown in Figure 12. As can be seen, both MS Excel and *Numerics* produce the same results with x, y, and z equaling 0.125, 0.2, and 0.35 respectively. Unit tests, like the one shown below, were developed for all verification tests in the *Numerics* library. The Nelder-Mead method is implicitly verified through verification of the MLE results for each distribution; i.e., if the MLE result for a distribution is correct, then the numerical method used to solve the MLE must also be correct.

```

''' <summary>
''' Test multidimensional function.
''' </summary>
1 reference
Public Function FXYZ(parms() As Double) As Double
    Dim x As Double = parms(0)
    Dim y As Double = parms(1)
    Dim z As Double = parms(2)
    Dim F As Double = (4 * x - 0.5) ^ 2 + (3 * y - 0.6) ^ 2 + (2 * z - 0.7) ^ 2
    Return F
End Function

''' <summary>
''' Nelder-Mead downhill simplex, sometimes referred to as Ameoba.
''' </summary>
0 references
<TestMethod()> Public Sub Test_NelderMead()
    Dim initial() As Double = {0.5, 0.5, 0.5}
    Dim lower() As Double = {0, 0, 0}
    Dim upper() As Double = {1, 1, 1}
    Dim solution() As Double = NelderMead.Minimize(AddressOf FXYZ, initial, lower, upper, 0.00000001)
    Dim x As Double = solution(0)
    Dim y As Double = solution(1)
    Dim z As Double = solution(2)

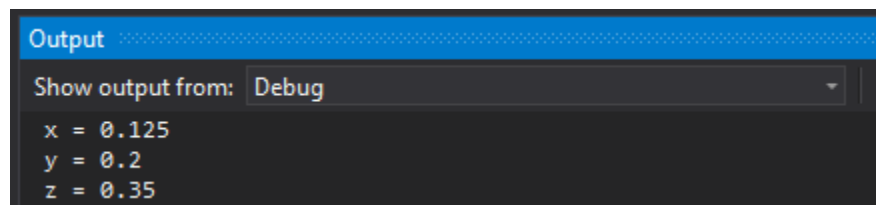
    Dim validX As Double = 0.125
    Dim validY As Double = 0.2
    Dim validZ As Double = 0.35

    Assert.AreEqual(Math.Abs(validX - x) / validX < 0.01, True)
    Assert.AreEqual(Math.Abs(validY - y) / validY < 0.01, True)
    Assert.AreEqual(Math.Abs(validZ - z) / validZ < 0.01, True)

    Debug.WriteLine("x = " & x.ToString)
    Debug.WriteLine("y = " & y.ToString)
    Debug.WriteLine("z = " & z.ToString)
End Sub

```

Figure 11 – Unit Test for the Nelder-Mead algorithm contained in *Numerics.dll*.



```

Output
Show output from: Debug
x = 0.125
y = 0.2
z = 0.35

```

Figure 12 – Unit Test output for the Nelder-Mead algorithm.

Probability Distributions

The distribution fitting analysis in RMC-BestFit fits thirteen different probability distributions to the input data. All probability distribution functionality is contained within *Numerics*. In most cases, the initial parameter values and parameter constraints are estimated using the Method of Moments (MOM), which equates the moments of the sample data with the moments of the probability distribution function. The MLE method for distribution fitting is then performed using the Nelder-Mead method described above.

Verification data sets come from two primary sources: 1) *The Gamma Family and Derived Distributions Applied in Hydrology* (Bobee & Ashkar, 1991), and 2) *Flood Frequency Analysis* (Rao & Hamed, 2000). Each test evaluates the MOM fit, the MLE fit, quantile estimates, and standard error estimates, when possible. RMC-BestFit results were verified using the textbook solutions found in (Bobee & Ashkar, 1991) and (Rao & Hamed, 2000), and results from *R-Stan* for the following distributions: Normal, Log-Normal, Gamma, Gumbel, Weibull, and Logistic.

The probability distribution parameterizations and estimation methods used in *Numerics* are consistent with those found in (Hosking & Wallis, 1997), (Asquith, 2011), and (Krishnamoorthy, 2016).

Normal and Related Distributions

All of the Normal (Gaussian) and related distributions were verified using examples found in *Flood Frequency Analysis* (Rao & Hamed, 2000). *Numerics* contains two log-Normal distributions. The first, named “Ln-Normal” is based on the natural logarithm, or log base e. This distribution is parameterized using real-space moments to be more intuitive for multi-disciplinary end-users of the software. The other distribution, named “Log-Normal,” is generalized so that the log base can be specified. Hydrologists typically use log base 10, so this is the default setting used in RMC-BestFit.

Normal

The Normal distribution was verified using the Tippecanoe River near Delphi, Indiana dataset provided in *Flood Frequency Analysis* (Rao & Hamed, 2000) and shown in Table 3. The MOM results are shown in Table 4, the MLE results are shown in Table 5 and Table 6, the results for the inverse CDF are provided in Table 7, and the results for the quantile standard error are shown in Table 8. All results are reported with the same significant digits as was reported in (Rao & Hamed, 2000).

Table 3 – Tippecanoe River near Delphi, Indiana dataset (Rao & Hamed, 2000).

Year	Flow (CFS)	Year	Flow (CFS)	Year	Flow (CFS)
1940	6,290	1957	18,800	1974	14,100
1941	2,700	1958	21,400	1975	14,100
1942	13,100	1959	22,600	1976	12,500
1943	16,900	1960	14,200	1977	7,530
1944	14,600	1961	11,000	1978	13,400
1945	9,600	1962	12,800	1979	17,600
1946	7,740	1963	15,700	1980	13,400
1947	8,490	1964	4,740	1981	19,200
1948	8,130	1965	6,950	1982	16,900
1949	12,000	1966	11,800	1983	15,500
1950	17,200	1967	12,100	1984	14,500
1951	15,000	1968	20,600	1985	21,900
1952	12,400	1969	14,600	1986	10,400
1953	6,960	1970	14,600	1987	7,460
1954	6,500	1971	8,900		
1955	5,840	1972	10,600		
1956	10,400	1973	14,200		

Table 4 – Normal Distribution Method of Moments (MOM) Results.

Parameter	Rao & Hamed (2000)	RMC-BestFit	% Difference
Mean (μ)	12,665	12,665	0.00%
Std. Deviation (σ)	4,710	4,710	0.00%

The results for MLE provided for this dataset by (Rao & Hamed, 2000) are incorrect. The MLE estimate for standard deviation is equal to the population standard deviation of the sample, not the sample standard deviation as reported by (Rao & Hamed, 2000). With this in mind, the MLE of the standard deviation is a biased estimator. The MLE results comparing (Rao & Hamed, 2000) with RMC-BestFit are shown in Table 5. The MLE results comparing *R-Stan* and RMC-BestFit are shown in Table 6. RMC-BestFit produces nearly identical results to *R-Stan*. Example code for *R-Stan* is provided in Figure 13 so that others will be able to reproduce these results.

Table 5 – Normal Distribution Maximum Likelihood Estimation (MLE) Results.

Parameter	Rao & Hamed (2000)	RMC-BestFit	% Difference
Mean (μ)	12,665	12,665	0.00%
Std. Deviation (σ)	4,710*	4,660.43	1.06%

*This should be the population standard deviation of the sample, which is 4,660.42.

 Table 6 – Normal Distribution MLE Results Compared to *R-Stan*.

Parameter	<i>R-Stan</i>	RMC-BestFit	% Difference
Mean (μ)	12,665.21	12,665.22	0.00%
Std. Deviation (σ)	4,660.40	4,660.43	0.00%

```
library(rstan)

# This is example code for R-Stan with the Normal distribution.
# Stan will automatically compile this block of code to significantly reduce runtimes.
stan_code <- 'data {int N; real x[N];}
              parameters {real mu; real<lower = 0> sigma;}
              model {for(n in 1:N){target += normal_lpdf(x[n] | mu, sigma);}}'
model <- stan_model(model_code=stan_code)

# Reference: "Flood Frequency Analysis", A.R. Rao & K.H. Hamed, CRC Press, 2000.
# Table 5.1.1 Tippecanoe River Near Delphi, Indiana (Station 43) Data.
gageData = c(6290, 2700, 13100, 16900, 14600, 9600, 7740, 8490, 8130, 12000, 17200, 15000,
             12400, 6960, 6500, 5840, 10400, 18800, 21400, 22600, 14200, 11000, 12800, 15700,
             4740, 6950, 11800, 12100, 20600, 14600, 14600, 8900, 10600, 14200, 14100, 14100,
             12500, 7530, 13400, 17600, 13400, 19200, 16900, 15500, 14500, 21900, 10400, 7460)

# Get the mean and standard deviation of the gage data.
m <- mean(gageData)
s <- sd(gageData)
# 12665.21
# 4709.742

# Estimate the posterior mode parameter set using Maximum Likelihood Estimation (MLE).
mle = optimizing(model, data=list(x=gageData, N=length(gageData)),
                algorithm="LBFGS", init=list(mu=m, sigma=s))

# Output the MLE results.
print(mle)
#      mu      sigma
# 12665.208 4660.398
```

 Figure 13 – Example code for *R-Stan* with the Normal Distribution.

The quantile estimate results for the 100-yr return period (or 0.99 non-exceedance probability) are provided in Table 7. These results were derived using the MOM parameters to have a 1:1 comparison with (Rao & Hamed, 2000). The minor differences are because *Numerics* uses a double-precision rational approximation to the inverse CDF, whereas (Rao & Hamed, 2000) uses a single-precision approximation. The CDF was verified for all distributions by plugging in the quantile value to ensure it computes the correct probability. The PDF of each distribution was validated implicitly through the MLE method; i.e., the MLE results can only be valid if the PDF is valid.

Table 7 – Normal Distribution Quantile Results.

Quantile	Rao & Hamed (2000)	RMC-BestFit	% Difference
$F^{-1}(0.99)$	23,624	23,622	0.01%

Quantile Standard Error

The quantile standard error for every distribution is estimated using a Taylor series approximation, often referred to as the delta method. The quantile standard error for the Normal distribution is estimated using Equation 9. This equation can be generalized for functions with any number of variables. The standard error is provided here because the calculations for the priors for quantiles in RMC-BestFit requires the partial derivatives of the inverse CDF with respect to each parameter. These partial derivatives are also required in Equation 9. Consequently, verification of the quantile standard error also provides verification of the methods used to estimate parameter variance and the partial derivatives. Results for the standard error for the 100-yr quantile using the MOM parameters are provided in Table 8.

$$Var Z = \left(\frac{\partial X}{\partial \mu}\right)^2 Var \mu + \left(\frac{\partial X}{\partial \sigma}\right)^2 Var \sigma + 2\left(\frac{\partial X}{\partial \mu}\right)\left(\frac{\partial X}{\partial \sigma}\right)Cov(\mu, \sigma) \tag{Equation 9}$$

Table 8 – Normal Distribution Quantile Standard Error.

Quantile	Rao & Hamed (2000)	RMC-BestFit	% Difference
$F^{-1}(0.99)$	1,309	1,309	0.00%

Log-Normal

The Log-Normal distribution was verified using the Wabash River at Lafayette, Indiana dataset provided in *Flood Frequency Analysis* (Rao & Hamed, 2000) and shown in Table 11. The Log-Normal distribution used in *Numerics* is generalized to work with any logarithmic base. This example uses the natural logarithm, base e.

Unfortunately, the book uses summary statistics that are significantly different than what would be generated using the data provided in the Table 11. Because the differences in summary statistics are sizeable, as shown in Table 9, a 1:1 comparison cannot truly be made. Rather than using the results reported in the book, the results are based on sample statistics derived from MS Excel (Table 10). Using these statistics, the MOM results are shown in Table 12. The MLE estimate for standard deviation is equal to the population standard deviation of the sample, not the sample standard deviation as reported by (Rao & Hamed, 2000). The MLE results comparing (Rao & Hamed, 2000) with RMC-BestFit are shown in Table 13. The MLE results comparing *R-Stan* and RMC-BestFit are shown in Table 14. RMC-BestFit produces identical results to *R-Stan*. Results for the inverse CDF are provided in Table 15, and the results for the quantile standard error are shown in Table 16.

Table 9 – Comparison of Summary Statistics for the Wabash River at Lafayette, Indiana dataset (Rao & Hamed, 2000).

Statistic	Rao & Hamed (2000)	MS Excel	% Difference
Mean	52,621	49,222	6.67%
Std. Dev.	25,200	18,908	28.53%

Table 10 – Summary Statistics for the Wabash River at Lafayette, Indiana dataset (Rao & Hamed, 2000).

Statistic	Value	Of Ln
Mean	49,222.35	10.7170
Std. Dev.	18,907.87	0.4501
Population Std. Dev.	18,796.32	0.4474

Table 11 – Wabash River at Lafayette, Indiana dataset (Rao & Hamed, 2000).

Year	Flow (CFS)	Year	Flow (CFS)	Year	Flow (CFS)	Year	Flow (CFS)
1907	41,500	1929	38,000	1951	50,600	1973	40,700
1908	57,000	1930	74,600	1952	41,900	1974	53,400
1909	44,000	1931	13,100	1953	35,000	1975	36,000
1910	49,000	1932	37,600	1954	16,500	1976	43,900
1911	31,000	1933	67,500	1955	35,300	1977	23,600
1912	45,900	1934	21,700	1956	30,000	1978	50,500
1913	19,000	1935	37,000	1957	52,600	1979	49,700
1914	41,100	1936	93,500	1958	99,000	1980	48,100
1915	37,300	1937	58,500	1959	89,000	1981	44,500
1916	76,000	1938	63,300	1960	39,500	1982	56,400
1917	33,200	1939	74,400	1961	55,400	1983	60,800
1918	61,200	1940	34,200	1962	46,000	1984	40,400
1919	76,000	1941	14,600	1963	63,000	1985	80,400
1920	59,800	1942	44,200	1964	58,300	1986	41,600
1921	44,400	1943	13,100	1965	36,500	1987	14,700
1922	58,400	1944	73,300	1966	14,600	1988	33,300
1923	53,600	1945	46,600	1967	64,900	1989	40,700
1924	59,800	1946	39,400	1968	68,500	1990	53,300
1925	63,300	1947	41,200	1969	69,100	1991	77,400
1926	57,700	1948	41,300	1970	42,600		
1927	64,000	1949	62,000	1971	31,000		
1928	63,500	1950	90,000	1972	39,400		

Table 12 – Log-Normal Distribution MOM Results.

Parameter	Rao & Hamed (2000)	RMC-BestFit	% Difference
Mean (μ)	10.7170	10.7170	0.00%
Std. Deviation (σ)	0.4501	0.4501	0.00%

Table 13 – Log-Normal Distribution MLE Results.

Parameter	Rao & Hamed (2000)	RMC-BestFit	% Difference
Mean (μ)	10.7170	10.7170	0.00%
Std. Deviation (σ)	0.4501*	0.4474	0.60%

* (Rao & Hamed, 2000) incorrectly estimates using the sample standard deviation. This should be the population standard deviation, which is 0.4474.

Table 14 – Log-Normal Distribution MLE Results Compared to R-Stan.

Parameter	R-Stan	RMC-BestFit	% Difference
Mean (μ)	10.7170	10.7170	0.00%
Std. Deviation (σ)	0.4474	0.4474	0.00%

Table 15 – Log-Normal Distribution Quantile Results.

Quantile	Rao & Hamed (2000)	RMC-BestFit	% Difference
$F^{-1}(0.99)$	128,538	128,538	0.00%

Table 16 – Log-Normal Distribution Quantile Standard Error.

Quantile	Rao & Hamed (2000)	RMC-BestFit	% Difference
$F^{-1}(0.99)$	11,935	11,935	0.00%

The Gamma Family of Distributions

The Gamma family of distributions were verified using examples found in *The Gamma Family and Derived Distributions Applied in Hydrology* (Bobee & Ashkar, 1991) and *Flood Frequency Analysis* (Rao & Hamed, 2000).

Exponential

The Exponential distribution was verified using the Wabash River at Lafayette, Indiana dataset provided in *Flood Frequency Analysis* (Rao & Hamed, 2000) and shown in Table 11. Summary statistics for this dataset are provided in Table 10. The MOM results are shown in Table 17, the MLE results are shown in Table 18, the results for the inverse CDF are provided in Table 20, and the results for the quantile standard error are shown in Table 21.

Table 17 – Exponential Distribution MOM Results.

Parameter	Rao & Hamed (2000)	RMC-BestFit	% Difference
Location (ξ)	30,314.48	30,314.48	0.00%
Scale (α)	18,907.87	18,907.87	0.00%

The MLE results are shown in Table 18. The error in the scale parameter is likely because the Nelder-Mead solver is stuck in a local maximum, rather than a global. This dataset is not well-suited for the Exponential distribution, as can be seen below in Figure 14. The Exponential distribution has the worst AIC, BIC, and RMSE of all fitted distributions for this dataset. For an alternative verification test, a synthetic data set was generated from a parent Exponential distribution with a location of 13,100 and scale of 36,122. Results are shown below in Table 19 and Figure 15. As can be seen, the percent difference between the theoretical MLE and the MLE produced by the Nelder-Mead method is sufficiently close to zero. The results for the inverse CDF are provided in Table 20, and the results for the quantile standard error are shown in Table 21. These results were based on the MOM parameters.

Table 18 – Exponential Distribution MLE Results.

Parameter	Rao & Hamed (2000)	RMC-BestFit	% Difference
Location (ξ)	13,100.00	13,100.00	0.00%
Scale (α)	36,122.35	35,816.48	0.85%

Table 19 – Exponential Distribution MLE Results for Synthetic Dataset.

Parameter	Theoretical	RMC-BestFit	% Difference
Location (ξ)	13,453.06	13,453.06	0.00%
Scale (α)	28,808.37	28,806.02	0.01%

Table 20 – Exponential Distribution Quantile Results.

Quantile	Rao & Hamed (2000)	RMC-BestFit	% Difference
$F^{-1}(0.99)$	143,471	143,471	0.00%

Table 21 – Exponential Distribution Quantile Standard Error.

Quantile	Rao & Hamed (2000)	RMC-BestFit	% Difference
$F^{-1}(0.99)$	15,986	15,986	0.00%

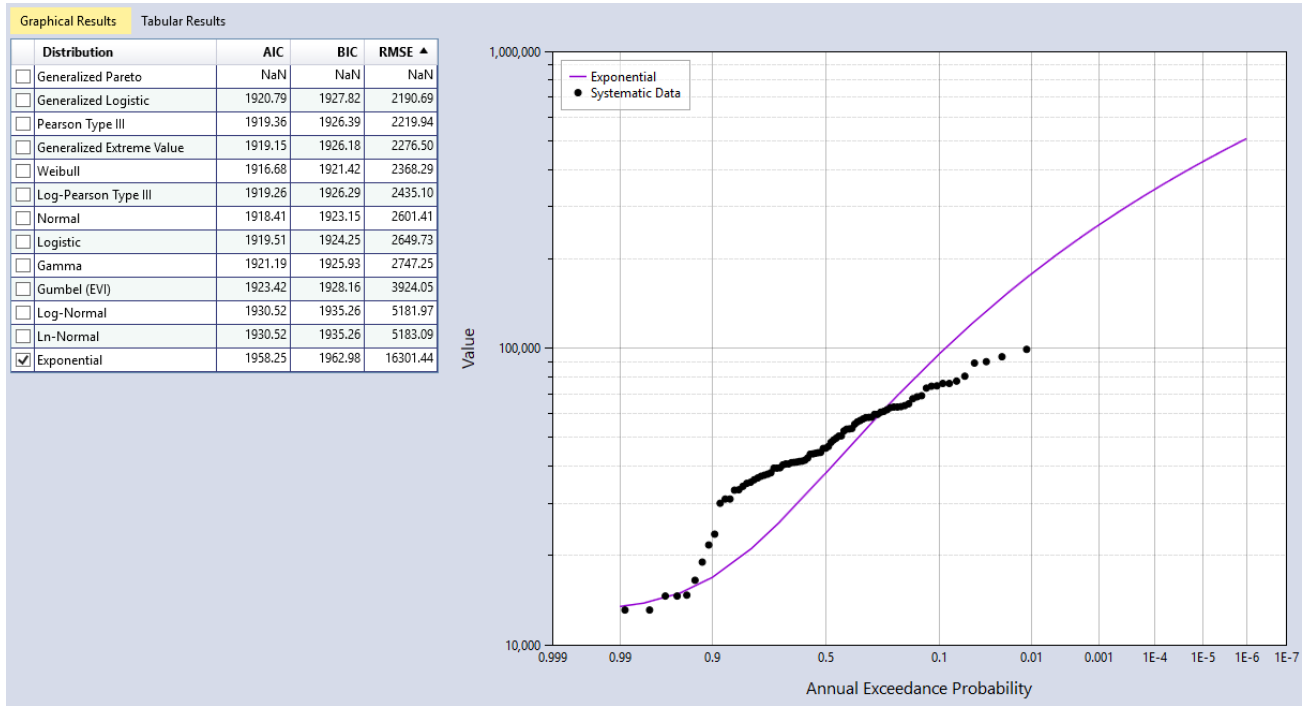


Figure 14 – Distribution Fitting Analysis for the Wabash River at Lafayette, Indiana dataset.

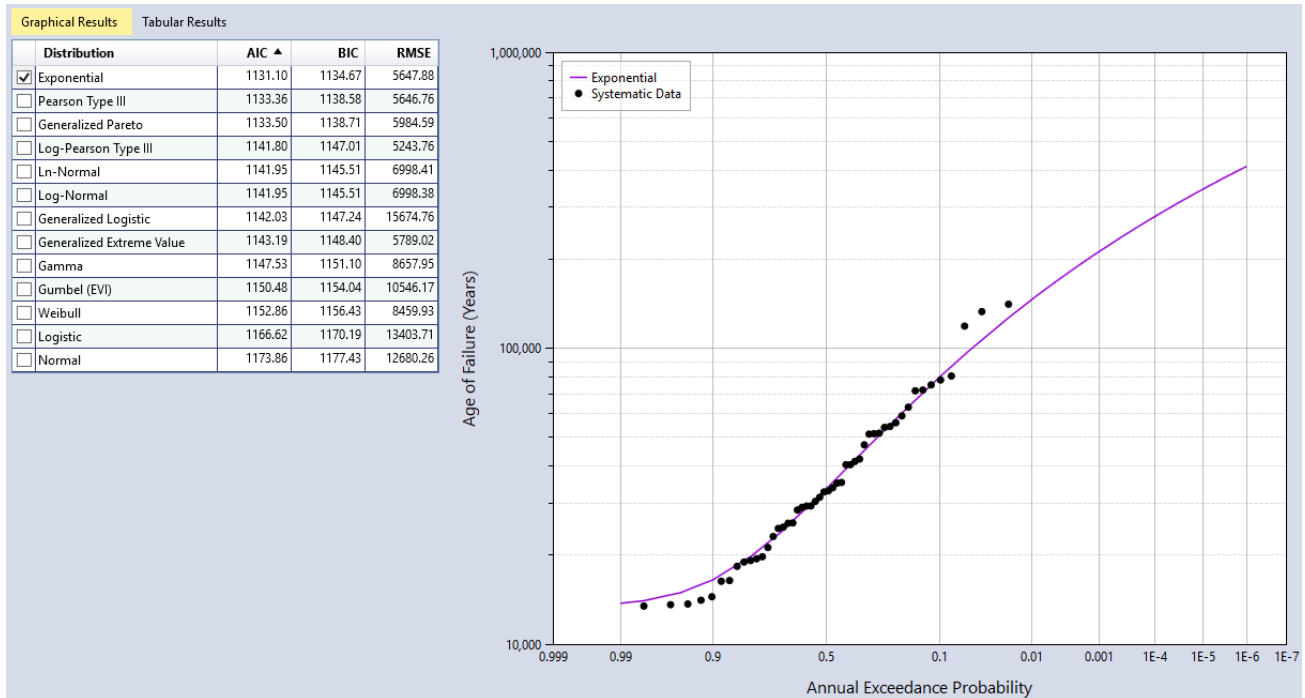


Figure 15 – Distribution Fitting Analysis for the Synthetic dataset.

Gamma

There are three different parameterizations for the Gamma distribution in common use: 1) With a scale parameter θ and a shape parameter κ ; 2) With an inverse scale parameter $\beta = 1/\theta$, called a rate parameter, and a shape parameter $\alpha = \kappa$; and 3) With a mean parameter $\mu = k\theta = \alpha/\beta$ and a shape parameter κ . *Numerics* uses the first parameterization, with a scale parameter θ and a shape parameter κ .

The Gamma distribution was verified using the Harricana River at Amos (Quebec, Canada) dataset provided in *The Gamma Family and Derived Distributions Applied in Hydrology* (Bobee & Ashkar, 1991) and shown in Table 22. The MOM results are shown in Table 23, the MLE results are shown in Table 24 and Table 25, the results for the inverse CDF are provided in Table 26, and the results for the quantile standard error are shown in Table 27. Results are reported with the same significant digits as was reported in (Bobee & Ashkar, 1991).

Table 22 – Harricana River at Amos (Quebec, Canada) (Bobee & Ashkar, 1991).

Year	Flow (CMS)	Year	Flow (CMS)	Year	Flow (CMS)
1915	122	1938	240	1961	125
1916	244	1939	230	1962	166
1917	214	1940	192	1963	99.1
1918	173	1941	195	1964	202
1919	229	1942	172	1965	230
1920	156	1943	173	1966	158
1921	212	1944	172	1967	262
1922	263	1945	153	1968	154
1923	146	1946	142	1969	164
1924	183	1947	317	1970	182
1925	161	1948	161	1971	164
1926	205	1949	201	1972	183
1927	135	1950	204	1973	171
1928	331	1951	194	1974	250
1929	225	1952	164	1975	184
1930	174	1953	183	1976	205
1931	98.8	1954	161	1977	237
1932	149	1955	167	1978	177
1933	238	1956	179	1979	239
1934	262	1957	185	1980	187
1935	132	1958	117	1981	180
1936	235	1959	192	1982	173
1937	216	1960	337	1983	174

Table 23 – Gamma Distribution MOM Results.

Parameter	Bobée & Ashkar (1991)	RMC-BestFit	% Difference
Scale (θ)	12.02357	12.02356	0.00%
Shape (κ)	15.91188	15.91188	0.00%

Table 24 – Gamma Distribution MLE Results.

Parameter	Bobée & Ashkar (1991)	RMC-BestFit	% Difference
Scale (θ)	11.32118	11.32103	0.00%
Shape (κ)	16.89937	16.89928	0.00%

Table 25 – Gamma Distribution MLE Results Compared to R-Stan.

Parameter	R-Stan	RMC-BestFit	% Difference
Scale (θ)	11.32136	11.32103	0.00%
Shape (κ)	16.89896	16.89928	0.00%

The quantile estimate results for the 100-yr return period (or 0.99 non-exceedance probability) and the standard error are provided in Table 26 and Table 27, respectively. These results were derived using the MLE parameters.

Table 26 – Gamma Distribution Quantile Results.

Quantile	Bobée & Ashkar (1991)	RMC-BestFit	% Difference
$F^{-1}(0.99)$	315.87	315.87	0.00%

Table 27 – Gamma Distribution Quantile Standard Error.

Quantile	Bobée & Ashkar (1991)	RMC-BestFit	% Difference
$F^{-1}(0.99)$	15.022	15.022	0.00%

Pearson Type III

The Pearson Type III (PIII) distribution was verified using the Harricana River at Amos (Quebec, Canada) dataset provided in *The Gamma Family and Derived Distributions Applied in Hydrology* (Bobee & Ashkar, 1991) and shown in Table 22. Verification results for this dataset are provided in Table 28 through Table 31.

In *Numerics*, the PIII distribution is parameterized by the end-user using the moments of the distribution, mean (μ), standard deviation (σ), and skew (γ). The true parameters (location, scale, and shape) are computed from the user-defined moments. This was done because the moments of the distribution are more intuitively defined by end-users. *Numerics* uses the same parameterization as (Hosking & Wallis, 1997), with the location parameter ξ , the scale parameter β , and the shape parameter α .

Table 28 – Pearson Type III Distribution MOM Results.

Parameter	Bobée & Ashkar (1991)	RMC-BestFit	% Difference
Mean (μ)	191.31739	191.31739	0.00%
Std. Dev. (σ)	47.96161	47.96161	0.00%
Skew (γ)	0.86055	0.86055	0.00%
Location (ξ)	79.84941	79.84941	0.00%
Scale (β)	20.63558	20.63657	0.00%
Shape (α)	5.40148	5.40148	0.00%

Table 29 – Pearson Type III Distribution MLE Results.

Parameter	Bobée & Ashkar (1991)	RMC-BestFit	% Difference
Mean (μ)	191.31739	191.31738	0.00%
Std. Dev. (σ)	47.01925	47.01928	0.00%
Skew (γ)	0.61897	0.61896	0.00%
Location (ξ)	39.38903	39.38849	0.00%
Scale (β)	14.55180	14.55163	0.00%
Shape (α)	10.44062	10.44067	0.00%

The quantile estimate results for the 100-yr return period (or 0.99 non-exceedance probability) and the standard error are provided in Table 30 and Table 31, respectively. These results were derived using the MLE parameters. The minor differences in standard error are a result of differences in the derivation of the frequency factor K. *Numerics*

estimates the frequency factor given the skewness coefficient through Cornish-Fisher transformation (Fisher & Cornish, 1960). Whereas, (Bobee & Ashkar, 1991) uses a polynomial approximation derived by the authors.

Table 30 – Pearson Type III Distribution Quantile Results.

Quantile	Bobée & Ashkar (1991)	RMC-BestFit	% Difference
$F^{-1}(0.99)$	321.48	321.48	0.00%

Table 31 – Pearson Type III Distribution Quantile Standard Error.

Quantile	Bobée & Ashkar (1991)	RMC-BestFit	% Difference
$F^{-1}(0.99)$	20.045	20.048	0.01%

Log-Pearson Type III

The Log-Pearson Type III (LPIII) distribution was verified using the Harricana River at Amos (Quebec, Canada) dataset provided in *The Gamma Family and Derived Distributions Applied in Hydrology* (Bobee & Ashkar, 1991) and shown in Table 22. Verification results for this dataset are provided in Table 32 through Table 35. The LPIII distribution uses the same parameterization as the PIII. The LPIII distribution used in *Numerics* is generalized to work with any logarithmic base following the procedures shown in (Bobee & Ashkar, 1991). Because the LPIII is parameterized with log-spaced moments, small errors in the MLE for log-moments can lead to larger errors in the real parameters, as shown in Table 33. These errors can be minimized by decreasing the tolerance in the Nelder-Mead solver; however, these differences are well within the acceptable range for verification.

Table 32 – Log-Pearson Type III Distribution MOM Results.

Parameter	Bobée & Ashkar (1991)	RMC-BestFit	% Difference
Mean (of log) (μ)	2.26878	2.26878	0.00%
Std. Dev (of log) (σ)	0.10699	0.10699	0.00%
Skew (of log) (γ)	-0.04061	-0.04061	0.00%
Location (ξ)	7.53821	7.53821	0.00%
Scale (β)	-0.00217	-0.00217	0.00%
Shape (α)	2,425.57481	2,425.57481	0.00%

Table 33 – Log-Pearson Type III Distribution MLE Results.

Parameter	Bobée & Ashkar (1991)	RMC-BestFit	% Difference
Mean (of log) (μ)	2.26878	2.26878	0.00%
Std. Dev (of log) (σ)	0.10621	0.10621	0.00%
Skew (of log) (γ)	-0.02925	-0.02925	0.00%
Location (ξ)	9.53033	9.53160	0.01%
Scale (β)	-0.00155	-0.00155	0.00%
Shape (α)	4,674.21790	4,675.85084	0.03%

The quantile estimate results for the 100-yr return period (or 0.99 non-exceedance probability) and the standard error are provided in Table 34 and Table 35, respectively. These results were derived using the MLE parameters. The minor differences in standard error are a result of differences in the derivation of the frequency factor K. *Numerics* estimates the frequency factor given the skewness coefficient through Cornish-Fisher transformation (Fisher & Cornish, 1960). Whereas, (Bobee & Ashkar, 1991) uses a polynomial approximation derived by the authors.

Table 34 – Log-Pearson Type III Distribution Quantile Results.

Quantile	Bobée & Ashkar (1991)	RMC-BestFit	% Difference
$F^{-1}(0.99)$	326.25	326.27	0.01%

Table 35 – Log-Pearson Type III Distribution Quantile Standard Error.

Quantile	Bobée & Ashkar (1991)	RMC-BestFit	% Difference
$F^{-1}(0.99)$	25.000	24.857	0.57%

Extreme Value Distributions

The extreme value distributions were verified using examples found in *Flood Frequency Analysis* (Rao & Hamed, 2000), synthetic data sets with *Palisade's @Risk*, and *R-Stan*.

Gumbel

The Gumbel distribution was verified using the Sugar Creek at Crawfordsville, Indiana dataset provided in *Flood Frequency Analysis* (Rao & Hamed, 2000) and shown in Table 36. Verification results are provided in Table 37 through Table 41.

Table 36 – Sugar Creek at Crawfordsville, Indiana dataset (Rao & Hamed, 2000).

Year	Flow (CFS)	Year	Flow (CFS)	Year	Flow (CFS)
1939	17,600	1958	15,100	1977	5,290
1940	3,660	1959	14,600	1978	12,200
1941	903	1960	7,300	1979	9,750
1942	5,050	1961	8,580	1980	7,390
1943	24,000	1962	15,100	1981	13,100
1944	11,400	1963	15,100	1982	7,190
1945	9,470	1964	21,800	1983	8,850
1946	8,970	1965	6,200	1984	6,290
1947	7,710	1966	2,130	1985	18,800
1948	14,800	1967	11,100	1986	9,740
1949	13,900	1968	14,300	1987	2,990
1950	20,800	1969	11,200	1988	6,950
1951	9,470	1970	6,670	1989	9,390
1952	7,860	1971	5,440	1990	12,400
1953	7,860	1972	9,370	1991	21,200
1954	2,730	1973	6,900		
1955	6,480	1974	9,680		
1956	18,200	1975	6,810		
1957	26,300	1976	7,730		

Table 37 – Gumbel Distribution MOM Results.

Parameter	Rao & Hamed (2000)	RMC-BestFit	% Difference
Location (ξ)	8,074.4	8,074.2	0.00%
Scale (α)	4,441.4	4,441.4	0.00%

Table 38 – Gumbel Distribution MLE Results.

Parameter	Rao & Hamed (2000)	RMC-BestFit	% Difference
Location (ξ)	8,049.6	8,049.60	0.00%
Scale (α)	4,478.6	4,478.60	0.00%

Table 39 – Gumbel Distribution MLE Results Compared to R-Stan.

Parameter	R-Stan	RMC-BestFit	% Difference
Location (ξ)	8,049.705	8,049.641	0.00%
Scale (α)	4,478.768	4,478.627	0.00%

Table 40 – Gumbel Distribution Quantile Results.

Quantile	Rao & Hamed (2000)	RMC-BestFit	% Difference
$F^{-1}(0.99)$	28,652	28,652	0.00%

Table 41 – Gumbel Distribution Quantile Standard Error.

Quantile	Rao & Hamed (2000)	RMC-BestFit	% Difference
$F^{-1}(0.99)$	2,486.5	2,486.5	0.00%

Weibull

RMC-BestFit supports the 2-parameter Weibull distribution with the parameterization commonly used in reliability analysis. The Weibull distribution was verified using the Tippecanoe River near Delphi, Indiana dataset provided in *Flood Frequency Analysis* (Rao & Hamed, 2000) and shown in Table 3 under the Normal distribution section. However, Rao and Hamed (2000) only provide solutions for the 3-parameter Weibull. Therefore, verification is performed using *R-Stan* and *Palisade's @Risk*. Unfortunately, neither of these products provide solutions based on method of moments, nor do they provide quantile standard error estimates. Therefore, verification results are only provided for MLE and quantile function estimations. The verification results are shown in Table 42 through Table 44.

Table 42 – Weibull Distribution MLE Results Compared to R-Stan.

Parameter	R-Stan	RMC-BestFit	% Difference
Scale (λ)	14,196.9496	14,197.2522	0.00%
Shape (κ)	2.9829	2.9828	0.00%

Table 43 – Weibull Distribution MLE Results Compared to Palisade's @Risk.

Parameter	@Risk	RMC-BestFit	% Difference
Scale (λ)	14,197.2476	14,197.2522	0.00%
Shape (κ)	2.9828	2.9828	0.00%

Table 44 – Weibull Distribution Quantile Results.

Quantile	@Risk	RMC-BestFit	% Difference
$F^{-1}(0.99)$	23,689.36	23,689.68	0.00%

Generalized Extreme Value

The Generalized Extreme Value distribution was verified using the White River near Nora, Indiana dataset provided in *Flood Frequency Analysis* (Rao & Hamed, 2000) and shown in Table 46. Verification results are provided in Table 45 through Table 49.

Table 45 – Generalized Extreme Value Distribution MOM Results.

Parameter	Rao & Hamed (2000)	RMC-BestFit	% Difference
Location (ξ)	11,012	11,012	0.00%
Scale (α)	6,209.4	6,209.3	0.00%
Shape (κ)	0.0736	0.0736	0.00%

Table 46 – White River near Nora, Indiana dataset (Rao & Hamed, 2000).

Year	Flow (CFS)	Year	Flow (CFS)	Year	Flow (CFS)
1930	23,200	1952	12,700	1974	13,200
1931	2,950	1953	9,740	1975	14,700
1932	10,300	1954	3,050	1976	14,300
1933	23,200	1955	8,830	1977	4,050
1934	4,540	1956	12,000	1978	14,600
1935	9,960	1957	30,400	1979	14,400
1936	10,800	1958	27,000	1980	19,200
1937	26,900	1959	15,200	1981	7,160
1938	23,300	1960	8,040	1982	12,100
1939	20,400	1961	11,700	1983	8,650
1940	8,480	1962	20,300	1984	10,600
1941	3,150	1963	22,700	1985	24,500
1942	9,380	1964	30,400	1986	14,400
1943	32,400	1965	9,180	1987	6,300
1944	20,800	1966	4,870	1988	9,560
1945	11,100	1967	14,700	1989	15,800
1946	7,270	1968	12,800	1990	14,300
1947	9,600	1969	13,700	1991	28,700
1948	14,600	1970	7,960		
1949	14,300	1971	9,830		
1950	22,500	1972	12,500		
1951	14,700	1973	10,700		

Table 47 – Generalized Extreme Value MLE Results.

Parameter	Rao & Hamed (2000)	RMC-BestFit	% Difference
Location (ξ)	10,849	10,849	0.00%
Scale (α)	5,745.6	5,745.6	0.00%
Shape (κ)	0.005	0.005	0.00%

The quantile estimate results for the 100-yr return period (or 0.99 non-exceedance probability) and the standard error are provided in Table 48 and Table 49, respectively. These results were derived using the MLE parameters. The difference in standard error estimates is likely due to rounding difference. The example in (Rao & Hamed, 2000) does not carry forward double precision through the full calculation of quantile variance.

Table 48 – Generalized Extreme Value Distribution Quantile Results.

Quantile	Rao & Hamed (2000)	RMC-BestFit	% Difference
$F^{-1}(0.99)$	36,977	36,978	0.00%

Table 49 – Generalized Extreme Value Distribution Quantile Standard Error.

Quantile	Rao & Hamed (2000)	RMC-BestFit	% Difference
$F^{-1}(0.99)$	5,142	5,136	0.12%

Generalized Pareto

The Generalized Pareto distribution was verified using the White River Flows at Mt. Carmel, Indiana dataset provided in *Flood Frequency Analysis* (Rao & Hamed, 2000) and shown in Table 50. Verification results are provided in Table 51 through Table 54.

Table 50 – White River Flows at Mt. Carmel, Indiana dataset (Threshold = 50,000 cfs) (Rao & Hamed, 2000).

Flow (CFS)	Flow (CFS)	Flow (CFS)	Flow (CFS)	Flow (CFS)	Flow (CFS)
126,000	56,400	105,000	56,400	61,000	50,900
148,000	128,000	93,700	112,000	155,000	63,500
66,000	106,000	277,000	76,400	96,500	63,500
156,000	110,000	85,700	116,000	89,100	152,000
136,000	232,000	77,300	51,400	77,900	51,000
122,000	60,400	122,000	59,800	70,500	285,000
183,000	60,400	106,000	63,900	73,400	114,000
162,000	50,800	93,300	81,900	180,000	197,000
85,200	100,000	79,000	88,200	83,700	106,000
56,800	55,900	130,000	62,300	302,000	132,000
56,600	167,000	126,000	162,000	133,000	83,700
138,000	53,700	57,800	67,200	92,100	67,200
81,000	56,700	64,700	85,500	105,000	110,000
51,800	126,000	162,000	51,000	235,000	202,000
90,700	100,000	71,900	286,000	213,000	127,000
139,000	59,500	63,500	73,800	96,100	90,600
160,000	164,000	81,500	61,300	77,100	126,000
118,000	81,800	51,000	60,800	73,900	73,900
50,600	56,400	84,400	91,300	55,400	86,500
137,000	124,000	108,000	134,000	55,200	181,000
151,000	64,600	185,000	106,000	87,800	141,000
172,000	77,300	55,800	70,800	52,600	79,700
52,600	65,900	94,600	106,000	106,000	97,800
248,000	72,500	82,800	122,000	93,000	57,300
152,000	65,100	146,000	149,000	147,000	77,200
64,500	80,800	66,500	53,700	61,800	133,000
61,500	69,800	57,700	85,300	101,000	82,900
143,000	53,000	78,700	144,000	154,000	55,000
108,000	195,000	85,100	54,800	52,000	62,000
53,000	128,000	129,000	116,000	121,000	51,700
134,000	114,000	75,700	67,500	86,700	54,500
115,000	110,000	104,000	56,500	57,300	51,600
84,100	149,000	139,000	86,700	97,500	103,000
105,000	74,100	50,600	91,500	112,000	134,000
85,400	75,900	53,500	105,000	88,500	71,700
76,900	99,300	178,000	134,000	76,200	57,000
99,100	168,000	110,000	97,300	140,000	63,900
73,700	70,800	50,800	84,000	87,400	60,700
122,000	104,000	76,000	141,000	154,000	81,900
62,500	125,000	130,000	52,600	95,100	171,000
54,300	77,300	67,300	124,000	131,000	111,000
58,000	97,300	149,000	196,000	131,000	50,400
144,000	140,000	78,400	84,200	54,900	50,500
55,800	54,900	96,600	54,500	78,800	69,700
127,000	66,000	83,300	74,500	101,000	88,900
55,800	199,000	68,400	104,000	224,000	76,600
107,000	99,800	84,300	57,200	54,800	

Table 51 – Generalized Pareto Distribution MOM Results.

Parameter	Rao & Hamed (2000)	RMC-BestFit	% Difference
Location (ξ)	50,169.23	50,170.13	0.00%
Scale (α)	55,443	55,441	0.00%
Shape (κ)	0.0956	0.0956	0.00%

Table 52 – Generalized Pareto Distribution MLE Results.

Parameter	Rao & Hamed (2000)	RMC-BestFit	% Difference
Location (ξ)	50,400	50,400	0.00%
Scale (α)	55,142.29	55,142.20	0.00%
Shape (κ)	0.0945	0.0945	0.00%

Table 53 – Generalized Pareto Distribution Quantile Results.

Quantile	Rao & Hamed (2000)	RMC-BestFit	% Difference
$F^{-1}(0.99)$	256,803	256,803	0.00%

Table 54 – Generalized Pareto Distribution Quantile Standard Error.

Quantile	Rao & Hamed (2000)	RMC-BestFit	% Difference
$F^{-1}(0.99)$	15,938	15,938	0.00%

The Logistic Distributions

The Logistic and Generalized Logistic distribution methods were verified using the examples provided in (Rao & Hamed, 2000).

Logistic

The Logistic distribution was verified using the Tippecanoe River near Delphi, Indiana dataset provided in *Flood Frequency Analysis* (Rao & Hamed, 2000) and shown in Table 3 under the Normal distribution section. The verification results are shown in Table 55 through Table 59.

Table 55 – Logistic Distribution MOM Results.

Parameter	Rao & Hamed (2000)	RMC-BestFit	% Difference
Location (ξ)	12,665	12,665	0.00%
Scale (α)	2,596.62	2,596.62	0.00%

Table 56 – Logistic Distribution MLE Results.

Parameter	Rao & Hamed (2000)	RMC-BestFit	% Difference
Location (ξ)	12,628	12,629	0.01%
Scale (α)	2,708.64	2,708.65	0.00%

Table 57 – Logistic Distribution MLE Results Compared to R-Stan.

Parameter	R-Stan	RMC-BestFit	% Difference
Location (ξ)	12,628.581	12,628.589	0.00%
Scale (α)	2,708.545	2,708.647	0.00%

Table 58 – Logistic Distribution Quantile Results.

Quantile	Rao & Hamed (2000)	RMC-BestFit	% Difference
$F^{-1}(0.99)$	24,597	24,597	0.00%

Table 59 – Logistic Distribution Quantile Standard Error.

Quantile	Rao & Hamed (2000)	RMC-BestFit	% Difference
$F^{-1}(0.99)$	1,684	1,684	0.00%

Generalized Logistic

The Generalized Logistic distribution was verified using the East Fork White River at Seymour near Delphi, Indiana dataset provided in *Flood Frequency Analysis* (Rao & Hamed, 2000) and shown in Table 60. Unfortunately, the book uses summary statistics that are different than what would be generated using the data provided in the table.

Therefore, a 1:1 comparison cannot be made. The differences in summary statistics are sizeable, as shown in Table 61. When using the summary statistics listed in the book, the MOM results are effectively identical, as shown in Table 62. However, when using the actual data set, the results are much different as shown in Table 63. The differences in results derived with RMC-BestFit are consistent with the differences in summary statistics. It can be seen that it is not possible to perform a true verification using this dataset.

Table 60 – East Fork White River at Seymour, Indiana dataset (Rao & Hamed, 2000).

Year	Flow (CFS)	Year	Flow (CFS)	Year	Flow (CFS)
1924	24,000	1947	33,000	1970	26,300
1925	7,920	1948	28,000	1971	27,900
1926	21,900	1949	78,500	1972	27,000
1927	47,100	1950	54,000	1973	22,700
1928	30,400	1951	28,600	1974	17,500
1929	36,100	1952	44,000	1975	46,400
1930	67,100	1953	13,300	1976	19,300
1931	7,030	1954	6,120	1977	12,700
1932	28,200	1955	11,100	1978	36,000
1933	40,100	1956	42,100	1979	39,900
1934	10,300	1957	33,400	1980	25,400
1935	11,100	1958	30,100	1981	30,200
1936	17,000	1959	32,100	1982	47,000
1937	65,600	1960	28,100	1983	39,800
1938	32,600	1961	59,400	1984	23,800
1939	36,200	1962	23,800	1985	29,600
1940	46,400	1963	52,000	1986	33,400
1941	3,650	1964	54,900	1987	15,400
1942	16,800	1965	25,600	1988	28,400
1943	44,800	1966	10,900	1989	26,700
1944	37,100	1967	33,700	1990	46,500
1945	42,900	1968	60,200	1991	61,200
1946	15,000	1969	39,200		

Table 61 – Summary statistics for the East Fork White River at Seymour, Indiana dataset (Rao & Hamed, 2000).

Statistic	Rao & Hamed (2000)	MS Excel	% Difference
Mean	32,714	32,272.35	1.36%
Std. Dev.	16,560.28	16,160.26	2.45%
Skewness	0.49051	0.51975	5.79%

Table 62 – Generalized Logistic Distribution MOM Results Using Book Summary Statistics.

Parameter	Rao & Hamed (2000)	RMC-BestFit	% Difference
Location (ξ)	31,892	31,892	0.00%
Scale (α)	9,030	9,030	0.00%
Shape (κ)	-0.05515	-0.05515	0.00%

Table 63 – Generalized Logistic Distribution MOM Results Using Actual Dataset.

Parameter	Rao & Hamed (2000)	RMC-BestFit	% Difference
Location (ξ)	31,892	31,425.30	1.47%
Scale (α)	9,030	8,800.29	2.58%
Shape (κ)	-0.05515	-0.05829	5.53%

Table 64 – Generalized Logistic Distribution MLE Results Using Actual Dataset.

Parameter	Rao & Hamed (2000)	RMC-BestFit	% Difference
Location (ξ)	30,911.83	30,622.11	0.94%
Scale (α)	9,305.02	9,026.14	3.04%
Shape (κ)	-0.14415	-0.13439	7.01%

The quantile estimate results for the 100-yr return period (or 0.99 non-exceedance probability) were derived using the MOM parameters provided by (Rao & Hamed, 2000) in order to have a 1:1 comparison.

Table 65 – Generalized Logistic Distribution Quantile Results.

Quantile	Rao & Hamed (2000)	RMC-BestFit	% Difference
$F^{-1}(0.99)$	79,117	79,117	0.00%

A simple expression cannot be obtained for the standard error of MLE estimates for the Generalized Logistic distribution. There are approximate numerical solutions available, but those were not implemented in *Numerics*. Table 66 shows the partial derivatives of the inverse CDF with respect for each parameter. These partial derivatives are required for handling quantile priors in the Bayesian estimation within RMC-BestFit.

Table 66 – Generalized Logistic Distribution Partial Derivatives.

Parameter	Rao & Hamed (2000)	RMC-BestFit	% Difference
$\partial F^{-1}(0.99)/\partial \xi$	1	1	0.00%
$\partial F^{-1}(0.99)/\partial \alpha$	6.51695	6.51696	0.00%
$\partial F^{-1}(0.99)/\partial \kappa$	-154,595.08	-154,595.18	0.00%

Goodness-of-Fit Measures

RMC-BestFit provides three goodness-of-fit (GOF) measures: the Akaike Information Criteria (AIC), the Bayesian Information Criteria (BIC), and Root Mean Square Error (RMSE). These measures indicate how well the distribution fits the input data, with a smaller value representing a better fit.

AIC and BIC are used for model selection among a finite set of models. The model with the lowest AIC or BIC is preferred. When comparing multiple distributions, additional parameters often yield larger, optimized log-likelihood values. AIC and BIC penalizes for more complex models, i.e., models with additional parameters. However, for BIC, the penalty is a function of the sample size, and so it is typically more severe than that of AIC. The formulas for AIC and BIC are shown in Equation 10 and Equation 11, respectively. To address potential over-fitting, RMC-BestFit implements a correction for small sample sizes for AIC.

$$AIC = 2k - 2 \ln(\hat{L}) + \frac{2k^2 + 2k}{n - k - 1} \tag{Equation 10}$$

$$BIC = \ln(n) k - 2 \ln(\hat{L}) \tag{Equation 11}$$

where k is the number of parameters; n is the sample size; and \hat{L} is the maximum value of the likelihood function for the model.

The formula for RMSE is provided in Equation 12. RMSE is computed based on the plotting positions of the input data. The user can change the plotting position coefficient, so this measure has a potential to be biased. To minimize this issue, the default plotting position coefficient in the input data interface is set to Weibull ($\alpha = 0$), which is unbiased.

$$RMSE = \sqrt{\frac{\sum_{i=1}^n (\hat{y}_i - y_i)^2}{n}} \tag{Equation 12}$$

where n is the sample size; \hat{y}_i is the predicted value for item i ; and y_i is the observed value for step i .

AIC and BIC were verified using *Palisade's @Risk* for the Weibull distribution fit to the Tippecanoe River near Delphi, Indiana dataset provided in *Flood Frequency Analysis* (Rao & Hamed, 2000) and shown in Table 3 under the Normal distribution section. RMSE is verified by computing the measure manually in MS Excel. Results are provided in Table 67.

Table 67 – Verification of Goodness-of-Fit Measures with *Palisade's @Risk*.

Measure	@Risk/Excel	RMC-BestFit	% Difference
AIC	950.36	950.36	0.00%
BIC	953.83	953.83	0.00%
RSME	553.48	553.48	0.00%

Bayesian Estimation

RMC-BestFit performs Bayesian estimation using a Markov Chain Monte Carlo (MCMC) algorithm to estimate distribution parameters given the specified input data and parent distribution. The Bayesian estimation method produces the most likely estimate for parameters (posterior mode) and a characterization of the parameter uncertainty. Several verification and validation tests were undertaken to ensure the Bayesian MCMC method employed by RMC-BestFit performs as expected. First, RMC-BestFit was verified using known theoretical solutions for the Normal distribution. Then, results from RMC-BestFit were compared with other widely used Bayesian software packages, such as *R-Stan*, *evdbayes*, and *Flike*. Finally, a comparison was made with flood frequency results from the Expected Moments Algorithm (EMA) (Cohn, Lane, & Baier, 1997) provided in the *HEC-SSP* software.

Bayesian Analysis Framework

In Bayesian analysis, the values of the flood frequency distribution parameters $\theta = (\theta_1, \theta_2, \dots, \theta_p)$ converge to a distribution rather than to a single best value. The uncertainty in the parameters is represented by a *prior* probability distribution $P(\theta)$, which is established based on information available *a priori*. This prior distribution is not derived from the observed flow data $D = (X_1, \dots, X_n)$, but instead comes from other sources that can be either subjective (e.g., expert opinion) or objective (e.g., previous statistical analyses or theory). After the prior distributions and the observed data are specified, Bayes' theorem (Equation 13) is used to combine the *a priori* information about the parameters with the observed data, using the likelihood $P(D|\theta)$ (Equation 14).

$$P(\theta|D) = \frac{P(D|\theta) \cdot P(\theta)}{\int P(D|\theta) \cdot P(\theta) \cdot d\theta} \quad \text{Equation 13}$$

$$P(D|\theta) = \prod_{i=1}^n f(X_i|\theta) \quad \text{Equation 14}$$

where $P(\theta|D)$ is the posterior probability density function (PDF) of θ ; $P(\theta)$ is the prior pdf of θ ; and $P(D|\theta)$ is the likelihood function. The posterior cumulative distribution function (CDF) of X now follows from the total probability theorem:

$$F(X) = \int F(X|\theta, D) \cdot P(\theta|D) \cdot d\theta \quad \text{Equation 15}$$

which is a probability-weighted sum of the CDFs under different posterior parameter sets $\theta_1, \theta_2, \dots, \theta_n$. Equation 15 is known as the Bayesian posterior predictive distribution, and is equivalent to the *expected probability of exceedance* concept first presented by (Beard, 1960). Stedinger (1983) and Kuczera (1999) refer to this integral as the design flood distribution, and it is considered the optimal estimator of an exceedance probability.

In most cases, there is not a closed form solution to the denominator of Equation 13. Therefore, Monte Carlo simulation techniques such as MCMC are required. The RMC-BestFit software employs an adaptive Differential Evolution Markov Chain (DE-MC_z) population-based sampler (ter Braak & Vrugt, 2008), which has proven to be very efficient. Several other MCMC algorithms have also been successfully used in flood frequency analysis [(Kuczera G., 1999); (Reis & Stedinger, 2005); (Viglione, Merz, Salinas, & Bloschl, 2013)].

Figure 16 illustrates the basic steps in Bayesian analysis. The Bayesian approach offers a framework that is well-suited to incorporate different sources of information, such as systematic flood records, historical floods, regional information, and other hydrologic information along with related uncertainties (Viglione, Merz, Salinas, & Bloschl, 2013). The Bayesian approach allows hydrologists to formally include their own expertise into the analysis by choosing a *prior* distributions. The possibility to combine this information with the observed data is even more important because, in hydrology, the samples are usually of limited size. Consequently, the Bayesian approach is more flexible and versatile than classical approaches.

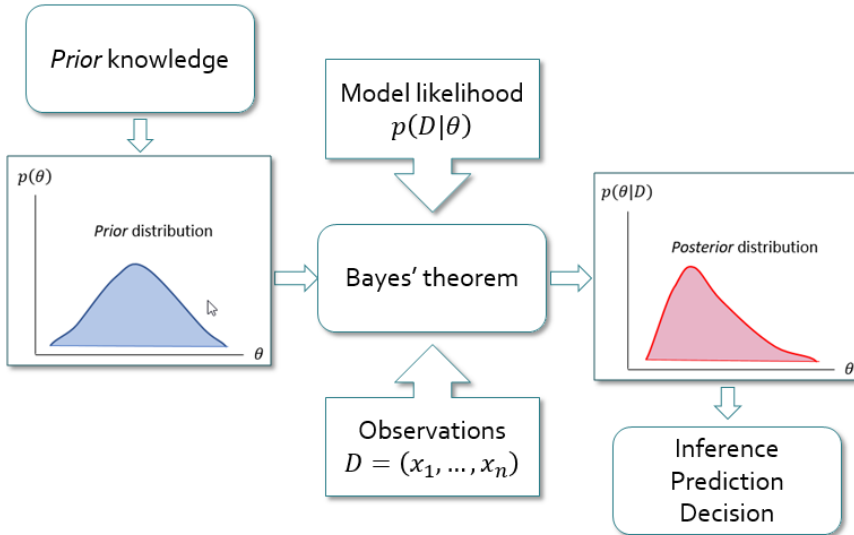


Figure 16 – Diagram Illustrating the Basic Steps in Bayesian Analysis (adapted from (Meylan, 2012), which was originally taken (Perreault, 2000)).

Theoretical Verification

The Normal distribution is fundamental to most statistical modeling with well-known theoretical properties (Gelman, et al., 2014). The Normal distribution has two parameters: mean (location) and standard deviation (scale). From an objective Bayesian perspective, when the distribution for both mean and standard deviation are unknown, the resulting posterior distribution of the population mean and standard deviation is given by the following equations:

$$F(\mu) = \Phi\left(\bar{x}, \frac{s}{\sqrt{n}}\right) \quad \text{Equation 16}$$

$$F(\sigma) = \sqrt{\frac{(n-1) \cdot s^2}{\chi^2_{(n-1)}}} \quad \text{Equation 17}$$

where μ and σ are the population mean and standard deviation, respectively; \bar{x} and s are the sample mean and standard deviation, respectively; n is the sample size; Φ is the Normal distribution; and χ^2 is the Chi-squared distribution with $n - 1$ degrees of freedom. The posterior predictive distribution is then given by:

$$F(X) = t_{n-1}\left(\frac{X - \bar{x}}{s \cdot \sqrt{1 + \frac{1}{n}}}\right) \quad \text{Equation 18}$$

where \bar{x} and s are the sample mean and standard deviation, respectively; n is the sample size; and t_{n-1} is the Student's t distribution with $n - 1$ degrees of freedom. This equation is equivalent to the *expected probability of exceedance* concept presented in (Beard, 1960) and (U.S. Geological Survey, 1982). The confidence intervals for a quantile are derived using a Noncentral-t distribution as shown in (Stedinger J. R., 1982). The $100(1 - 2\alpha)\%$ confidence interval for the quantile X_p is:

$$[\bar{x} + s \cdot \zeta_\alpha(p), \bar{x} + s \cdot \zeta_{1-\alpha}(p)] \quad \text{Equation 19}$$

where \bar{x} and s are the sample mean and standard deviation, respectively; ζ is the Noncentral-t distribution with $n - 1$ degrees of freedom and noncentrality $\Phi^{-1}(p) \cdot \sqrt{n}$, where Φ^{-1} is the standard Normal variate of the desired probability, p , of exceedance.

Verification tests were performed using synthetic datasets for different sample sizes: $n = 30, 100, \text{ and } 500$. The Log-Normal (base 10) distribution was used for the verification testing because it is has traditionally been used for demonstration purposes in flood frequency analysis [(U.S. Geological Survey, 1982), (Stedinger J. R., 1982), (Stedinger J. R., 1983), (Stedinger & Cohn, 1986), and (Reis & Stedinger, 2005)].

Default Flat Priors

RMC-BestFit automatically develops default flat (uniform) priors for the selected distribution, given the input data. The goal of this routine is to develop prior distributions that have minimal impact on the posterior distributions. This approach is sometimes referred to as vague priors, or weakly informative priors. Weakly informative priors contain information to keep the posterior within reasonable bounds without fully capturing one's scientific knowledge about the underlying parameter (Gelman, et al., 2014). There are two approaches to developing a weakly informative prior as described by Gelman et al (2014):

1. Start with some version of an uninformative prior distribution and then add enough information so that inferences are constrained to be reasonable.
2. Start with a strong, highly informative prior and broaden it to account for uncertainty in one's prior beliefs and in the applicability of any historically based prior distributions to new data.

RMC-BestFit develops default flat priors by first considering the parent distribution and parameter support, and then peeking at the data to determine broad upper and lower constraints for the parameters. This ensures the prior distributions for parameters are somewhat centered near the likelihood, but with a much larger spread. The typical end-user of RMC-BestFit will likely not have much advanced training in Bayesian statistics. Therefore, the routine for default flat priors ensures the user will get reasonable results "out of the box." The default flat priors used in RMC-BestFit are verified through comparison with other Bayesian software (see the Comparison with R-Stan and Comparison with Evdbayes sections).

Ever since Laplace advocated the principles of insufficient reason in the late eighteenth century, a flat, or uniform, distribution has been the obvious choice for an uninformative prior distribution (Efron & Hastie, 2016). However, uniform priors are not transformation invariant. This means that the uniform priors can lead to bias, especially with scale parameters. Figure 17 through Figure 19 show the RMC-BestFit results with default flat priors compared to the theoretical distributions. The posterior marginal distributions for mean agree well. However, the RMC-BestFit results for the posterior marginal for standard deviation are biased and slightly shifted to the right of the theoretical distribution. This leads to a slight shift in the credible intervals and posterior predictive distribution as seen in Figure 19.

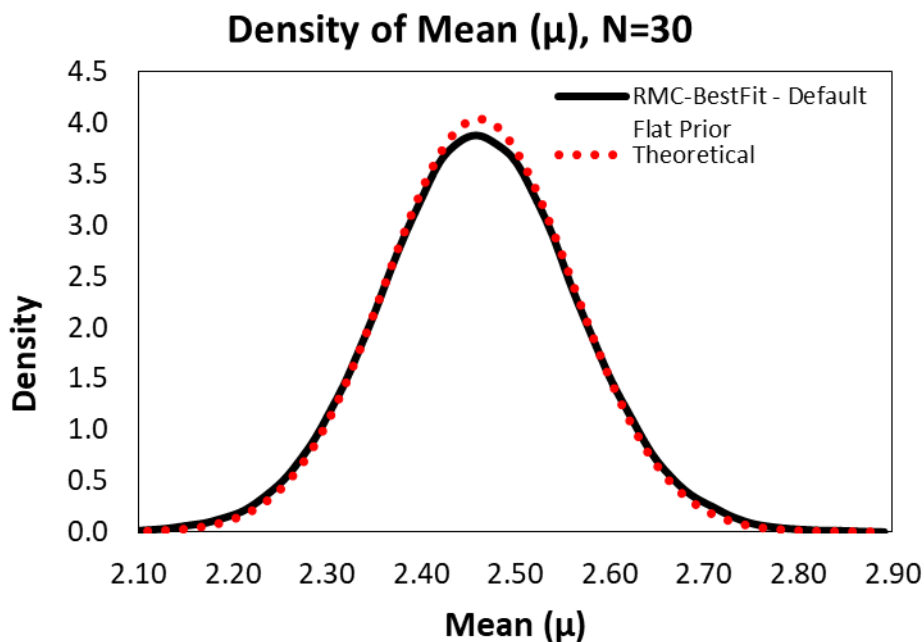


Figure 17 – Comparison of RMC-BestFit with Default Flat Priors with the Theoretical Distribution for Mean ($N = 30$).

Density of Standard Deviation (σ), N=30

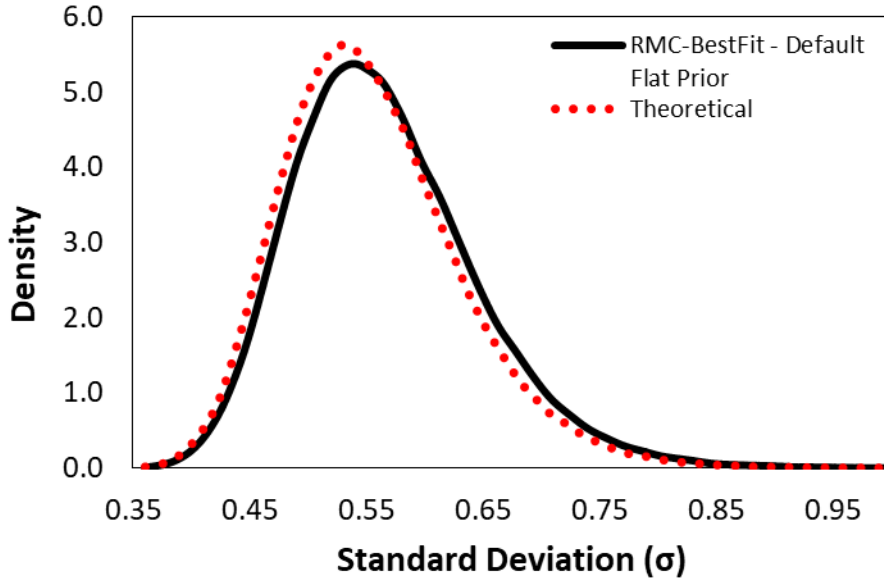


Figure 18 – Comparison of RMC-BestFit with Default Flat Priors with the Theoretical Distribution for Standard Deviation (N = 30).

Log-Normal Distribution, with Default Flat Priors, N = 30

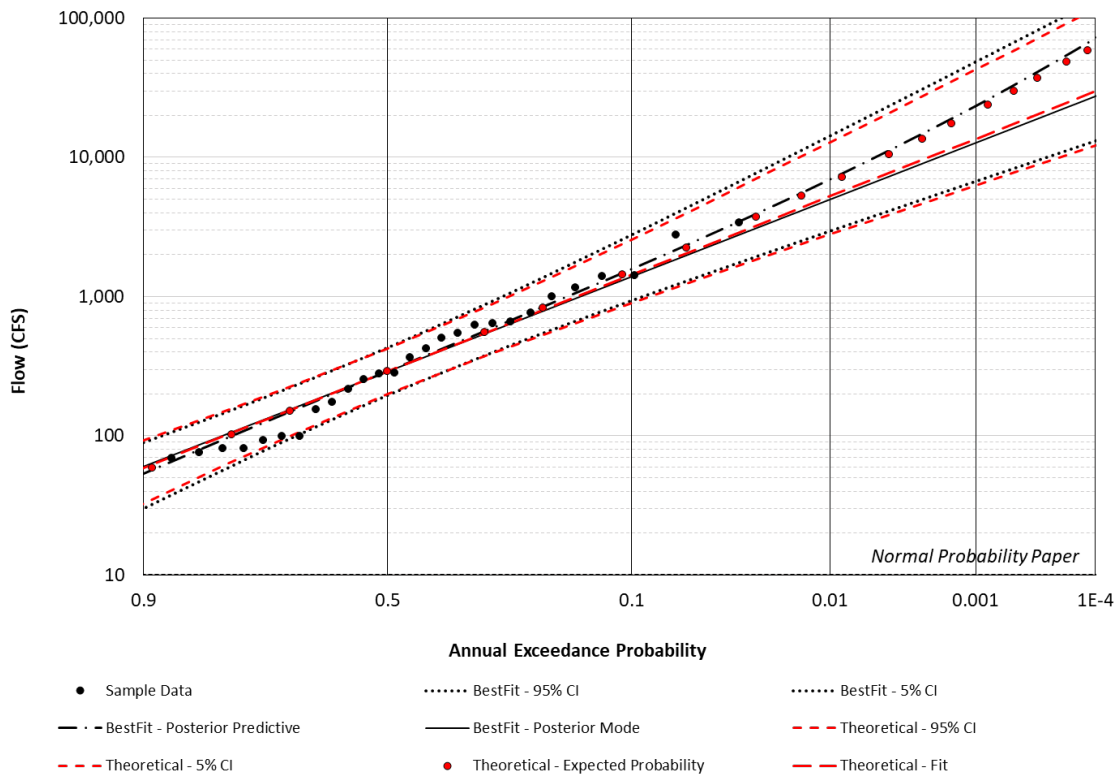


Figure 19 – Comparison of RMC-BestFit Frequency Curve with Default Flat Priors with the Theoretical Distribution (N = 30).

As the sample size increases, the influence of the prior distribution on posterior inferences decreases. In addition, the posterior marginal and joint distributions approach asymptotic Normality as the sample size approaches infinity. Figure 20 through Figure 25 illustrate this point. Using the default flat priors with RMC-BestFit with a sample size of 100 results in very close agreement with the theoretical distributions. When the sample size is 500, there is near perfect agreement with the theoretical distributions. However, it is important to note that in practice a sample size of 500 is rarely possible for flood frequency analysis.

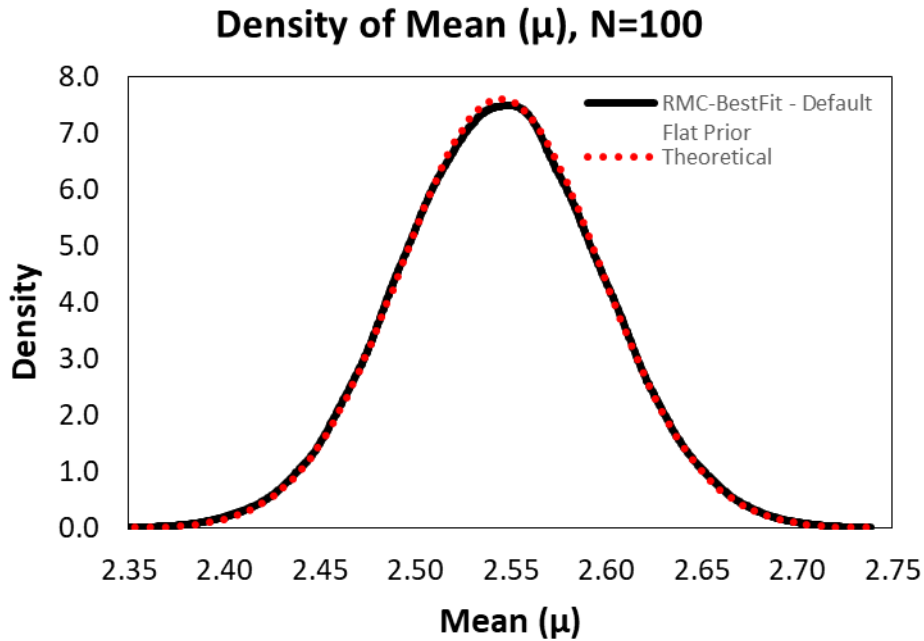


Figure 20 – Comparison of RMC-BestFit with Default Flat Priors with the Theoretical Distribution for Mean (N = 100).

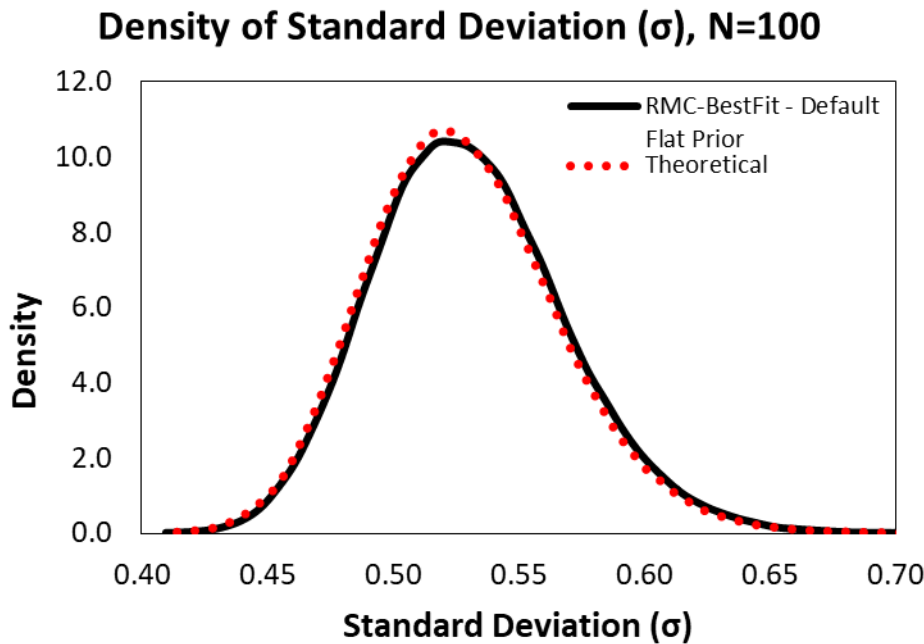


Figure 21 – Comparison of RMC-BestFit with Default Flat Priors with the Theoretical Distribution for Standard Deviation (N = 100).

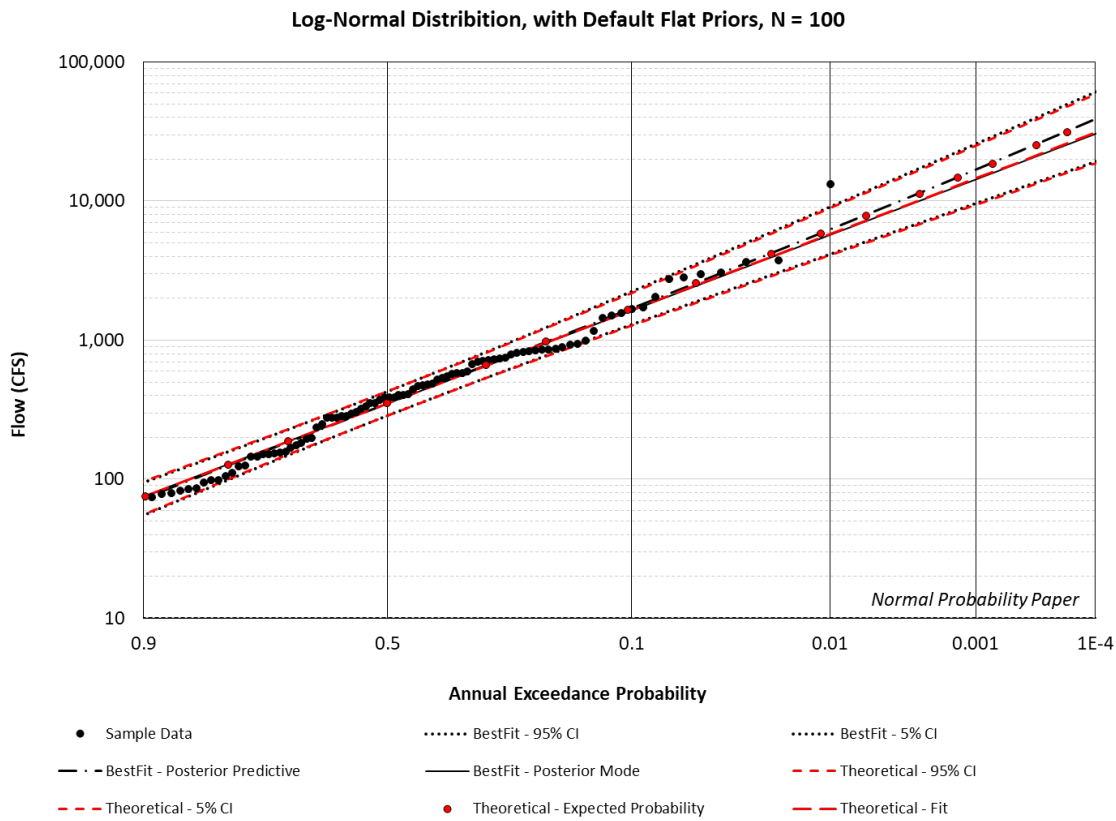


Figure 22 – Comparison of RMC-BestFit Frequency Curve with Default Flat Priors with the Theoretical Distribution (N = 100).

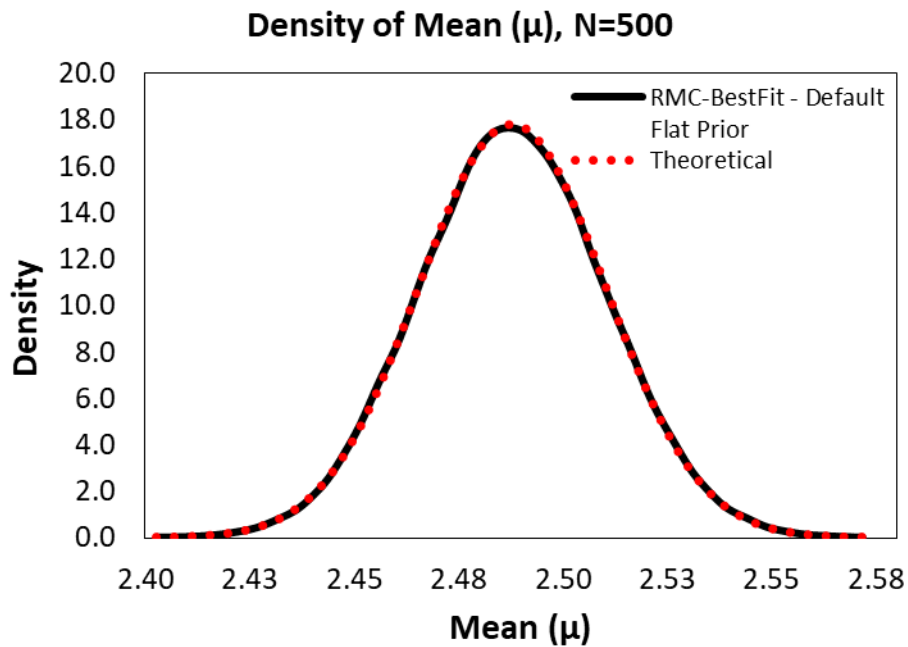


Figure 23 – Comparison of RMC-BestFit with Default Flat Priors with the Theoretical Distribution for Mean (N = 500).

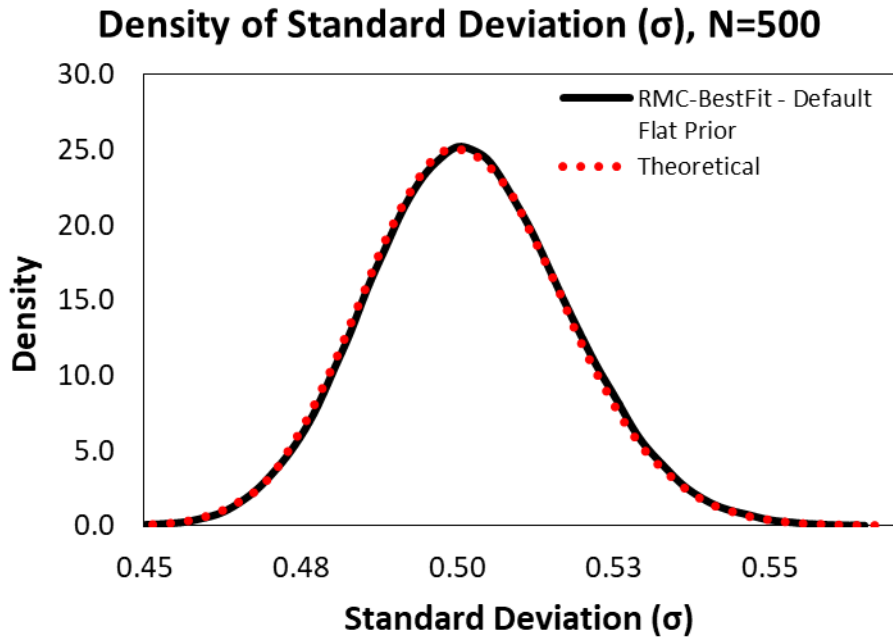


Figure 24 – Comparison of RMC-BestFit with Default Flat Priors with the Theoretical Distribution for Standard Deviation ($N = 500$).

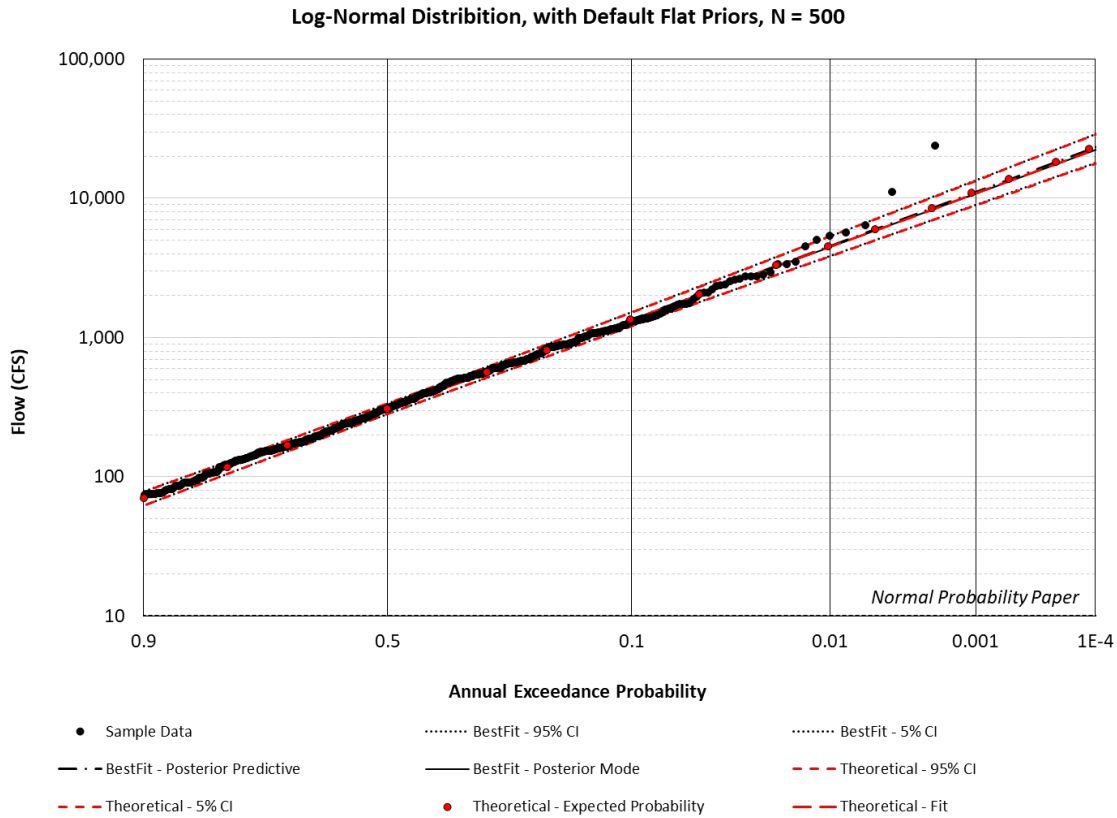


Figure 25 – Comparison of RMC-BestFit Frequency Curve with Default Flat Priors with the Theoretical Distribution ($N = 500$).

Jeffreys' Prior

As previously stated, uniform priors are not transformation invariant. As a consequence, a more sophisticated version of Laplace's principle was put forward by Jeffreys beginning in the 1930s. Jeffreys' prior does in fact transform correctly under parameter changes. Jeffreys' prior is considered an objective, or uninformative prior. The term "uninformative prior" is often interpreted to mean "gives Bayesian posterior intervals that closely match frequentist confidence intervals." With this in mind, "uninformative" has a positive connotation, implying that the use of such a prior does not bias the resulting inference (Efron & Hastie, 2016). For location-scale models, Jeffreys' prior for the location parameter is still a uniform distribution. However, for the scale parameter, σ , the prior is simply:

$$f(\sigma) = \frac{1}{\sigma} \quad \text{Equation 20}$$

For demonstration purposes, Jeffreys' prior was implemented programmatically in *RMC.BestFit.dll*. Figure 26 through Figure 28 show that using Jeffreys' prior results in near perfect agreement with the theoretical distributions. The results from RMC-BestFit when using the default flat priors versus Jeffreys' prior are consistent with other examples in literature (Efron & Hastie, 2016).

RMC-BestFit does not formally support the use of Jeffreys' prior. In most applied contexts, there is no clear advantage to a truly uninformative prior like Jeffreys' when sufficiently vague or weak priors will suffice. The bias shown in Figure 19 would certainly not affect the statistical inference or change decisions in practice. The next section demonstrates that the same unbiased results from Jeffreys' prior can be achieved using other weakly informative priors.

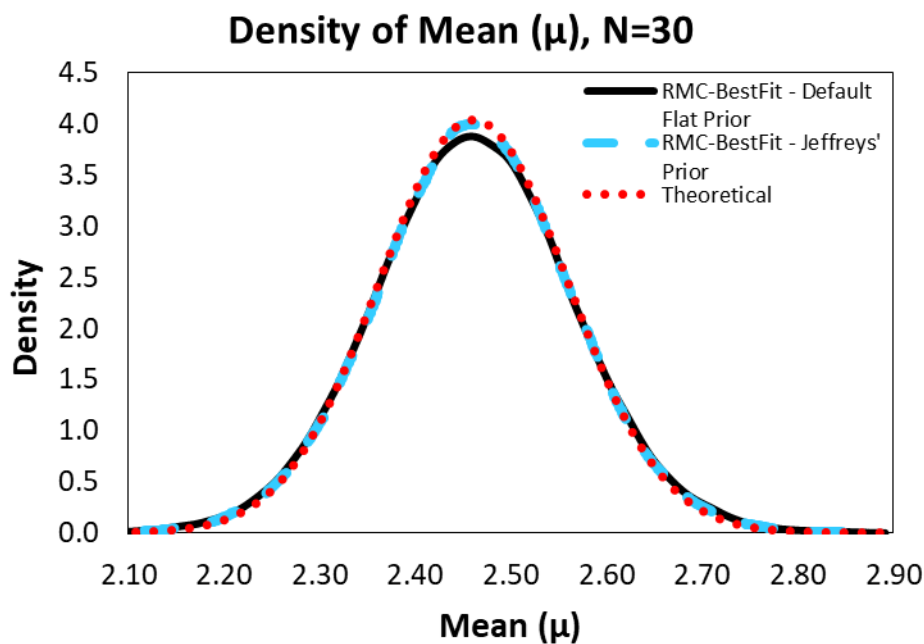


Figure 26 – Comparison of RMC-BestFit with Jeffreys' Prior with the Theoretical Distribution for Mean ($N = 30$).

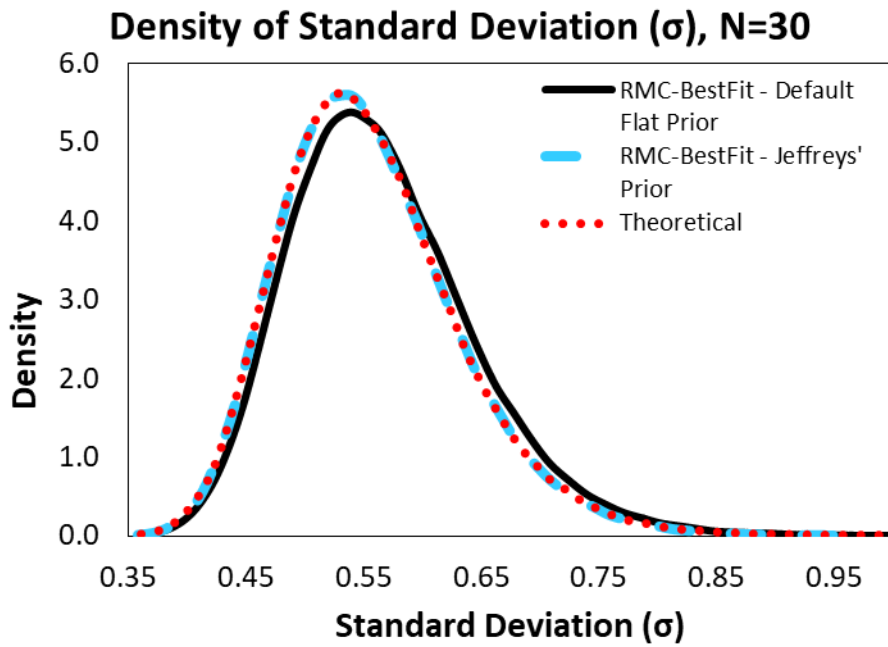


Figure 27 – Comparison of RMC-BestFit with Jeffreys' Prior with the Theoretical Distribution for Standard Deviation (N = 30).

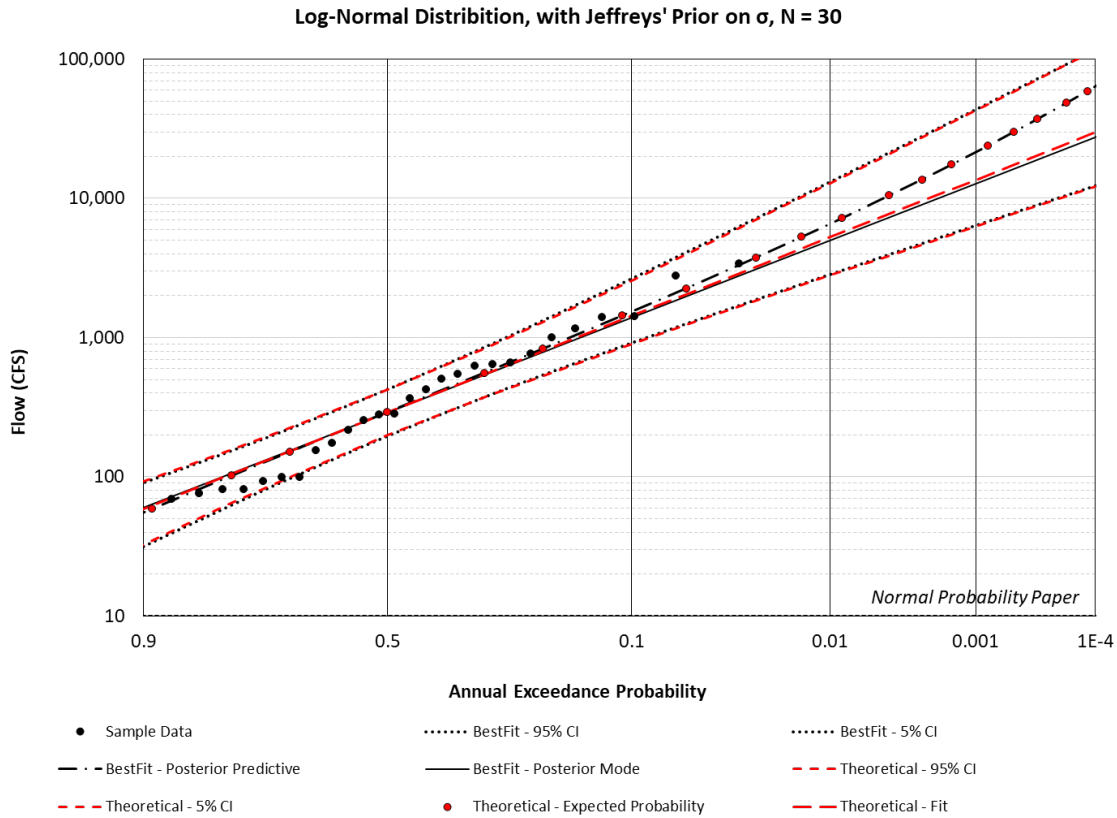


Figure 28 – Comparison of RMC-BestFit Frequency Curve with Jeffreys' Prior with the Theoretical Distribution (N = 30).

Other Weakly Informative Priors

RMC-BestFit allows the user to select prior distributions from several options:

- Exponential
- Gamma
- Generalized Beta
- Ln-Normal
- Noncentral-t
- Normal
- PERT
- Student-t
- Triangular
- Truncated Normal
- Uniform

There are other priors for the scale parameter that will produce the same unbiased posterior distributions as Jeffreys' prior. For example, an Exponential distribution can be used for the prior for standard deviation, with the rate parameter for the Exponential distribution equal to the sample standard deviation of the data, as shown in Figure 29 through Figure 31. In addition, the Ln-Normal distribution can be used as shown in Figure 32 and Figure 33, so long as the variance is large enough to not overly influence the posterior.

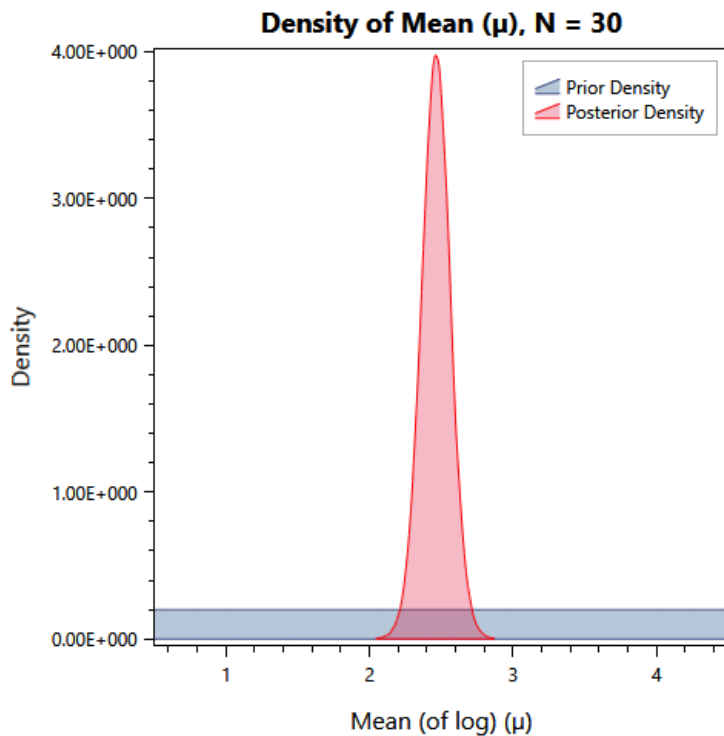


Figure 29 – Default Flat Prior and Posterior for the Mean Parameter in RMC-BestFit.

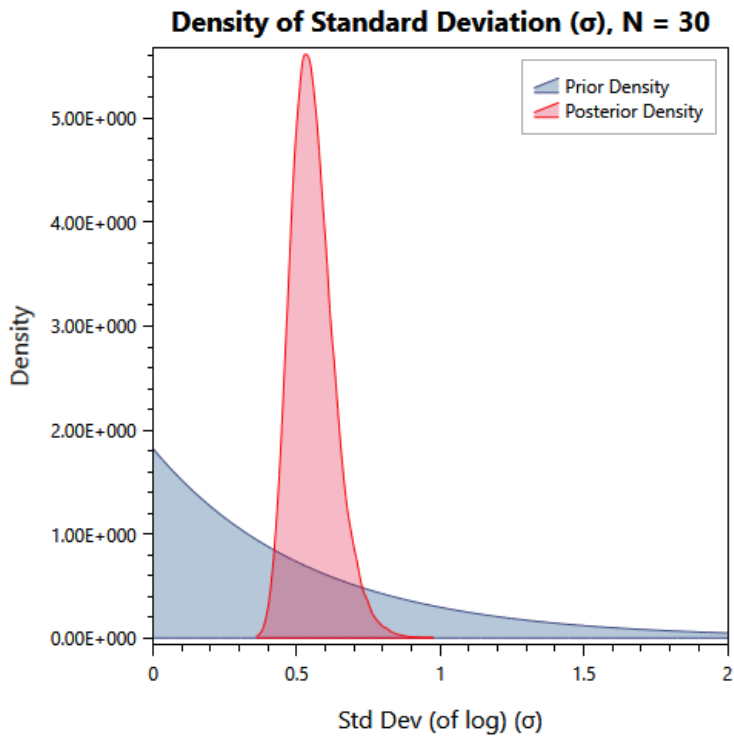


Figure 30 – Exponential Prior and Posterior Distributions for the Standard Deviation Parameter in RMC-BestFit.

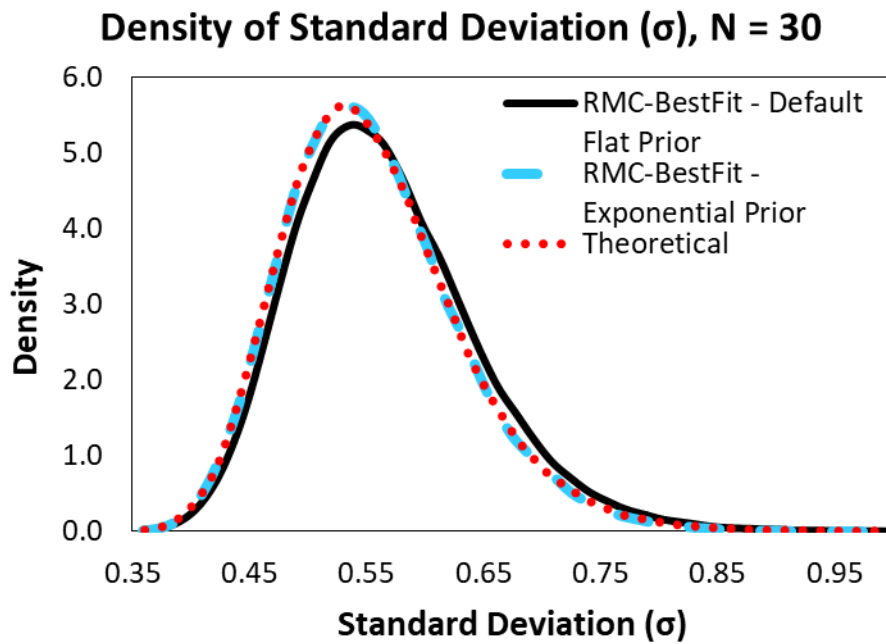


Figure 31 – Comparison of RMC-BestFit with an Exponential Prior with the Theoretical Distribution for Standard Deviation ($N = 30$).

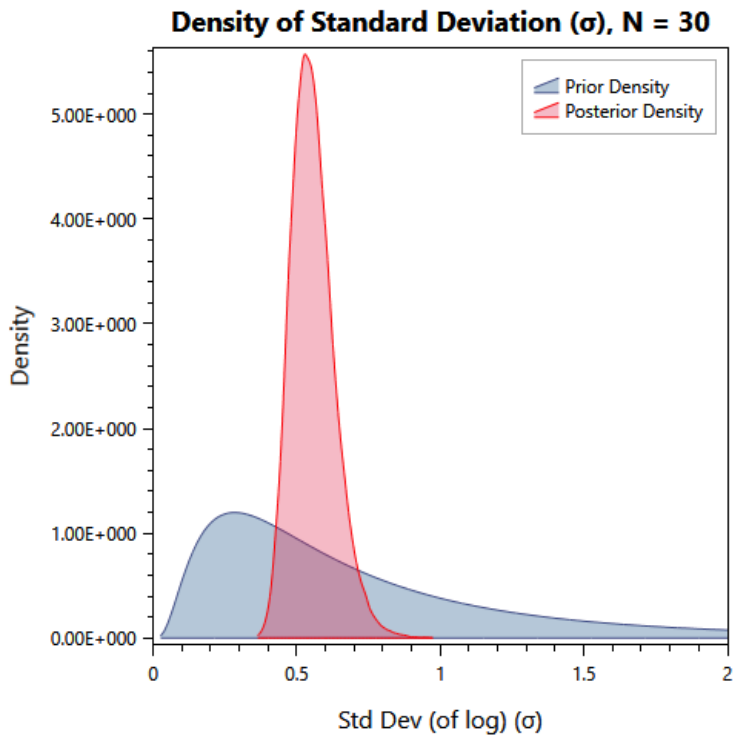


Figure 32 – Ln-Normal Prior and Posterior Distributions for the Standard Deviation Parameter in RMC-BestFit.

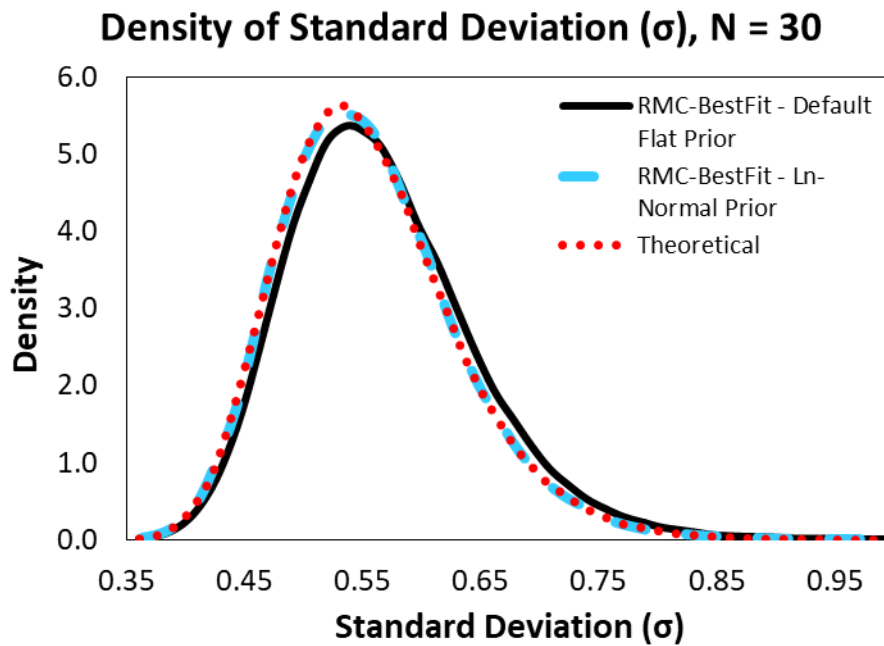


Figure 33 – Comparison of RMC-BestFit with a Ln-Normal Prior with the Theoretical Distribution for Standard Deviation (N = 30).

Conjugate Priors

If the posterior distributions of the parent distribution parameters are in the same probability distribution family as the prior distributions, then the priors are called conjugate priors. In practice, conjugate priors have been popular because of the simpler computation of the posterior distributions. The MCMC sampler employed in RMC-BestFit does not require conjugate or conditionally conjugate priors, like that of a Gibbs sampler. Therefore, in a strict sense, conjugate priors are not implemented in RMC-BestFit. However, priors can be selected from the same family as the posterior. For example, the prior for the mean can be set as a Normal distribution centered at the sample mean, with very wide variance so as to not bias the posterior as shown in Figure 34. The prior for the standard deviation can be set as a Gamma distribution as shown in Figure 35 and Figure 36. When setting “uninformative” priors in this manner, it is important to set the variance very wide to not overly constrain the posterior. However, in general, rather than using the Gamma distribution, it is recommended to use the Exponential distribution as an alternative uninformative prior for scale parameters in RMC-BestFit, as previously demonstrated.

Virtually all methods for deriving an uninformative prior are dependent on the model $f(X|\theta)$. Therefore, there is no pure or correct approach that is strictly uninformative. Furthermore, if the data likelihood is truly dominant, then the choice among relatively flat or weakly informative priors will not matter. Nevertheless, it is important to verify that the posterior density is proper and to determine the sensitivity of posterior inferences to the choice of priors.

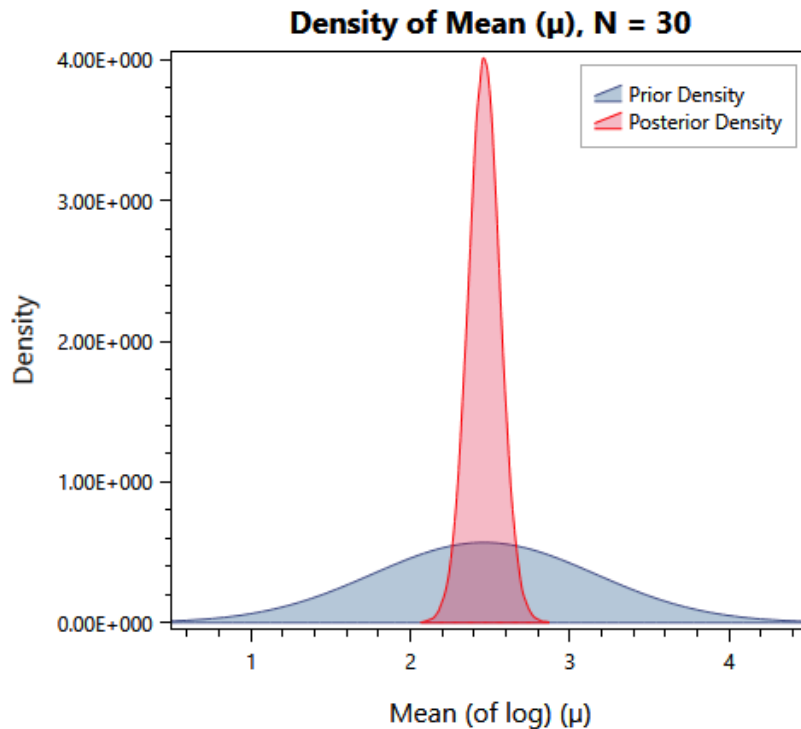


Figure 34 – Normal Prior and Posterior for the Mean Parameter in RMC-BestFit.

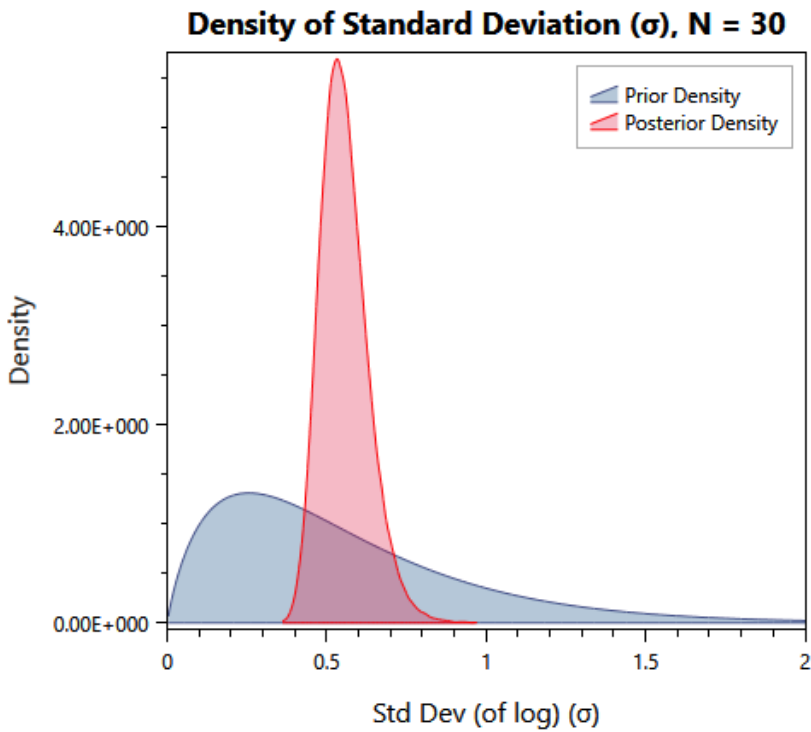


Figure 35 – Gamma Prior and Posterior Distributions for the Standard Deviation Parameter in RMC-BestFit.

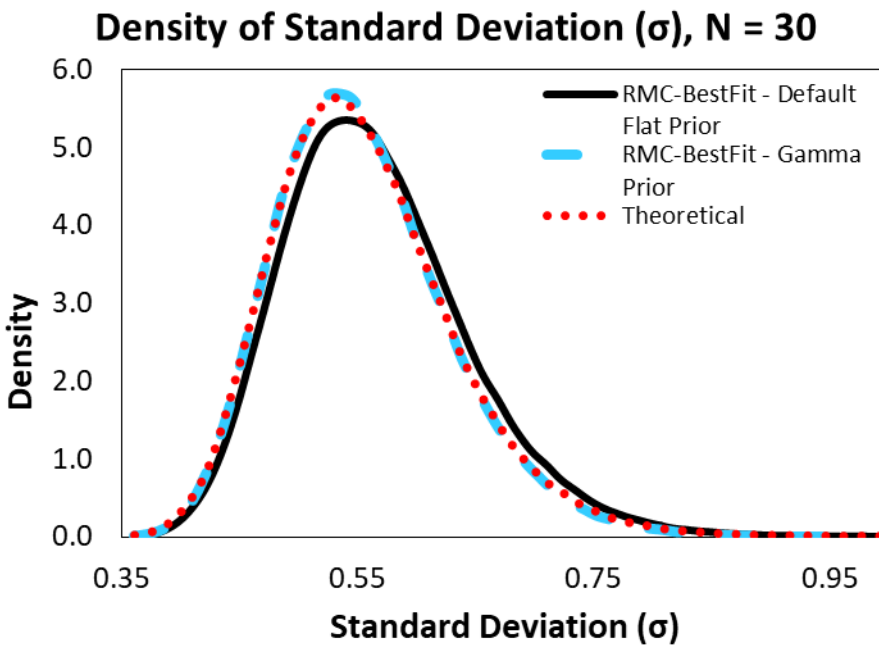


Figure 36 – Comparison of RMC-BestFit with a Gamma Prior with the Theoretical Distribution for Standard Deviation ($N = 30$).

Informative Priors

An informative prior provides specific, scientific information about the parameter. Prior information can be obtained from regional analysis, causal modeling, or expert elicitation. In flood frequency, an example of an informative prior would be the use of a regional skew (Kuczera G. , 1983) for the LPIII distribution as described in Bulletin 17B (U.S. Geological Survey, 1982) and 17C (U.S. Geological Survey, 2018). The “weighted skew” equation provided in Bulletin 17B and 17C is the standard formula for the average of two independent Normal distributions:

$$E(X_{at\ site}, Y_{regional}) = \frac{\mu_X \cdot \sigma_Y^2 + \mu_Y \cdot \sigma_X^2}{\sigma_X^2 + \sigma_Y^2} \quad \text{Equation 21}$$

$$Var(X_{at\ site}, Y_{regional}) = \frac{\sigma_X^2 \cdot \sigma_Y^2}{\sigma_X^2 + \sigma_Y^2} \quad \text{Equation 22}$$

where μ_X and σ_X^2 are the at-site mean and variance for the skew parameter, respectively; and μ_Y and σ_Y^2 are the regional mean and variance of the skew parameter.

The weighted skew equations provide a means for verifying the use of informative priors in RMC-BestFit. Large sample theory postulates that as sample sizes approach infinity, marginal and joint distributions become asymptotically Normally distributed. For a finite sample size n , this Normal approximation is typically more accurate for conditional and marginal distributions of components of the parent distribution than for the full joint distribution. As the sample size increases, the influence of the prior distribution on posterior inferences will decrease because the data likelihood will dominate. Taking this into account, regional prior information is most valuable when the at-site sample sizes are small relative to the effective sample size of the regional information.

A verification was performed using inflows at Blakely Mountain Dam in Arkansas. In 2019, a hydrologic hazard assessment was performed which included a paleoflood analysis. The systematic gage record included 91 years of data. Historical flood data dating back to 1870 was incorporated into the analysis, for a total record length of 149 years. The paleoflood analysis provided data dating back to at least 5,000 years of age. Historical and paleoflood data were incorporated using intervals and perception thresholds, so the effective record lengths were much shorter than the full 5,000 years. The posterior mode for the skew parameter, and the marginal mean and standard deviation of skew, for each dataset are shown in Table 68.

Regional skew information was obtained from a USGS regional study of Arkansas, Oklahoma, and Louisiana (Wagner, Krieger, & Veilleux, 2016). From the USGS study, the regional skew was determined to be -0.17 with a mean-square error (MSE) of 0.12. This information was incorporated into the Bayesian analysis by setting the prior for the skew parameter of LPIII to be Normally distributed with a mean of -0.17 and standard deviation of 0.35, or $\sqrt{0.12}$.

Verification results for each dataset are provided in Table 69 through Table 71 and illustrated in Figure 37 through Figure 39. The results from RMC-BestFit strongly agree with the theoretical approximation. The at-site posterior marginal distributions are not quite Normally distributed and exhibit some skewness. Therefore, the results will not match precisely with the theoretical solution. Nevertheless, the theoretical Normal approximation serves as a useful comparison.

Generally, the stronger the prior (i.e., the more informative), the greater the influence it will have on the posterior. Yet, the asymptotic results formalize the notion that the importance of the prior distribution diminishes as the sample size increases (Gelman, et al., 2014). When the at-site sample sizes are small, the prior distribution is a critical part of the model specification. However, when the at-site sample sizes are very large, the prior distribution has little influence, and the data likelihood dominates the posterior. The results below confirm that the influence of the regional skew diminishes as the at-site data increases.

Further verification of informative priors for parameters are provided in the Comparison with Flike and Comparison with EMA sections. Verification of informative priors on quantiles is provided in the Comparison with Viglione et al. (2013) and Comparison with Evdbayes sections.

Table 68 – Summary Statistics for the At-Site Skew Parameter for Each Dataset at Blakely Mountain Dam.

Skew (of log)	Systematic	Historical	Paleoflood
Joint Posterior Mode	-0.4204	-0.4559	-0.3558
Marginal Mean (μ)	-0.3478	-0.3972	-0.3426
Marginal Std. Deviation (σ)	0.2821	0.2569	0.1749

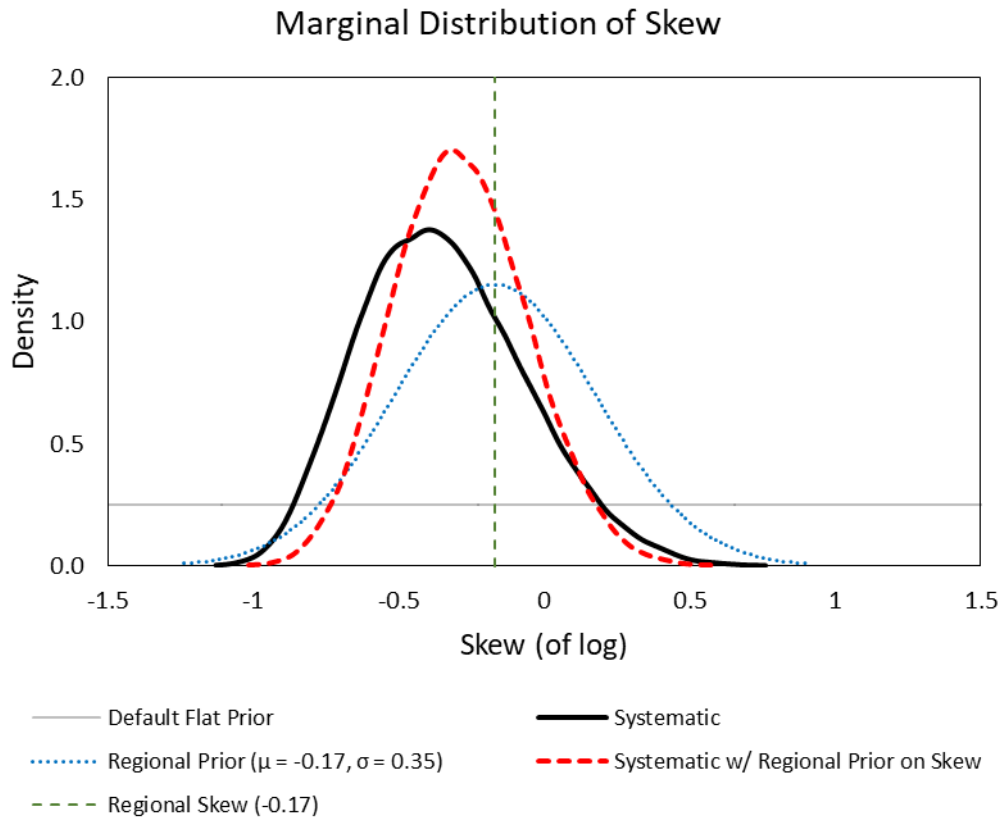


Figure 37 – Marginal Distribution of Skew in RMC-BestFit for Systematic Data Only.

Table 69 – Posterior Skew Statistics in RMC-BestFit Compared to the Theoretical Solution for Systematic Data Only.

Skew (of log)	Theoretical	RMC-BestFit
Joint Posterior Mode	-0.3206	-0.3113
Marginal Mean (μ)	-0.2769	-0.2864
Marginal Std. Deviation (σ)	0.2187	0.2288

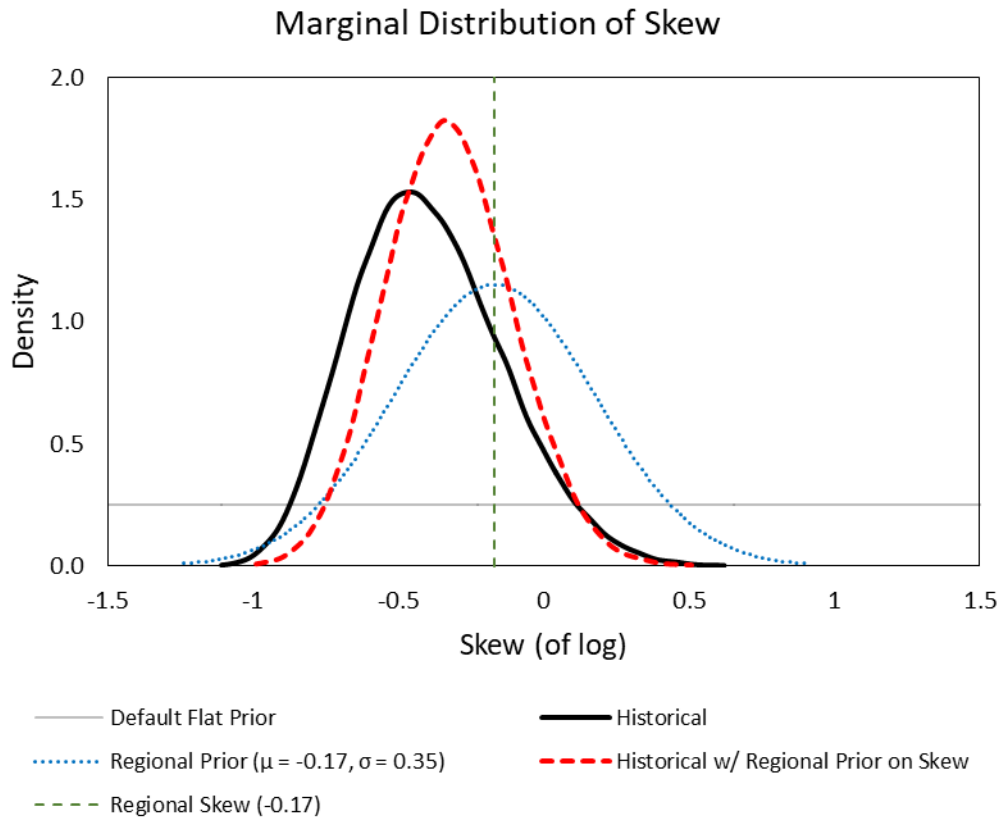


Figure 38 – Marginal Distribution of Skew in RMC-BestFit for Systematic and Historical Data.

Table 70 – Posterior Skew Statistics in RMC-BestFit Compared to the Theoretical Solution for Systematic and Historical Data.

Skew (of log)	Theoretical	RMC-BestFit
Joint Posterior Mode	-0.3545	-0.3507
Marginal Mean (μ)	-0.3166	-0.3240
Marginal Std. Deviation (σ)	0.2063	0.2166

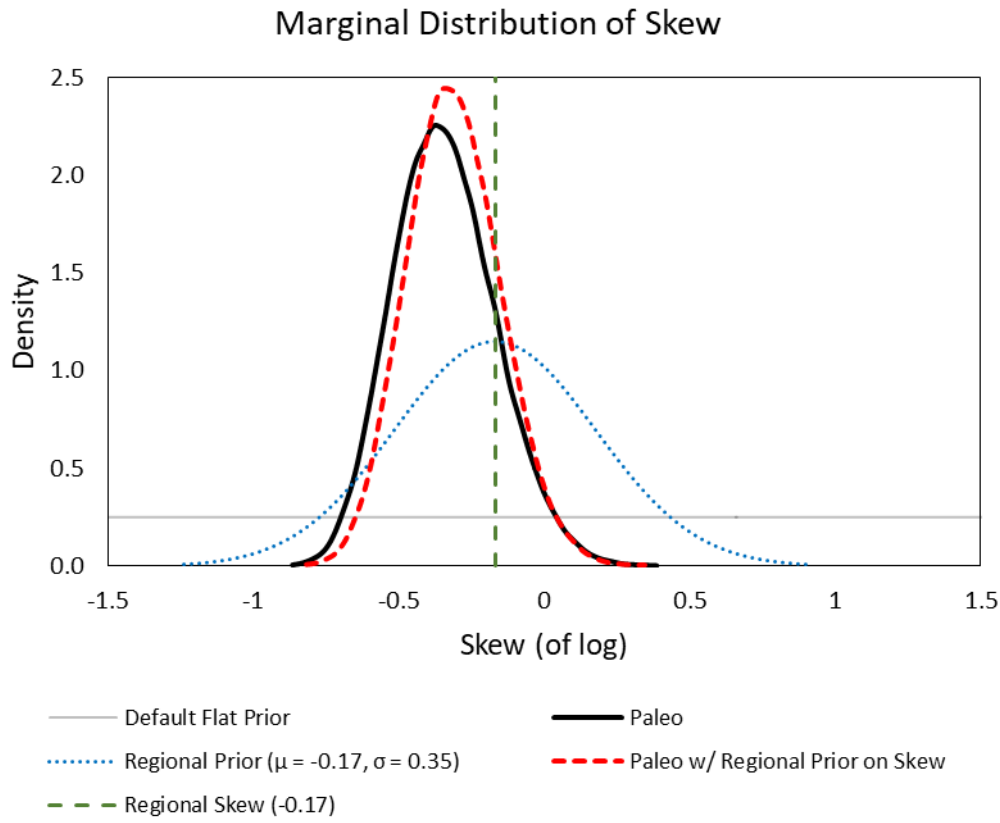


Figure 39 – Marginal Distribution of Skew in RMC-BestFit for Systematic, Historical and Paleoflood Data.

Table 71 – Posterior Skew Statistics in RMC-BestFit Compared to the Theoretical Solution for Systematic, Historical and Paleoflood Data.

Skew (of log)	Theoretical	RMC-BestFit
Joint Posterior Mode	-0.3181	-0.3165
Marginal Mean (μ)	-0.3075	-0.3105
Marginal Std. Deviation (σ)	0.1561	0.1600

Comparison with R-Stan

This section provides additional verification of the MCMC algorithm used in RMC-BestFit and the appropriateness of the default flat priors. Results from RMC-BestFit were compared to results from *R-Stan*, which is a widely used high-level programming language for performing Bayesian statistical inference with MCMC sampling. *R-Stan* employs a state-of-the-art Hamiltonian Monte Carlo sampler capable of working with very complex models (Gelman, et al., 2014). RMC-BestFit utilizes an adaptive Differential Evolution Markov Chain (DE-MC_z) population-based sampler (ter Braak & Vrugt, 2008) for performing MCMC sampling, which is also a very efficient sampler.

Similar to RMC-BestFit, *R-Stan* uses default uniform priors. The key difference is that *R-Stan* defaults to a uniform distribution bounded between negative infinity and positive infinity; whereas, RMC-BestFit develops weakly informative default flat priors that take into consideration the model and parameter support, and are broadly constrained by the data. A verification was performed to ensure the default flat priors in RMC-BestFit produced comparable results with *R-Stan* for the following distributions: Gumbel, Logistic, Normal, and Weibull. Both samplers were configured to be compatible with the following settings:

- 4 chains.
- Thinning rate of 20.
- Warm-up of 3,000 draws.
- 100,000 total posterior draws.

Verification results are provided in the following subsections. Example code for *R-Stan* is provided in Figure 48 so that others will be able to reproduce these results. In each case, RMC-BestFit produces nearly identical results to *R-Stan*, which provides high confidence in the MCMC algorithm and the default priors.

Gumbel

The Gumbel distribution was verified using the Sugar Creek at Crawfordsville, Indiana dataset provided in *Flood Frequency Analysis* (Rao & Hamed, 2000) and shown in Table 36. Summary statistics results for the Gumbel distribution parameters are provided in Table 72 and Table 73. Kernel density plots are provided in Figure 40 and Figure 41.

Table 72 – Parameter Summary Statistics for the Gumbel Distribution from *R-Stan*.

Parameter	Mean	Std. Dev.	2.5%	50%	97.5%
Location (ξ)	8,060.56	677.60	6,742.87	8,056.17	9,409.39
Scale (α)	4,654.65	522.15	3,757.72	4,611.37	5,797.42

Table 73 – Parameter Summary Statistics for the Gumbel Distribution from RMC-BestFit.

Parameter	Mean	Std. Dev.	2.5%	50%	97.5%
Location (ξ)	8,059.04	678.34	6,742.18	8,051.37	9,418.29
Scale (α)	4,656.04	518.77	3,761.00	4,614.79	5,791.56

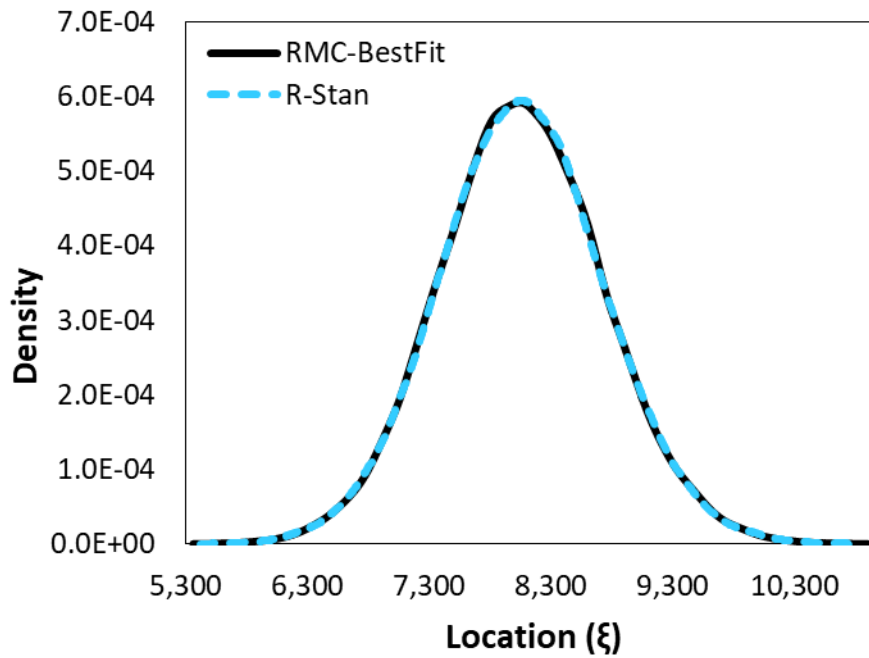


Figure 40 – Comparison of RMC-BestFit with R-Stan for the Gumbel Distribution Location Parameter.

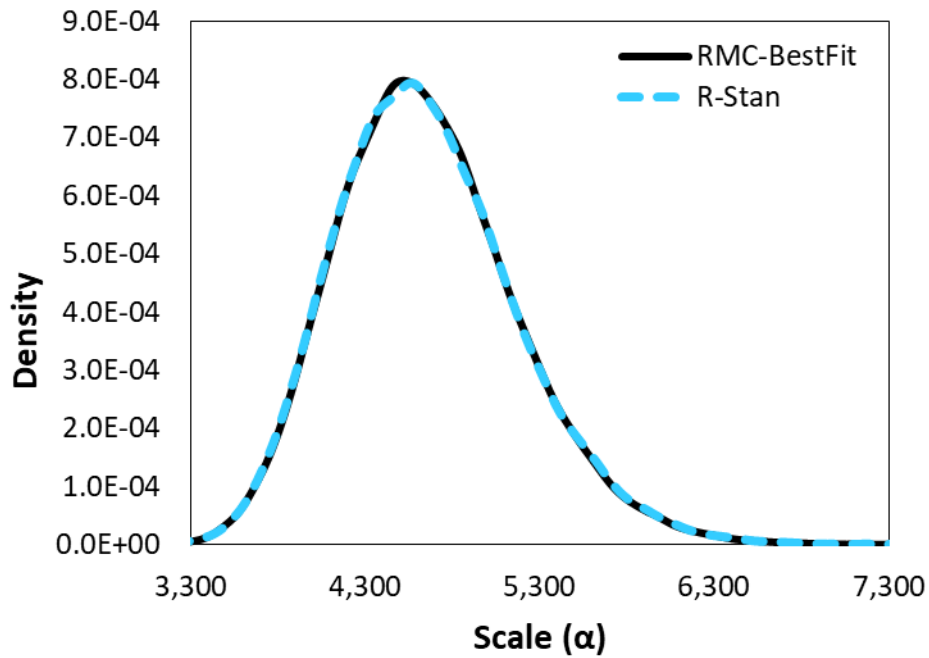


Figure 41 – Comparison of RMC-BestFit with R-Stan for the Gumbel Distribution Scale Parameter.

Logistic

The Logistic distribution was verified using the Tippecanoe River near Delphi, Indiana dataset provided in *Flood Frequency Analysis* (Rao & Hamed, 2000) and shown in Table 3 under the Normal distribution section. Summary statistics results for the Logistic distribution parameters are provided in Table 74 and Table 75. Kernel density plots are provided in Figure 42 and Figure 43.

Table 74 – Parameter Summary Statistics for the Logistic Distribution from R-Stan.

Parameter	Mean	Std. Dev.	2.5%	50%	97.5%
Location (ξ)	12,626.30	713.55	11,225.80	12,629.17	14,028.70
Scale (α)	2,823.36	347.23	2,226.02	2,794.33	3,584.00

Table 75 – Parameter Summary Statistics for the Logistic Distribution from RMC-BestFit.

Parameter	Mean	Std. Dev.	2.5%	50%	97.5%
Location (ξ)	12,630.79	714.36	11,224.60	12,630.88	14,038.12
Scale (α)	2,821.31	349.51	2,222.60	2,792.57	3,591.59

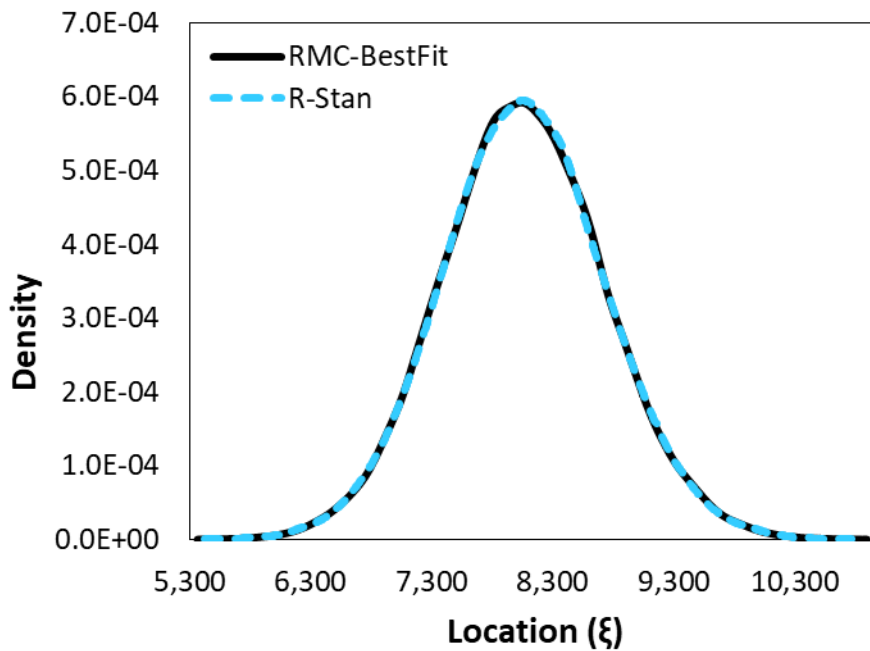


Figure 42 – Comparison of RMC-BestFit with R-Stan for the Logistic Distribution Location Parameter.

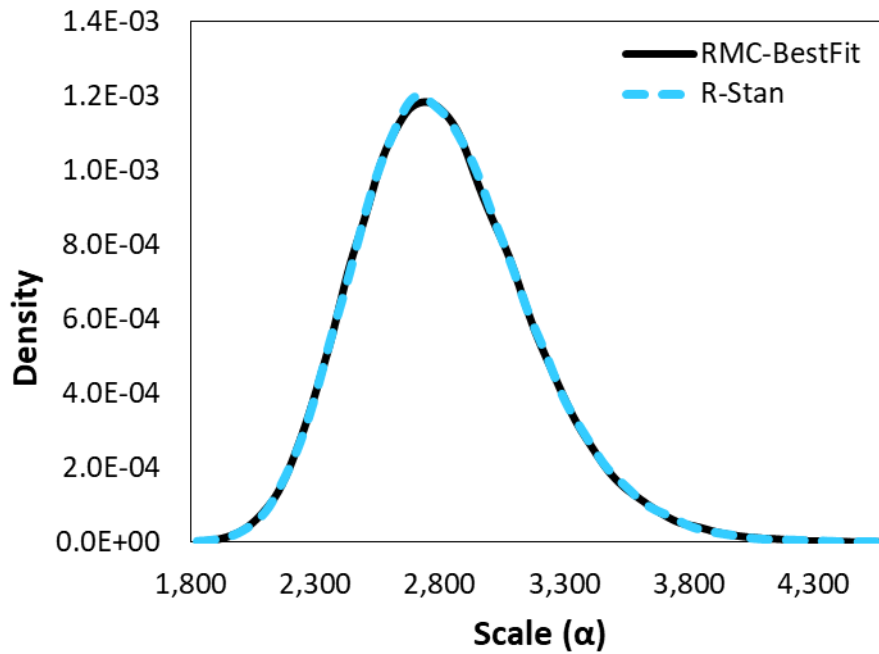


Figure 43 – Comparison of RMC-BestFit with R-Stan for the Logistic Distribution Scale Parameter.

Normal

The Normal distribution was verified using the Tippecanoe River near Delphi, Indiana dataset provided in *Flood Frequency Analysis* (Rao & Hamed, 2000) and shown in Table 3 under the Normal distribution section. Summary statistics results for the Normal distribution parameters are provided in Table 76 and Table 77. Kernel density plots are provided in Figure 44 and Figure 45.

Table 76 – Parameter Summary Statistics for the Normal Distribution from R-Stan.

Parameter	Mean	Std. Dev.	2.5%	50%	97.5%
Mean (μ)	12,662.15	702.90	11,270.56	12,663.38	14,048.01
Std. Deviation (σ)	4,840.77	517.27	3,958.41	4,796.07	5,979.78

Table 77 – Parameter Summary Statistics for the Normal Distribution from RMC-BestFit.

Parameter	Mean	Std. Dev.	2.5%	50%	97.5%
Mean (μ)	12,668.00	701.98	11,288.64	12,669.17	14,059.29
Std. Deviation (σ)	4,840.15	516.12	3,957.46	4,795.30	5,977.51

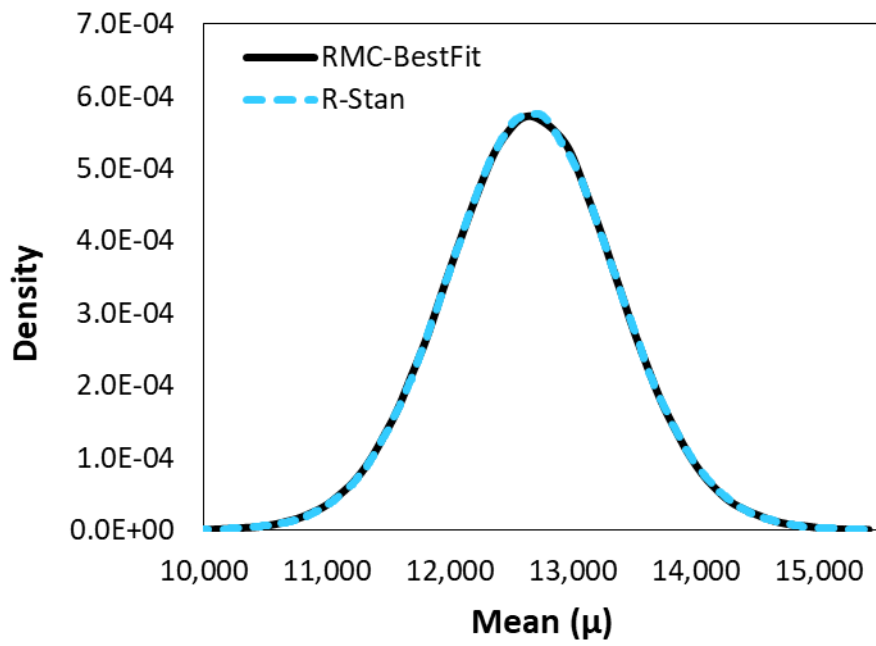


Figure 44 – Comparison of RMC-BestFit with R-Stan for the Normal Distribution Mean Parameter.

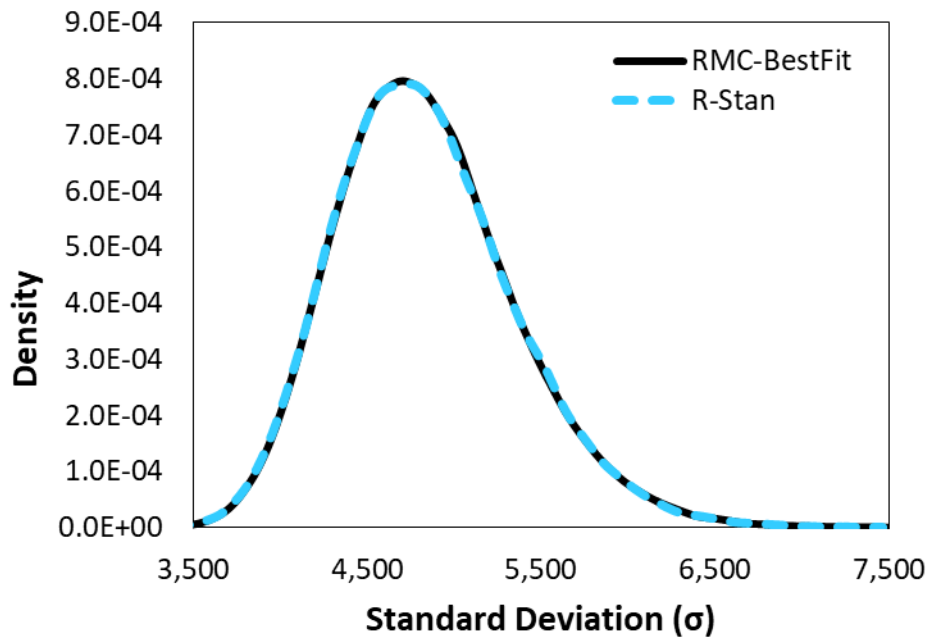


Figure 45 – Comparison of RMC-BestFit with R-Stan for the Normal Distribution Std. Deviation Parameter.

Weibull

The Weibull distribution was verified using the Tippecanoe River near Delphi, Indiana dataset provided in *Flood Frequency Analysis* (Rao & Hamed, 2000) and shown in Table 3 under the Normal distribution section. Summary statistics results for the Weibull distribution parameters are provided in Table 78 and Table 79. Kernel density plots are provided in Figure 46 and Figure 47.

Table 78 – Parameter Summary Statistics for the Weibull Distribution from R-Stan.

Parameter	Mean	Std. Dev.	2.5%	50%	97.5%
Scale (λ)	14,294.43	744.91	12,869.45	14,282.53	15,800.01
Shape (κ)	2.9800	0.3400	2.3400	2.9700	3.6700

Table 79 – Parameter Summary Statistics for the Weibull Distribution from RMC-BestFit.

Parameter	Mean	Std. Dev.	2.5%	50%	97.5%
Scale (λ)	14,293.56	745.62	12,865.77	14,280.83	15,793.87
Shape (κ)	2.9785	0.3390	2.3428	2.9680	3.6744

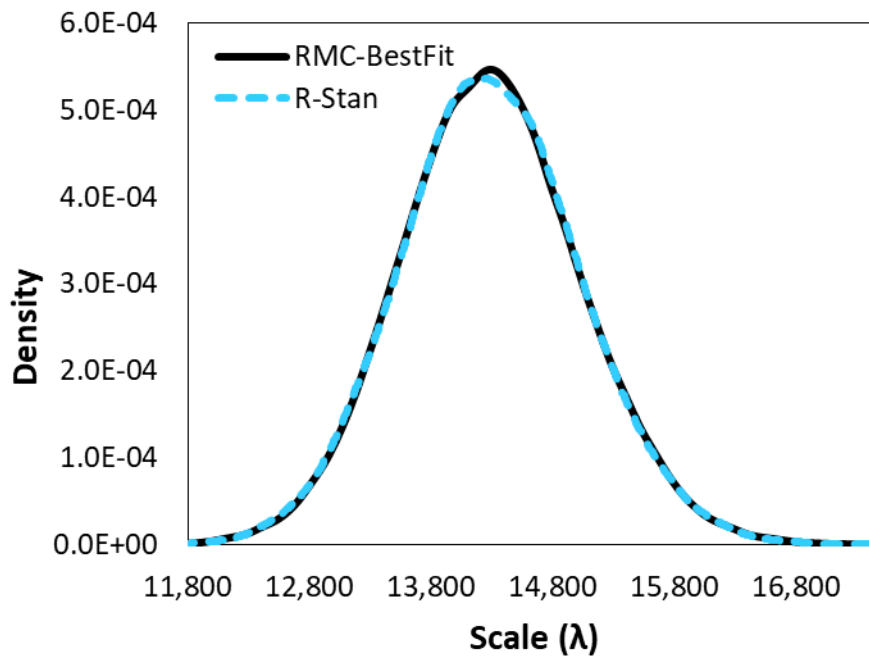


Figure 46 – Comparison of RMC-BestFit with R-Stan for the Weibull Distribution Scale Parameter.

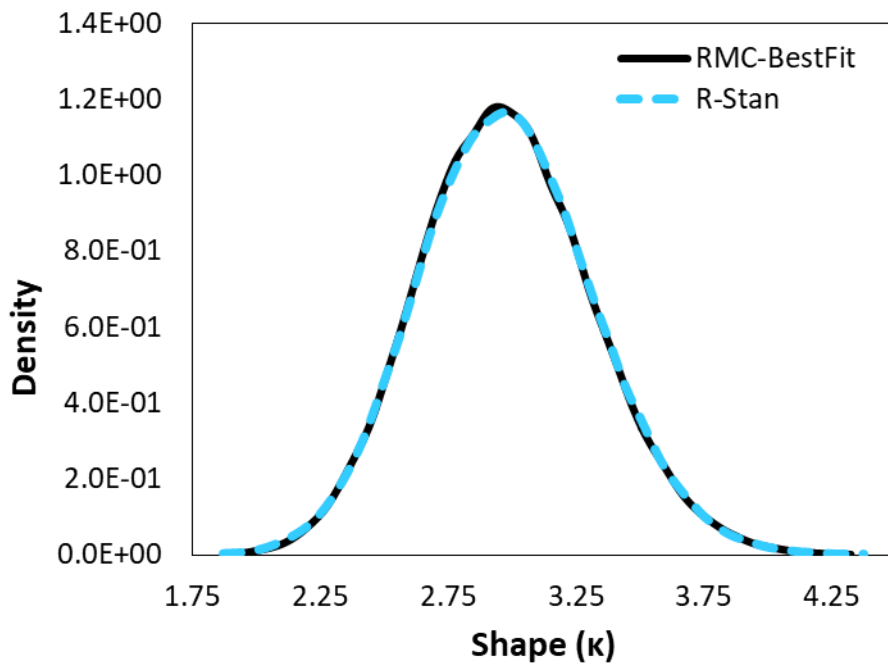


Figure 47 – Comparison of RMC-BestFit with R-Stan for the Weibull Distribution Shape Parameter.

```

library(rstan)

# This is example code for R-Stan with the Normal distribution.
# Stan will automatically compile this block of code to significantly reduce runtimes.
stan_code <- 'data {int N; real x[N];}
              parameters {real mu; real<lower = 0> sigma;}
              model {for(n in 1:N){target += normal_lpdf(x[n] | mu, sigma);}}'
model <- stan_model(model_code=stan_code)

# Reference: "Flood Frequency Analysis", A.R. Rao & K.H. Hamed, CRC Press, 2000.
# Table 5.1.1 Tippecanoe River Near Delphi, Indiana (Station 43) Data.
gageData = c(6290, 2700, 13100, 16900, 14600, 9600, 7740, 8490, 8130, 12000, 17200, 15000,
             12400, 6960, 6500, 5840, 10400, 18800, 21400, 22600, 14200, 11000, 12800, 15700,
             4740, 6950, 11800, 12100, 20600, 14600, 14600, 8900, 10600, 14200, 14100, 14100,
             12500, 7530, 13400, 17600, 13400, 19200, 16900, 15500, 14500, 21900, 10400, 7460)

# Get the mean and standard deviation of the gage data.
m <- mean(gageData)
s <- sd(gageData)
# 12665.21
# 4709.742

# Estimate the posterior mode parameter set using Maximum Likelihood Estimation (MLE).
mle = optimizing(model, data=list(x=gageData, N=length(gageData)),
                 algorithm="LBFSGS", init=list(mu=m, sigma=s))

# Output the MLE results.
print(mle)
#      mu      sigma
# 12665.208 4660.398

# Perform Bayesian estimation using R-Stan.
# Simulation settings are compatible with RMC-BestFit.
options(mc.cores = parallel::detectCores())
fit <- sampling(model, data=list(x=gageData, N=length(gageData)),
               warmup=15000, iter=515000, chains=4, thin=20)

# Output the summary statistics for the Bayesian estimated parameters.
print(fit, probs=c(0.025, 0.5, 0.975))

#      mean se_mean  sd  2.5%  50%  97.5%  n_eff Rhat
# mu  12667.57  2.23 702.61 11290.92 12666.72 14058.52 99450 1
# sigma 4839.08  1.65 518.56 3953.29 4795.90 5980.64 98257 1
# lp__ -466.13  0.00  1.02 -468.86 -465.82 -465.13 100699 1

# Plot Markov Chain trace plots.
stan_trace(fit, inc_warmup = FALSE)

# Plot kernel density estimates for each parameter.
stan_dens(fit, pars = "mu")
stan_dens(fit, pars = "sigma")

# Write parameter sets to text file.
list_of_draws <- extract(fit, pars = "mu")
lapply(list_of_draws, write, "Normal_mu.txt", append=FALSE)
list_of_draws <- extract(fit, pars = "sigma")
lapply(list_of_draws, write, "Normal_sigma.txt", append=FALSE)

```

Figure 48 – Example code for R-Stan for MCMC Sampling with the Normal Distribution.

Comparison with Viglione et al. (2013)

Viglione et al. (2013) and (Skahill, Viglione, & Byrd, 2016) present a Bayesian analysis framework for combining and evaluating the worth of different types of additional data (i.e., temporal, spatial, and causal) in a flood frequency analysis. Temporal information expansion is directed toward collecting information on the flood behavior before (or after) the systematic data period (Viglione, Merz, Salinas, & Bloschl, 2013). Spatial information expansion is based on using flood information from neighboring catchments to improve flood frequency estimates at the site of interest. Causal information expansion analyzes the generating mechanisms of floods in the catchment of interest (Merz & Bloschl, 2008).

Temporal information is added to the Bayesian analysis through the inclusion of interval- and threshold-censored data in the likelihood function as discussed in the Maximum Likelihood Estimation (MLE) section. Regional information on distribution parameters can be incorporated through the use of informative priors, as shown in the Informative Priors section. Causal information is incorporated into the analysis by first defining the prior distribution for a flood quantile:

$$h(Q_p) = N(\mu_p, \sigma_p) \tag{Equation 23}$$

where Q_p is the flood discharge for a specific annual exceedance probability P ; and $h(\cdot)$ is the PDF of the Normally distributed variable Q_p . Q_p is determined from the inverse cdf $F^{-1}(\cdot)$ of the parent distribution conditional on the parameters:

$$Q_p = F^{-1}(P|\theta) \tag{Equation 24}$$

The inverse CDF is then plugged into the PDF of the quantile prior to get:

$$\pi(\theta) = h(F^{-1}(P|\theta)) \tag{Equation 25}$$

During the Bayesian MCMC routine, the likelihood of the various components are multiplied by the quantile prior $\pi(\theta)$ to calculate a posterior distribution of the parameters, which is consistent with a reasonable range of Q_p . The overall likelihood function is then constructed by multiplying all of the components:

$$L(D|\theta) = L_S(D|\theta) \cdot L_L(D|\theta) \cdot L_I(D|\theta) \cdot \pi(\theta) \tag{Equation 26}$$

It can be seen in Equation 26 that the causal indicator $\pi(\theta)$ behaves similarly to a penalty function, in that it rewards parameter sets that produce a reasonable likelihood of Q_p and discounts those that do not. All other things being equal, parameter sets that do not agree well with $h(Q_p)$ will have lower likelihoods than those that do.

Skahill et al. (2016) independently revisited components of the example originally profiled by (Viglione, Merz, Salinas, & Bloschl, 2013), performing eight distinct MCMC simulations using the Kamp at Zwettl dataset. A summary of the simulations performed are provided in Table 80.

Table 80 – Summary of the Eight Distinct MCMC Simulation (Skahill, Viglione, & Byrd, 2016).

MCMC Simulation	Data of the Kamp at Zwettl
1	Systematic data (1951-2001)
2	Systematic data (1951-2005)
3	Systematic data (1951-2001) + temporal information expansion
4	Systematic data (1951-2005) + temporal information expansion
5	Systematic data (1951-2001) + causal information expansion
6	Systematic data (1951-2005) + causal information expansion
7	Systematic data (1951-2001) + temporal + causal information expansion
8	Systematic data (1951-2005) + temporal + causal information expansion

For each MCMC simulation, the posterior mode (PM) estimate for the GEV parameters and the 100-yr and 1,000-yr discharges, including the 90% credible interval, were provided in (Skahill, Viglione, & Byrd, 2016). The same eight simulations were performed using RMC-BestFit and compared with the results from Skahill et al. (2016). The default flat priors for the GEV were used with 100,000 posterior parameter sets. Results are provided in Table 81 through Table 83. RMC-BestFit produces nearly identical results for each scenario.

Table 81 – Comparison RMC-BestFit with (Skahill, Viglione, & Byrd, 2016) for Posterior Mode Parameters for the GEV Distribution.

MCMC Simulation	Skahill et al. (2016) - GEV Parameters			RMC-BestFit - GEV Parameters		
	Location (ξ)	Scale (α)	Shape (κ)	Location (ξ)	Scale (α)	Shape (κ)
1	42.9	20.2	-0.096	42.9	20.2	-0.096
2	41.7	20.7	-0.310	41.8	20.7	-0.310
3	43.4	21.7	-0.222	43.3	21.6	-0.221
4	42.6	21.5	-0.281	42.7	21.5	-0.279
5	41.9	21.0	-0.313	41.8	21.0	-0.312
6	41.6	20.8	-0.333	41.6	20.8	-0.333
7	42.7	21.8	-0.291	42.7	21.8	-0.292
8	42.5	21.5	-0.313	42.5	21.6	-0.311

Table 82 – Comparison RMC-BestFit with (Skahill, Viglione, & Byrd, 2016) for the 100-yr Quantile.

MCMC Simulation	Skahill et al. (2016) - Q_{100} (m ³ /s)			RMC-BestFit - Q_{100} (m ³ /s)		
	PM	5%	95%	PM	5%	95%
1	160	130	288	160	128	288
2	253	184	542	253	184	545
3	217	176	291	216	176	291
4	244	197	331	244	197	331
5	258	193	307	257	192	307
6	269	217	317	269	216	317
7	253	206	299	254	207	299
8	264	220	308	263	220	308

Table 83 – Comparison RMC-BestFit with (Skahill, Viglione, & Byrd, 2016) for the 1,000-yr Quantile.

MCMC Simulation	Skahill et al. (2016) - Q_{1000} (m ³ /s)			RMC-BestFit - Q_{1000} (m ³ /s)		
	PM	5%	95%	PM	5%	95%
1	241	183	649	240	163	654
2	543	317	1853	544	310	1952
3	399	278	647	396	274	656
4	497	347	818	495	339	836
5	557	335	702	554	329	725
6	604	418	747	604	411	768
7	527	369	671	529	362	684
8	571	418	708	568	410	725

The method for incorporating a quantile prior proposed by Viglione et al. (2013), and described above, is similar to the weighting of two independent and Normally distributed estimates using Equation 21 and Equation 22 from the Informative Priors section. Accordingly, a comparison was performed between RMC-BestFit and the theoretical weighting method.

Simulation #1 used the systematic Kamp at Zwetl dataset for years 1951-2001. Simulation #3 combined the systematic dataset with historical (temporal) information dating back to year 1600. The mean and standard deviation of the at-site 500-year quantile for the two datasets are shown in Table 84.

In Viglione et al. (2013), expert elicitation was used to determine a prior for the 500-year quantile (0.002 exceedance probability), which was set as a Normal distribution with mean of 480 m³/s and standard deviation of 80 m³/s. Simulation #5 was performed using the systematic data plus the quantile prior. Simulation #7 used the systematic data plus the historical data and the quantile prior. Results for each dataset are provided in Table 85 and Table 86 and illustrated in Figure 49 and Figure 50, respectively.

The results from RMC-BestFit agree reasonably well with the theoretical approximation. However, recall that the theoretical approximation assumes the two estimates are Normally distributed. It can be seen in Figure 49 that the quantile distribution for simulation #1 (systematic data only) exhibits considerable skewness. Therefore, it would be unreasonable to expect the theoretical weighting solution to match RMC-BestFit since the Normality assumption is not satisfied. As the at-site data increases, the Normality assumption becomes more reasonable and the theoretical approximation can be expected to perform better. Figure 50 shows the quantile distribution for simulation #3 (historical data), which has less skewness than simulation #1. As expected, the theoretical solution more closely matches RMC-BestFit for this dataset as shown in Table 86.

Table 84 – Summary Statistics for the At-Site 500-Year Quantile for Kamp at Zwetl.

Q ₅₀₀ (m ³ /s)	Simulation #1	Simulation #3
Mean (μ)	264.67	350.73
Std. Deviation (σ)	148.02	87.93

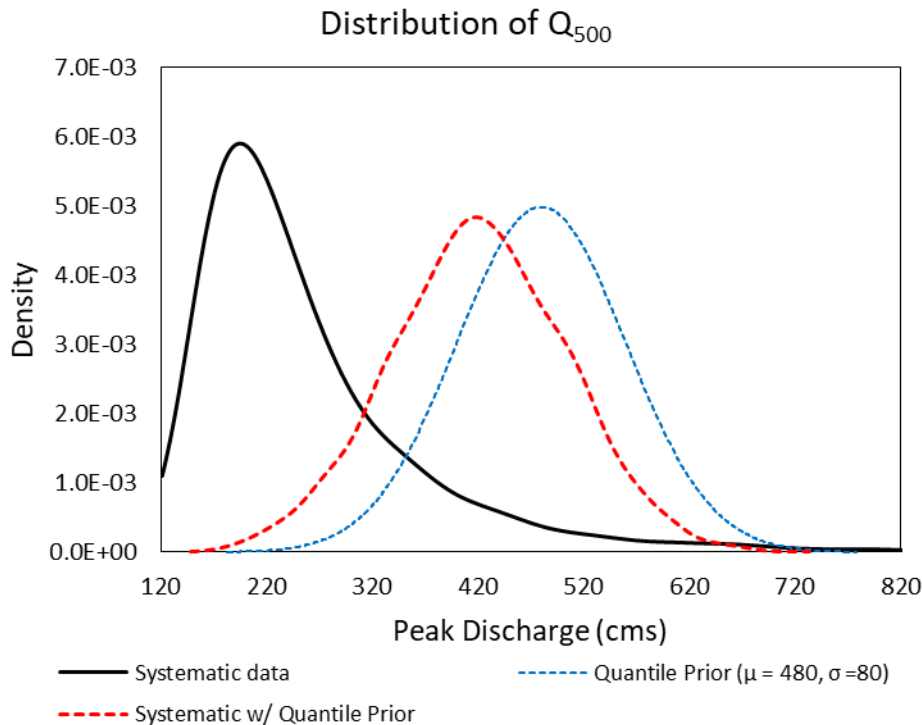


Figure 49 – Distributions of Quantile Q₅₀₀ in RMC-BestFit for MCMC Simulation #5.

Table 85 – Posterior Quantile Statistics in RMC-BestFit Compared to the Theoretical Solution for MCMC Simulation #5.

Q_{500} (m ³ /s)	Theoretical	RMC-BestFit
Mean (μ)	431.32	421.37
Std. Deviation (σ)	70.38	83.75

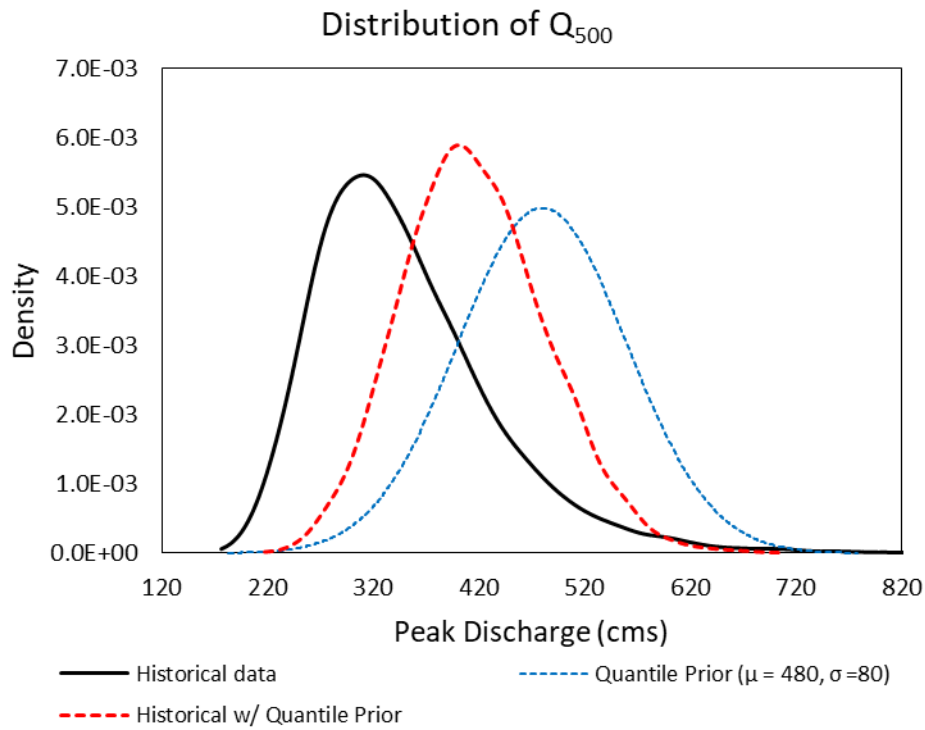


Figure 50 – Distributions of Quantile Q_{500} in RMC-BestFit for MCMC Simulation #7.

Table 86 – Posterior Quantile Statistics in RMC-BestFit Compared to the Theoretical Solution for MCMC Simulation #7.

Q_{500} (m ³ /s)	Theoretical	RMC-BestFit
Mean (μ)	421.46	416.10
Std. Deviation (σ)	59.17	67.65

Comparison with Evdbayes

The *evdbayes* package is an add-on package for the R programming environment that provides functions for the Bayesian analysis of extreme value models using MCMC (Stephenson & Ribatet, 2006). The *evdbayes* package provides several options for priors, including an option for setting priors on distribution quantiles following the approach used in (Coles & Tawn, 1996). This same approach is also implemented in RMC-BestFit.

A prior distribution can be constructed in terms of the quantiles $(q_{p_1}, q_{p_2}, q_{p_3})$ for specified exceedance probabilities $p_1 < p_2 < p_3$. Since $q_{p_1} > q_{p_2} > q_{p_3}$ it is easier to work with differences $(\bar{q}_{p_1}, \bar{q}_{p_2}, \bar{q}_{p_3})$, where $\bar{q}_{p_i} = q_{p_i} - q_{p_{i-1}}$. The number of exceedance probabilities must be equal to the number of distribution parameters. For example, for the GEV distribution there must be three quantile priors with three quantile differences. The priors on the quantile differences are assumed to be independent and Gamma distributed with $\bar{q}_{p_1} \sim \text{Gamma}(\alpha_i, \beta_i)$. This leads to the prior density for the GEV quantiles as:

$$\pi(\theta) = |J| \cdot \prod_{i=1}^3 \bar{q}_{p_i} \tag{Equation 27}$$

where J is the Jacobian of the transformation from $(q_{p_1}, q_{p_2}, q_{p_3})$ to $\theta = (\xi, \alpha, \kappa)$. More details on this method can be found in (Coles & Tawn, 1996) and (Smith, 2005). This approach for quantile priors has been generalized to work for any of the thirteen probability distributions offered in RMC-BestFit.

First, before verifying the method for quantile priors, a comparison was performed with uninformative priors using the Kamp at Zwettl dataset from 1951-2001 (Vigione, Merz, Salinas, & Bloschl, 2013). Example code for *evdbayes* is provided in Figure 51 so that others will be able to reproduce these results. The *evdbayes* package provides summary statistics for the GEV parameters, return period plots, and the posterior predictive distribution. For this comparison, the default flat priors were used in RMC-BestFit with 100,000 posterior parameter sets. In *evdbayes*, the priors for parameters are set to be a multivariate Normal distribution with very large variances in order to make them uninformative. Summary statistics of the verification results are provided in Table 87 and Table 88, and a frequency curve plot comparing curves is provided in Figure 52. It can be seen that RMC-BestFit and *evdbayes* produce effectively identical results. In addition, Figure 52 provides further confirmation that RMC-BestFit is correctly computing the posterior predictive distribution.

Table 87 – Parameter Summary Statistics from Evdbayes with Uninformative Priors.

Parameter	Mean	Std. Dev.	2.5%	50%	97.5%
Location (ξ)	42.3582	3.335	35.98100	42.2910	49.1315
Scale (α)	20.9698	2.703	16.31164	20.7482	26.8899
Shape (κ)	-0.1252	0.129	-0.4056	-0.1154	0.9938

Table 88 – Parameter Summary Statistics from RMC-BestFit with Uninformative Priors.

Parameter	Mean	Std. Dev.	2.5%	50%	97.5%
Location (ξ)	43.0466	3.4184	36.6124	42.9615	49.9683
Scale (α)	21.5134	2.8006	16.6868	21.2830	27.6154
Shape (κ)	-0.1162	0.1312	-0.4020	-0.1065	0.1107

```

library(evd)
library(evdbayes)
library(coda)

# This is example code with evdbayes with the GEV distribution and uninformative priors.
# Kamp at Zwettl, 1951-2001. Dataset from Viglione (2013).
gageData = c(135, 52, 45, 95, 54, 94, 95, 56, 140, 72, 50.9, 54, 105, 53, 62, 51, 58, 39, 62, 68,
             44, 52, 36, 60, 100, 41.2, 60.2, 19.7, 50.6, 35.6, 46.1, 42, 26, 32.1, 89.1, 29,
             58.3, 46.4, 20.9, 17, 74.4, 22.6, 73.2, 41.8, 34.6, 120, 43, 23.7, 56.9, 30.4, 21.8)

# Estimate the posterior mode parameter set using Maximum Likelihood Estimation (MLE).
mle <- fgev(x=gageData, method="Nelder-Mead", std.err = FALSE)
print(mle)
# Estimates
#      loc      scale      shape
# 42.91251 20.20805 0.09625

# Set up MCMC inputs
gevCovMatrix <- diag(c(1000, 1000, 10))
gevPriors <- prior.norm(mean=c(0,0,0), cov=gevCovMatrix)
initialVals <- c(as.numeric(mle$param[1]), as.numeric(mle$param[2]), as.numeric(mle$param[3]))
gevPosteriors <- posterior(n=2000000, init=initialVals, prior=gevPriors, lh="gev",
                          data=gageData, psd=c(5,.1,.1), burn=60000, thin=as.integer(20))

# Run MCMC
gevMCMC <- mcmc(gevPosteriors)

# Output the summary statistics for the Bayesian estimated parameters.
summary(gevMCMC)
# Note: The sign of the shape parameter (xi) is reverse of the
# Hosking parameterization (kappa) used in RMC-BestFit.
#
#      Mean      SD Naive SE Time-series SE
# mu    42.3582  3.335 0.0107066   0.0113403
# sigma 20.9698  2.703 0.0086788   0.0095153
# xi     0.1252  0.129 0.0004143   0.0004477
#
#      2.5%      25%      50%      75%      97.5%
# mu    35.98100 40.09090 42.2910 44.5371 49.1315
# sigma 16.31164 19.06830 20.7482 22.6337 26.8899
# xi    -0.09938 0.03437 0.1154 0.2049 0.4056

# Plot Markov chain trace plots and kernel density estimates for each parameter.
plot(gevMCMC)

# Plot frequency curve with confidence intervals.
rl.pst(gevMCMC, lh="gev", ylim=c(10,2000), ci=0.95)
print(rl.pst(gevMCMC, lh="gev", ylim=c(10,2000), ci=0.95))

# Plot posterior predictive curve.
rl.pred(gevMCMC, lh="gev", qlim=c(10,3000))
print(rl.pred(gevMCMC, lh="gev", qlim=c(10,3000)))

```

Figure 51 – Example code for evdbayes with uninformative priors.

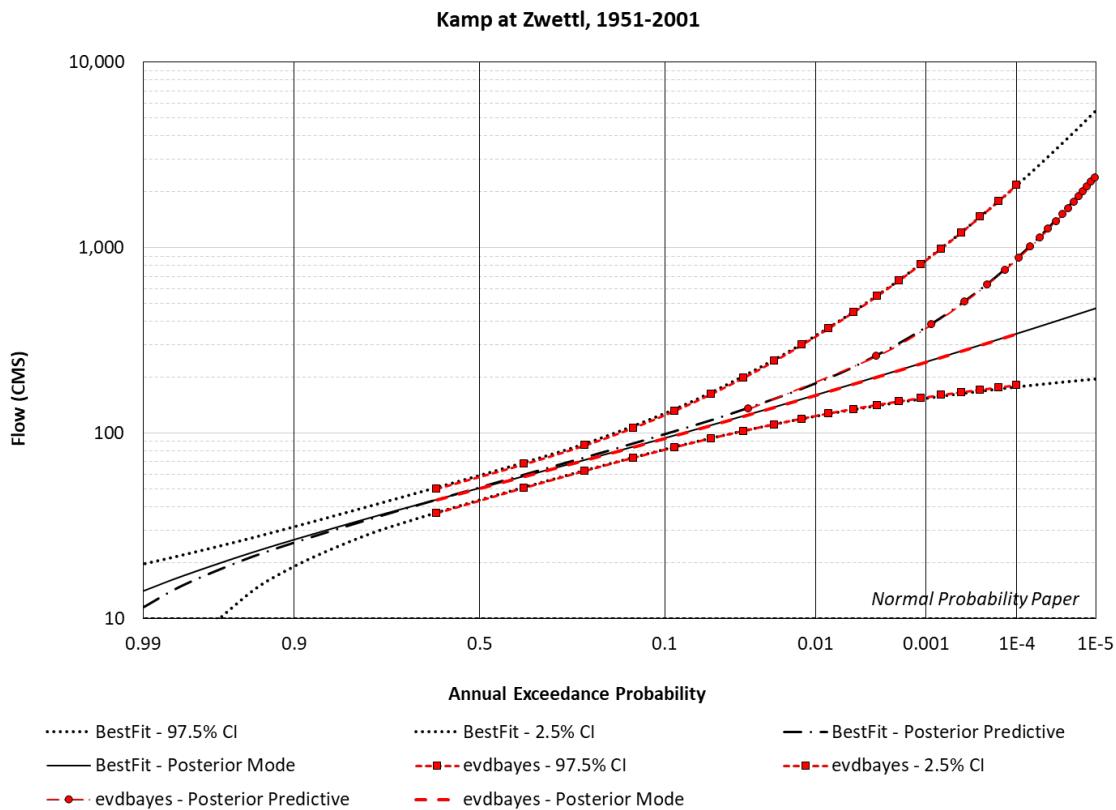


Figure 52 – Comparison of RMC-BestFit with Evdbayes with Uninformative Priors.

The next verification compared RMC-BestFit with *evdbayes* with informative priors on quantiles. In RMC-BestFit, the user specifies priors on quantiles using a Normal distribution because it is more intuitive than specifying the Gamma distributed quantile differences. The Gamma distributions for quantile differences are estimated automatically in the code behind. Using the mean and variance of the difference between two independent Normal distributions, the scale and shape parameters of the Gamma distribution are then estimated using the direct method of moments. Table 89 provides a summary of the prior distributions used for this example.

Table 89 – Summary of Prior Distributions on Quantiles.

Exceedance Probability	Normal Distribution for Quantiles		Gamma Distribution for Differences	
	Mean	Std. Dev.	Scale	Shape
0.1	100	20	4.00	25.00
0.01	250	40	13.33	11.25
0.001	500	60	20.80	12.02

Example code for *evdbayes* with informative priors is provided in Figure 54. Summary statistics of the verification results are provided in Table 90 and Table 91, and a frequency curve plot comparing curves is provided in Figure 53. RMC-BestFit and *evdbayes* produce nearly identical results.

Table 90 – Parameter Summary Statistics from Evdbayes with Informative Priors on Quantiles.

Parameter	Mean	Std. Dev.	2.5%	50%	97.5%
Location (ξ)	41.4307	3.0918	35.5680	41.3467	47.7391
Scale (α)	20.7700	2.4520	16.3861	20.6195	26.0375
Shape (κ)	-0.2694	0.0488	-0.3608	-0.2709	-0.1699

Table 91 – Parameter Summary Statistics from RMC-BestFit with Informative Priors on Quantiles.

Parameter	Mean	Std. Dev.	2.5%	50%	97.5%
Location (ξ)	41.4281	3.1001	35.5634	41.3612	47.7805
Scale (α)	20.7617	2.4513	16.4351	20.5992	25.9730
Shape (κ)	-0.2690	0.0490	-0.3614	-0.2703	-0.1689

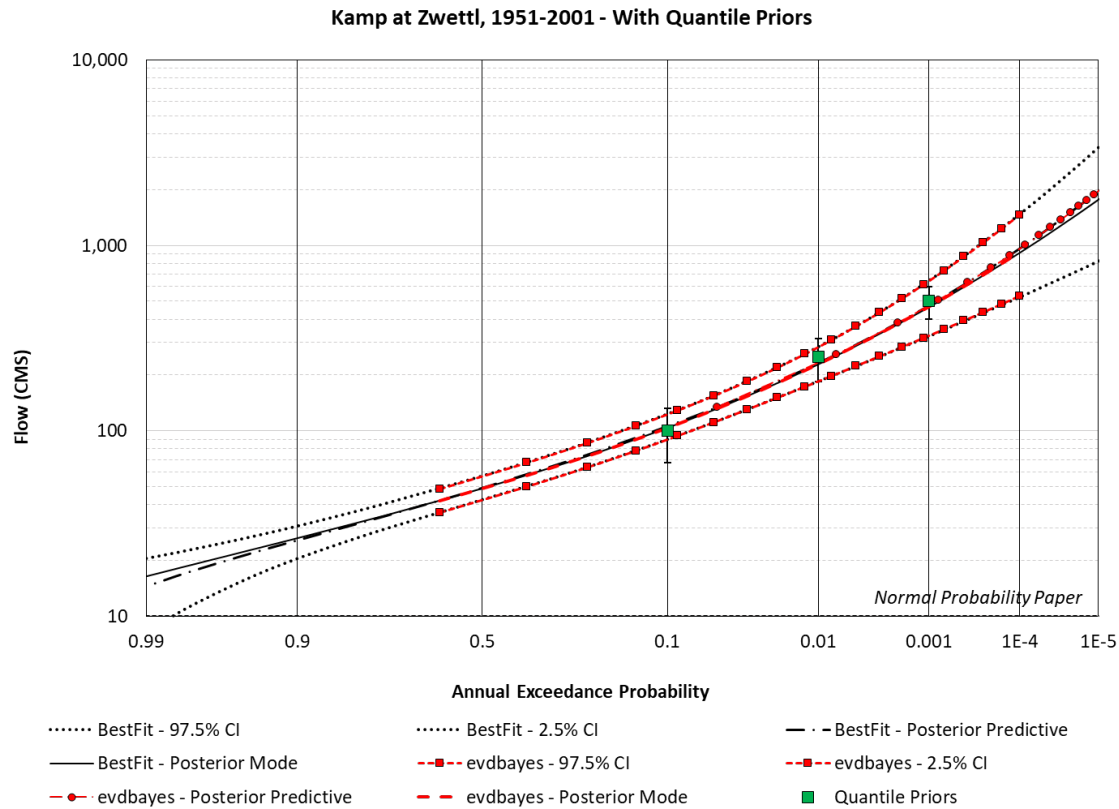


Figure 53 – Comparison of RMC-BestFit with Evdbayes with Informative Priors on Quantiles.

```

library(evd)
library(evdbayes)
library(coda)

# This is example code with evdbayes with the GEV distribution and Informative priors.
# Kamp at Zwettl, 1951-2001. Dataset from Viglione (2013).
gageData = c(135, 52, 45, 95, 54, 94, 95, 56, 140, 72, 50.9, 54, 105, 53, 62, 51, 58, 39, 62, 68,
             44, 52, 36, 60, 100, 41.2, 60.2, 19.7, 50.6, 35.6, 46.1, 42, 26, 32.1, 89.1, 29,
             58.3, 46.4, 20.9, 17, 74.4, 22.6, 73.2, 41.8, 34.6, 120, 43, 23.7, 56.9, 30.4, 21.8)

# Estimate the posterior mode parameter set using Maximum Likelihood Estimation (MLE).
mle <- fgev(x=gageData, method="Nelder-Mead", std.err = FALSE)
print(mle)
#      loc      scale  shape
# 42.91251 20.20805 0.09625

# Set up MCMC inputs
gevPriors <- prior.quant(shape=c(25,6.25,6.25), scale=c(4,24,40))
initialVals <-c(as.numeric(mle$param[1]), as.numeric(mle$param[2]),as.numeric(mle$param[3]))
gevPosteriors <- posterior(n=2000000, init=initialVals, prior=gevPriors, lh="gev",
                          data=gageData, psd=c(5,.1,.1), burn=60000, thin=as.integer(20))

# Estimate maximum a posteriori (MAP)
map <- mposterior(data=gageData, init=initialVals, prior=gevPriors, lh="gev", method="Nelder-Mead",
                  control=list(maxit=20000))
print(map)
# 41.2176265 19.9717628 0.2817834

# Run MCMC
gevMCMC <- mcmc(gevPosteriors)

# Output the summary statistics for the Bayesian estimated parameters.
summary(gevMCMC)
# Note: The sign of the shape parameter kappa is reverse of the
# Hosking parameterization used in RMC-BestFit.
#
#      Mean      SD Naive SE Time-series SE
# mu  41.4307 3.0918 0.0099271  0.0105737
# sigma 20.7700 2.4520 0.0078727  0.0086493
# xi    0.2694 0.0488 0.0001567  0.0001637
#
#      2.5%  25%  50%  75%  97.5%
# mu  35.5680 39.3004 41.3467 43.4675 47.7391
# sigma 16.3861 19.0696 20.6195 22.3158 26.0375
# xi    0.1699 0.2376 0.2709 0.3028 0.3608

# Plot Markov chain trace plots and kernel density estimates for each parameter.
plot(gevMCMC)

# Plot frequency curve with confidence intervals.
rl.pst(gevMCMC, lh="gev", ylim=c(10,2000), ci=0.95)
print(rl.pst(gevMCMC, lh="gev", ylim=c(10,2000), ci=0.95))

# Plot posterior predictive curve.
rl.pred(gevMCMC, lh="gev", qlim=c(10,3000))
print(rl.pred(gevMCMC, lh="gev", qlim=c(10,3000)))

```

Figure 54 – Example code for evdbayes with Informative Priors on Quantiles.

Comparison with Flike

A comparison was made with *Flike* (Kuczera G. , 1999), which is a Bayesian flood frequency analysis software developed by Professor George Kuczera from the School of Civil Engineering at the University of Newcastle, Australia. *Flike* is compliant with the recent major revision of Australian industry guidelines for flood estimation, documented in the update of Australian Rainfall and Runoff (ARR). *Flike* uses a novel importance sampling approach for estimating the posterior rather than Bayesian MCMC. In addition, *Flike* samples prior distributions using a multivariate Normal distribution, with the default priors set to have very large variances in order to make them uninformative.

There are a number of self-training examples on the *Flike* website⁷. The examples most comparable with RMC-BestFit are examples 3 through 6. Example #3 demonstrates a flood frequency analysis using the procedures described in Australian Rainfall and Runoff Book 3: Peak Discharge Estimation⁸. Specifically, this example covers the fitting of a LPIII distribution to an annual maximum series for the Hunter River at Singleton. Results are shown in Figure 55. *Flike* does not output the posterior mode; however, it does provide the posterior predictive distribution and the posterior mean quantile curve. For this example, a comparison was made with the credible intervals and the posterior predictive distribution. As can be seen, RMC-BestFit and *Flike* produce the same results.

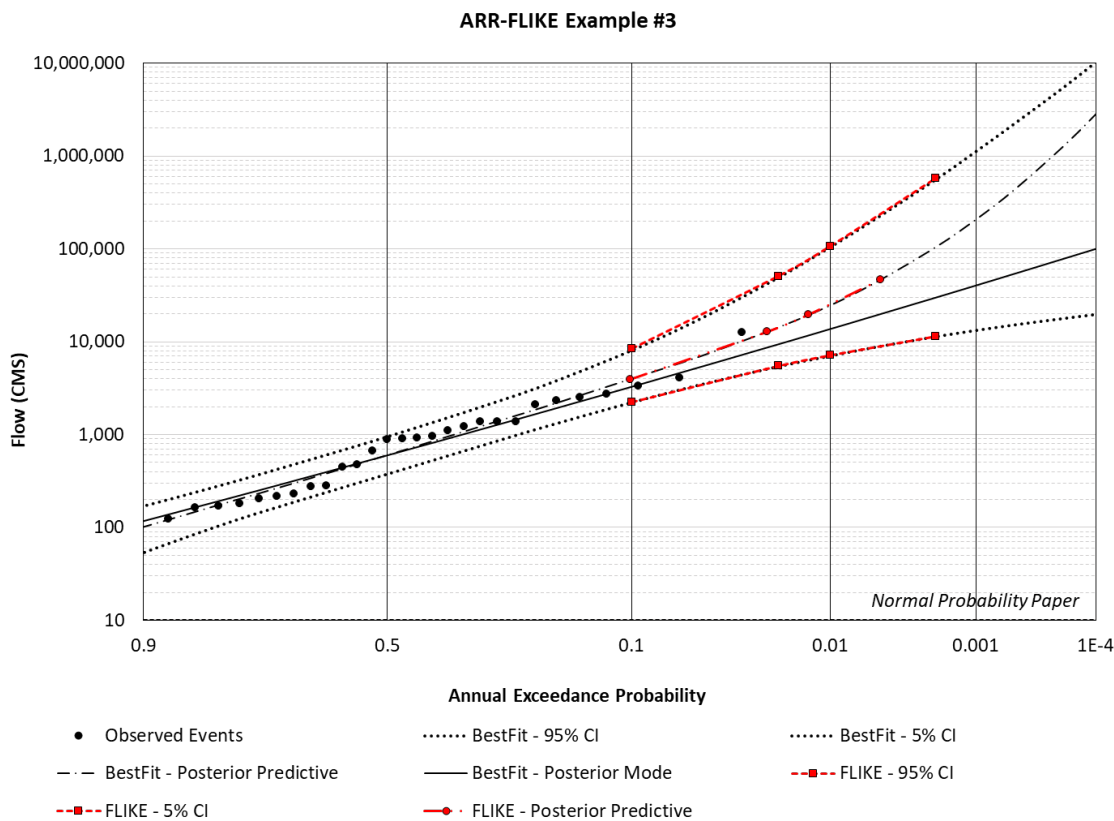


Figure 55 – Comparison of RMC-BestFit and *Flike* for Example #3.

Example #4 is a continuation of Example #3 and it examines the benefit of using binomial censored historical flood information. RMC-BestFit doesn't permit right censored thresholds. Nevertheless, RMC-BestFit can still replicate the binomial-censored example using an interval and setting the upper bound to be extremely large, approaching infinity. Results for Example #4 are shown in Figure 56. RMC-BestFit and *Flike* produce the same results for this example.

⁷ <https://flike.tuflow.com>

⁸ <http://arr.ga.gov.au/arr-guideline>

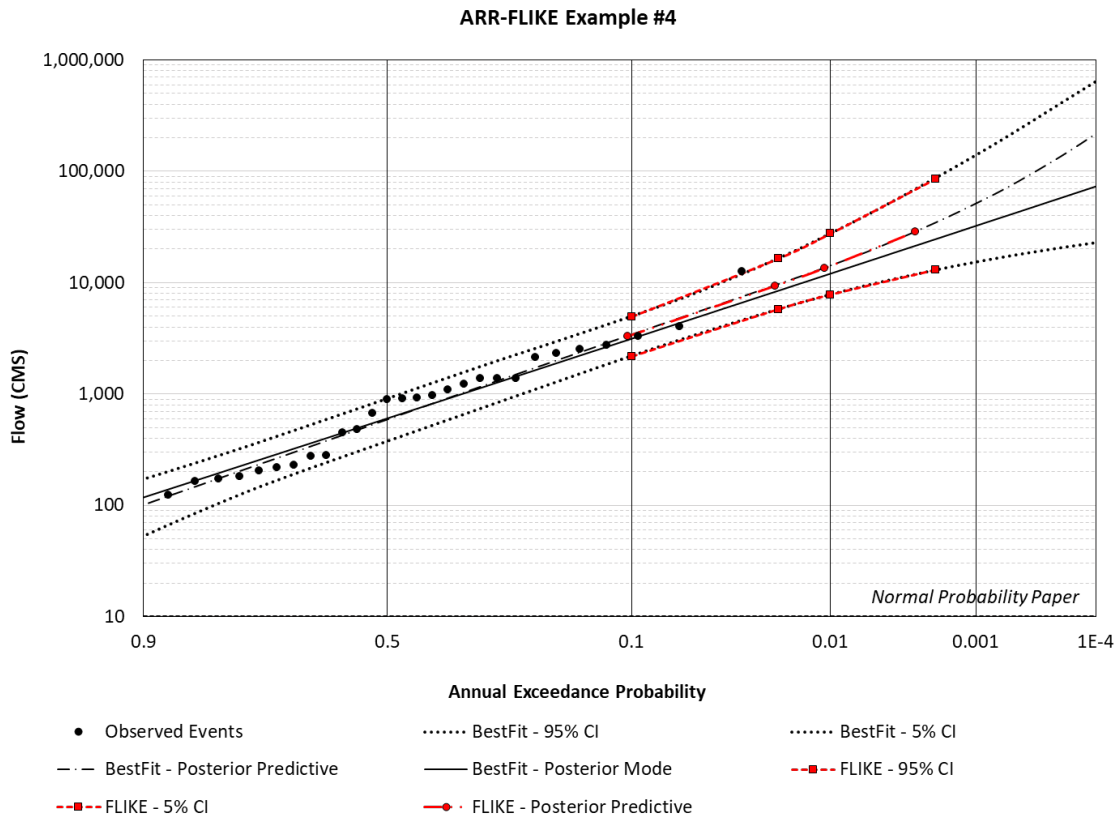


Figure 56 – Comparison of RMC-BestFit and Flike for Example #4.

Example #5 examines the use of regional information, building on Example #3. In this example, a regional skew analysis was performed and the regional skew was estimated to be 0.00 with a MSE of 0.09. This information was incorporated into the Bayesian analysis by setting the prior for the skew parameter of LPIII to be Normally distributed with a mean of 0.00 and standard deviation of 0.30. The *Flike* website only provides results for the credible intervals and posterior mean quantile for this example. Therefore, only the credible intervals were compared. As shown in Figure 57, RMC-BestFit and *Flike* produce the same credible intervals for this example.

Example #6 is a two-part example demonstrating censoring using the MGBT. The example uses 56 years of annual maximum discharges for the Wimmera River at Glynwylin. In the first part of this example, the GEV distribution was fit to the at-site data without removal of low outliers. The *Flike* website only provides results for the credible intervals for this example. Results are shown in Figure 58 below. RMC-BestFit and *Flike* results are equivalent. Next, the MGBT test was used to remove low outliers and replace them with a left-censored threshold. This approach is consistent with Bulletin 17C (U.S. Geological Survey, 2018), and is implemented in *HEC-SSP* and RMC-BestFit. The results for part two of Example #6 are shown in Figure 59. Again, RMC-BestFit and *Flike* produce the same results.

ARR-FLIKE Example #5

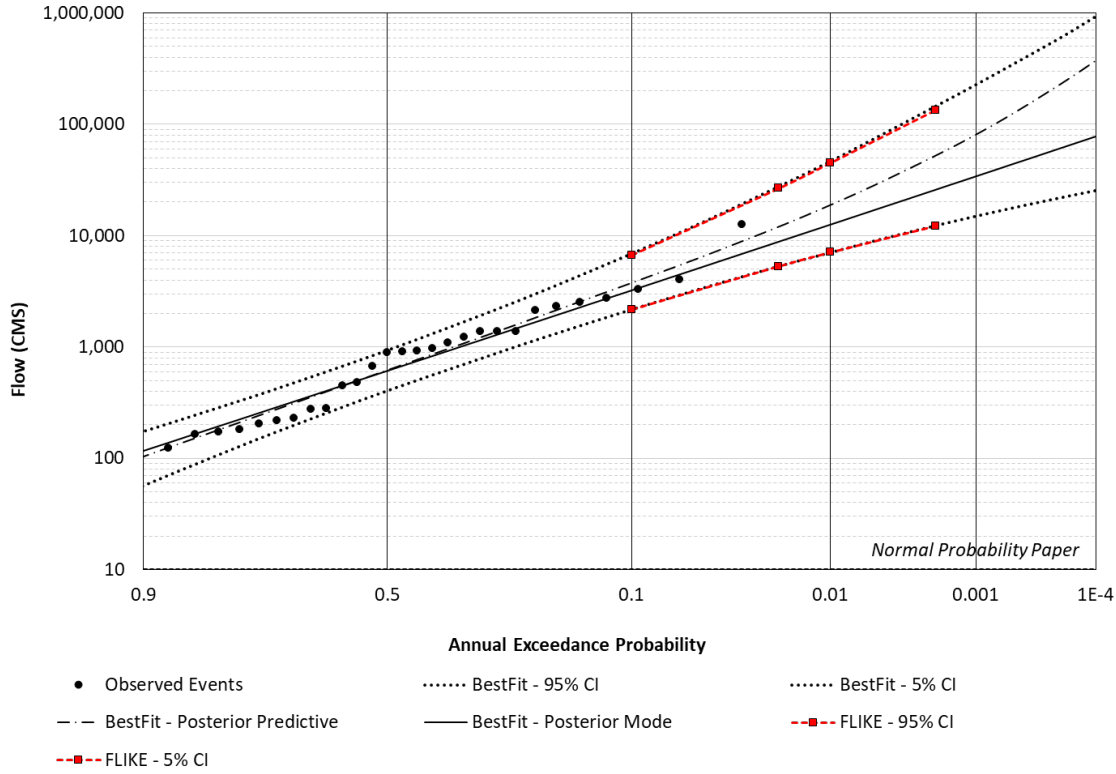


Figure 57 – Comparison of RMC-BestFit and Flike for Example #5.

ARR-FLIKE Example #6a

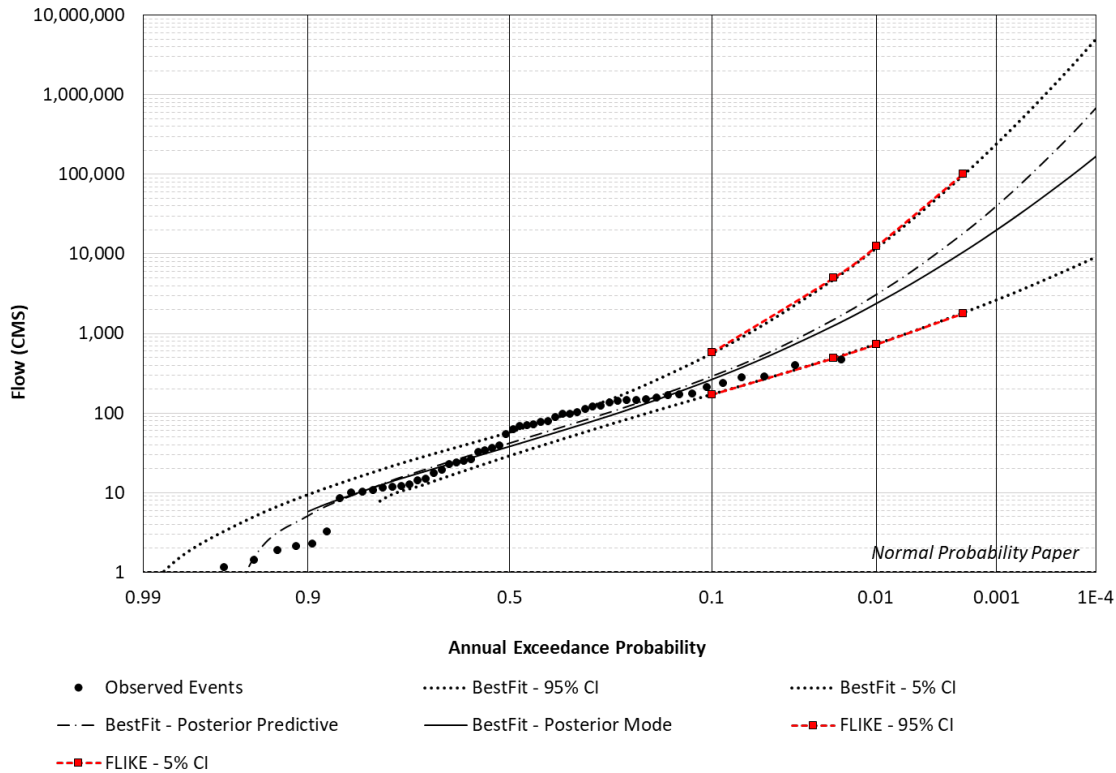


Figure 58 – Comparison of RMC-BestFit and Flike for Example #6a.

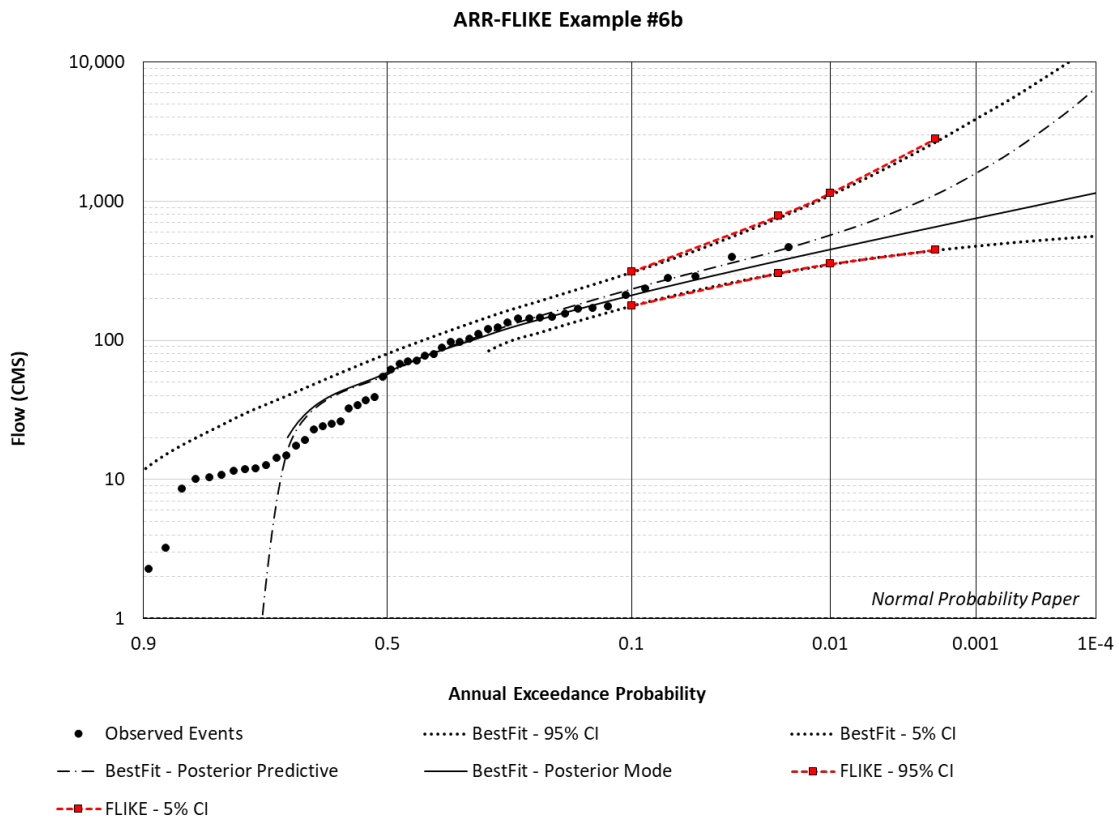


Figure 59 – Comparison of RMC-BestFit and Flike for Example #6b.

Comparison with EMA

The currently accepted flood-frequency methodology in the United States, described in Bulletin 17C (U.S. Geological Survey, 2018), recommends fitting the LPIII distribution using the Expected Moments Algorithm (EMA). EMA is a major improvement over the Bulletin 17B guidelines (U.S. Geological Survey, 1982), and is capable of incorporating historical and paleoflood information into flood frequency studies.

EMA was developed as an alternative to MLE and the Bulletin 17B (U.S. Geological Survey, 1982) method for incorporating historical information in flood frequency studies (Cohn, Lane, & Baier, 1997). EMA was shown to achieve greater efficiency than the B17B adjustment for censored data, and nearly achieving the efficiency of MLE while avoiding some of the numerical complications. However, in the cases where there is no censored data, EMA and B17B are identical and exhibit substantial bias as compared to MLE (Cohn, Lane, & Baier, 1997).

It would be unreasonable to expect a Bayesian estimation approach to perfectly match a moments-based fitting approach, such as EMA, or vice versa. The two estimation methods are very different from a theoretical perspective. Nevertheless, comparisons of RMC-BestFit and EMA were performed to provide some insight into how the methods may differ in practice. These comparisons do not validate or invalidate either method.

RMC-BestFit was compared with EMA for the 82 USGS gage sites (see Table 1 for a listing) used for testing in Bulletin 17C. Several additional sites have been compared during risk assessments performed as part of the USACE Dam Safety program, including studies with historical and paleoflood data. In general, for most sites, RMC-BestFit produces similar results to EMA. In cases where there is only systematic data, EMA is identical with the method of moments (MOM), which means the estimators can be biased and less efficient than MLE and Bayesian estimation. Consequently, in those cases, the quantile standard error and confidence intervals for EMA are sometimes wider than RMC-BestFit. In addition, MOM can be more sensitive than Bayesian estimation for sites with only one or two events that are much larger than the rest of the data. In these scenarios, the data likelihood used for MLE and Bayesian estimation is less influenced by single large values.

An example of this behavior is seen at site 01439500 Bush Kill at Shoemaker, PA, where out of 102 years of record, the largest event is more than double the next highest peak. There is only systematic data in this example. As can be seen in Figure 60, the EMA fit pulls upwards towards the highest peak as compared to the RMC-BestFit results. Furthermore, the EMA confidence intervals are considerably wider than the credible intervals from RMC-BestFit. A comparison of the computed parameters and resulting log-likelihood is provided in Table 92. As expected, the posterior mode from RMC-BestFit produces a slightly higher log-likelihood than the EMA fit.

Table 92 – Comparison of RMC-BestFit and EMA parameters for USGS 01439500 Bush Kill at Shoemaker, PA.

Parameter	EMA	RMC-BestFit
Mean (of log) (μ)	3.3327	3.3327
Std. Dev (of log) (σ)	0.2322	0.2306
Skew (of log) (γ)	0.9725	0.7839
Log-Likelihood	-858.3656	-857.4655

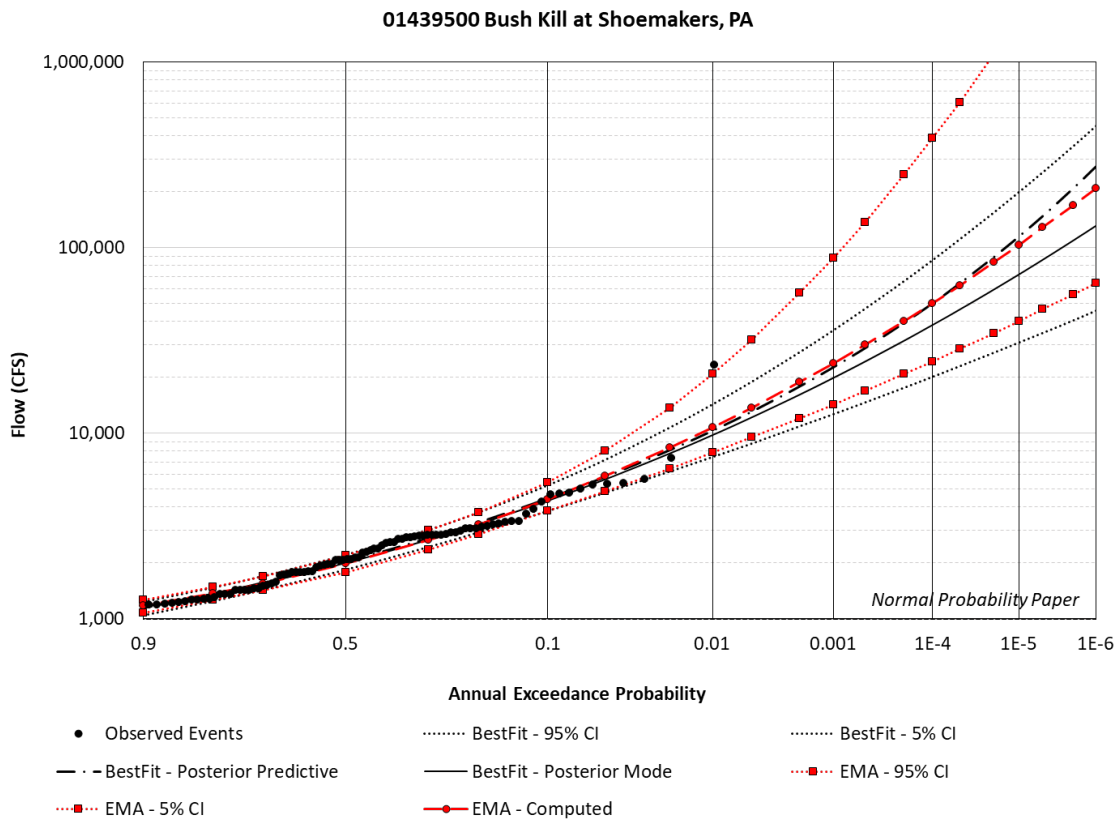


Figure 60 – Comparison of RMC-BestFit and EMA for USGS 01439500 Bush Kill at Shoemaker, PA.

Poor agreement between RMC-BestFit and EMA can also be expected in cases where there are many low outliers and the data is very negatively skewed. If the absolute value of the skewness coefficient is greater than 2, then the MLE method cannot produce a solution for the shape parameter of the PIII or LPIII (Bobee & Ashkar, 1991). This implies that the MLE estimate for the shape parameter is biased. If the absolute value of skew is greater than approximately 1.25, it is not recommended to use PIII/LPIII with MLE (Bobee & Ashkar, 1991). If the absolute value of skew is greater than 2, the method of “conditional maximum likelihood” must be applied. Conditional MLE is performed by first fixing the location parameter to the smallest value of the sample if the skew is positive, or the largest value of the sample if the skew is negative. Then, the scale and shape parameters are solved for, conditionally on the fixed location parameter. In cases where the absolute value of skew is greater than 1.25 and approaching 2, Bayesian estimation will automatically produce results that are similar to conditional MLE.

Example #2 from Appendix 10 of Bulletin 17C (U.S. Geological Survey, 2018) provides a good example of this behavior. This example is from USGS site 11274500 Orestimba Creek near Newman, CA, which has 30 low outliers. The results from RMC-BestFit for this site are shown in Figure 61. The skewness of the data is approximately -1.75. The posterior mode for the location parameter of LPIII is ~15,000, which is very close the largest value of the sample of 12,000 cfs. This demonstrates that the Bayesian approach will automatically produce results similar to conditional MLE. A comparison of RMC-BestFit with EMA is provided in Figure 62. Both methods produce similar confidence intervals, but the computed curve from EMA provides a less biased fit for the right-hand tail. When integrating over the confidence intervals from EMA, an expected probability curve can be computed. Figure 63 shows that the posterior predictive distribution from RMC-BestFit closely matches the expected probability curve from EMA for this site.

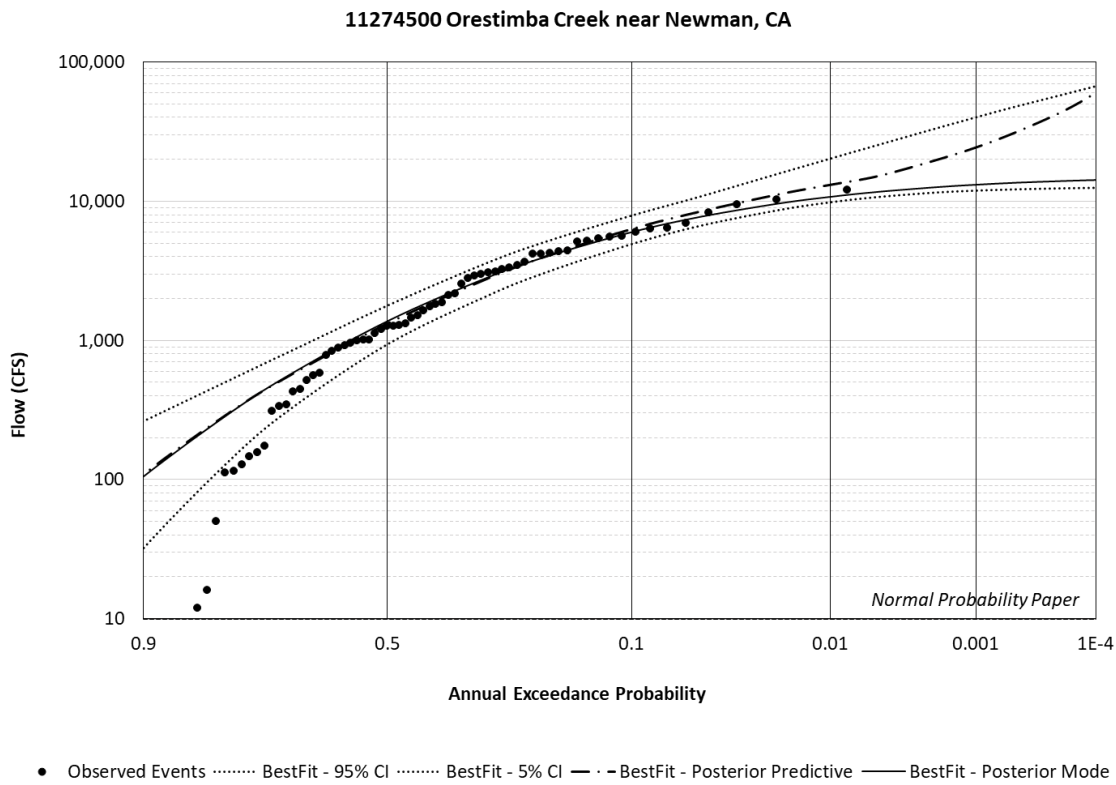


Figure 61 – RMC-BestFit Results for USGS 11274500 Orestimba Creek near Newman, CA.

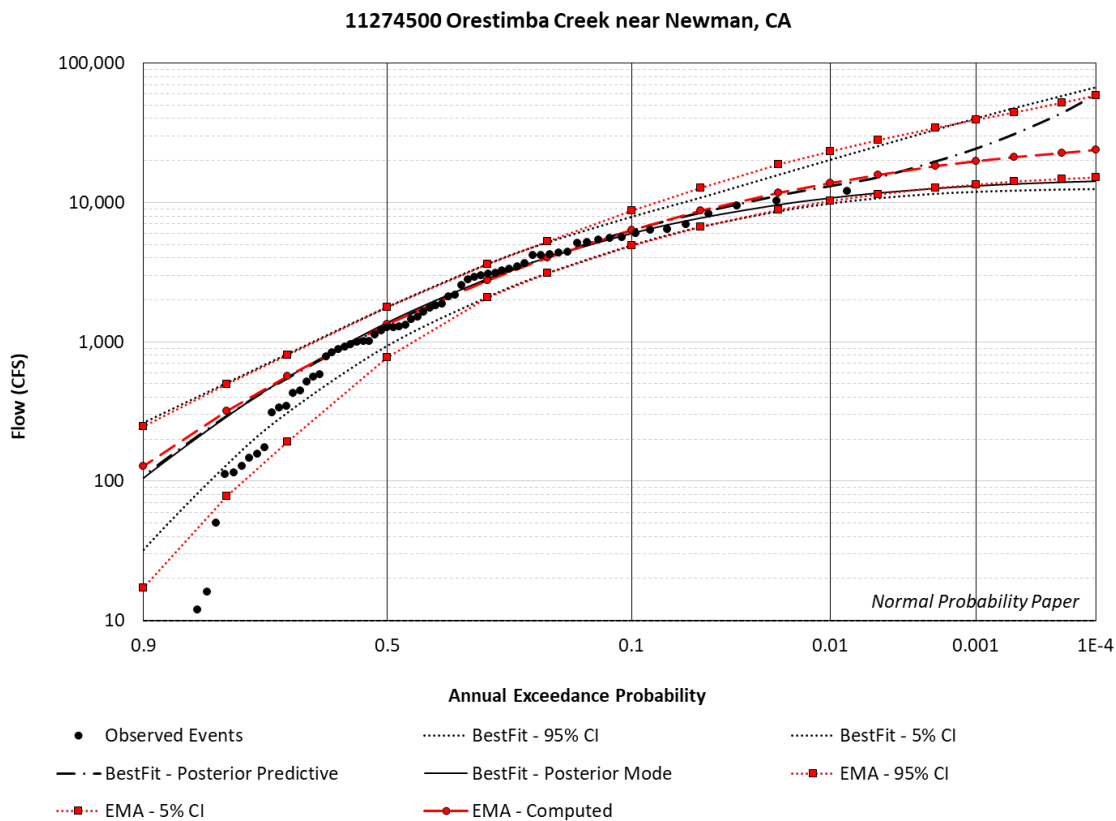


Figure 62 – Comparison of RMC-BestFit and EMA for USGS 11274500 Orestimba Creek near Newman, CA.

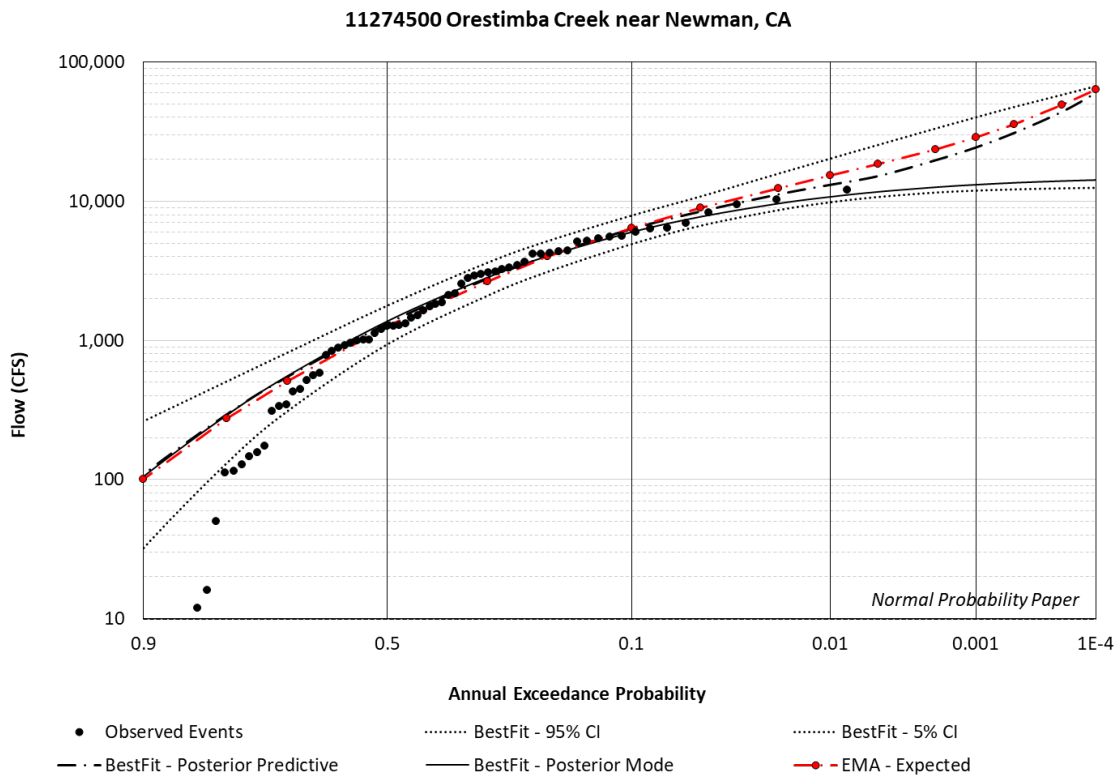


Figure 63 – Comparison of RMC-BestFit Posterior Predictive with the EMA Expected Probability Curve for USGS 11274500 Orestimba Creek near Newman, CA.

In cases where there is historical data incorporated with intervals and perception thresholds, RMC-BestFit and EMA will generally produce similar results. For example, RMC-BestFit was compared to EMA for site 11446500 American River at Fair Oaks, CA, which is example #7 from Appendix 10 in Bulletin 17C (U.S. Geological Survey, 2018). In this example, there is a major historical flood in 1862 and four paleoflood events dating back over 1,000 years. Results of the comparison are shown in Figure 64. For this example, the differences between EMA and RMC-BestFit are inconsequential, and the computed curve from EMA and the posterior mode from RMC-BestFit, along with the confidence intervals, are very consistent.

A final comparison was performed using Example #10 provided in the *HEC-SSP* example download. This example is for USGS station 01470500 Schuylkill River, PA, and it includes historical data, a perception threshold and regional skew. The regional skew is 0.001 with an MSE of 0.064. In RMC-BestFit, the regional skew is entered as an informative prior on skew that is Normally distributed with a mean of 0.001 and standard deviation 0.253. As shown in Figure 65, RMC-BestFit and EMA produce virtually identical results for this example.

A more comprehensive investigation into the similarities and differences between RMC-BestFit and EMA, and the respective limitations of each, is planned for a future report.

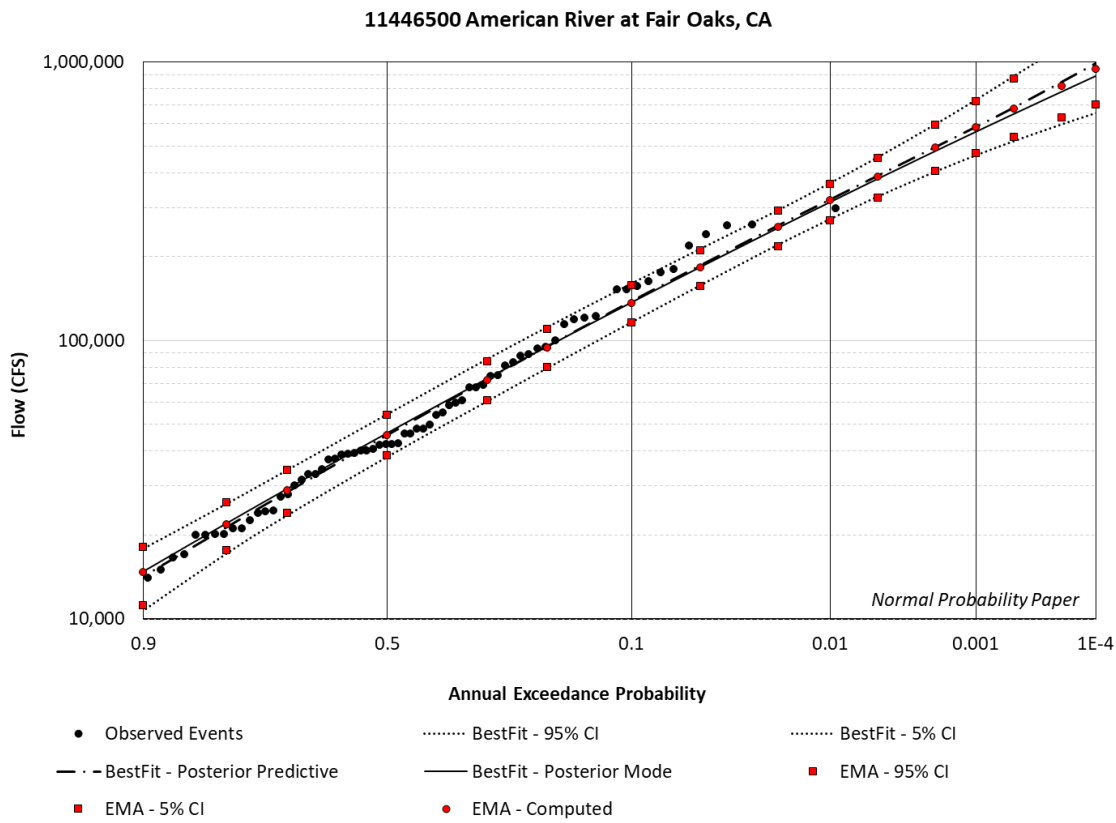


Figure 64 – Comparison of RMC-BestFit and EMA for USGS 11446500 American River at Fair Oaks, CA.

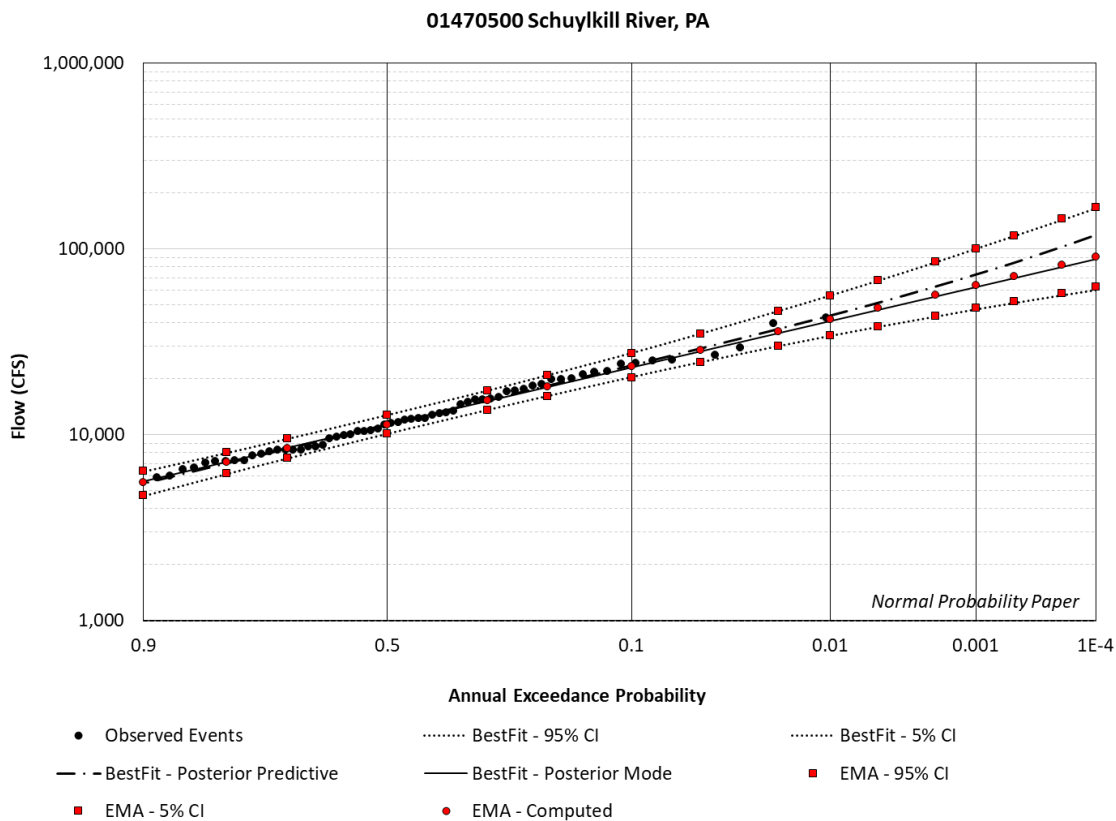


Figure 65 – Comparison of RMC-BestFit and EMA for USGS 01470500 Schuylkill River, PA.

Conclusion

As demonstrated in this report, the computational methods used in RMC-BestFit have been verified. The Multiple Grubbs-Beck Test and Hirsch-Stedinger plotting positions were verified with *HEC-SSP* using 82 test sites. Nonparametric summary statistics were verified with *Palisade's @Risk*. Probability distribution functionality, Maximum Likelihood Estimation, and goodness-of-fit measures were verified using textbook examples, *R-Stan*, and *Palisade's @Risk*. Bayesian estimation was verified using theoretical posterior distributions, and other state-of-the-art software, such as *R-Stan*, *evdbayes*, *Flike*, and *HEC-SSP*. In all cases, RMC-BestFit produced valid results. Any minor differences in precision between methods were inconsequential and would not lead to a different statistical inference.

References

- Asquith, W. H. (2011). *Distributional Analysis with L-moment Statistics using the R Environment for Statistical Computing*. Lubbock, TX: Create Space Independent Publishing Platform.
- Beard, L. R. (1960, July). Probability Estimates Based on Small Normal-Distribution Samples. *Journal of Geophysical Research*.
- Bobee, B., & Ashkar, F. (1991). *The Gamma Family and Derived Distributions Applied in Hydrology*. Littleton, CO: Water Resources Publications.
- Cohn, T. A., England, J. F., Berenbrock, C. E., Mason, R. R., Stedinger, J. R., & Lamontagne, J. R. (2013). A generalized Grubbs-Beck test statistic for detecting multiple potentially influential low outliers in flood series. *Water Resources Research*, 49(8), 5047-5058.
- Cohn, T. A., Lane, W. M., & Baier, W. G. (1997). An Algorithm for Computing Moments-Based Flood Quantile Estimates When Historical Flood Information is Available. *Water Resources Research*, 2089-2096.
- Coles, S. G., & Tawn, J. A. (1996). A Bayesian Analysis of Extreme Rainfall Data. *Journal of the Royal Statistical Society*, 463-478.
- Efron, B., & Hastie, T. (2016). *Computer Age Statistical Inference: Algorithms, Evidence and Data Science*. New York, NY: Cambridge University Press.
- Fisher, R. A., & Cornish, E. A. (1960). The percentile points of distributions having known cumulants. *Technometrics*, 2(2), 209-225.
- Gelman, A., Carlin, J. B., Stern, H. S., Dunson, D. B., Vehtari, A., & Rubin, D. B. (2014). *Bayesian Data Analysis* (Third ed.). Boca Raton, FL: CRC Press.
- Hirsch, R. M., & Stedinger, J. R. (1987). Plotting Positions for Historical Floods and Their Precision. *Water Resources Research*, 715-727.
- Hosking, J. R., & Wallis, J. R. (1997). *Regional Frequency Analysis: An Approach Based on L-Moments*. Cambridge, UK: Cambridge University Press.
- Jongejan, R. (2018). *Uncertainty in Hydrology: An evaluation of USACE methodology for estimating and portraying hydrologic uncertainty*.
- Krishnamoorthy, K. (2016). *Handbook of Statistical Distributions with Applications*. Boca Raton, FL: CRC Press.
- Kuczera, G. (1983). A Bayesian Surrogate for Regional Skew in Flood Frequency Analysis. *Water Resources Research*, 19, 821-832.
- Kuczera, G. (1999). Comprehensive at-site flood frequency analysis using Monte Carlo Bayesian inference. *Water Resources Research*, 1551-1557.
- Merz, R., & Blöschl, G. (2008). Flood frequency hydrology: 1. Temporal, spatial, and causal expansion of information. *Water Resources Research*.
- Meylan, P. (2012). *Predictive Hydrology: A Frequency Analysis Approach*. Enfield, New Hampshire: Science Publishers.
- O'Connell, D. R., Ostenaar, D. A., Levish, D. R., & Klinger, R. E. (2002). Bayesian flood frequency analysis with paleohydrologic bound data. *Water Resources Research*, 38(5). Retrieved from doi:10.1029/2000WR000028
- Perreault, L. (2000). *Bayesian retrospective analysis of a break in sequences of hydrologic random variables*. Paris: ENGREF.
- Press, W. H., Teukolsky, S. A., Vetterling, W. T., & Flannery, B. P. (2017). *Numerical Recipes: The Art of Scientific Computing*. (3rd ed.). Cambridge, UK: Cambridge University Press.
- Rao, A., & Hamed, K. H. (2000). *Flood Frequency Analysis*. Boca Raton, FL: CRC Press LLC.

- Reis, D. S., & Stedinger, J. R. (2005). Bayesian MCMC flood frequency analysis with historical information. *Journal of Hydrology*, 97-116.
- Skahill, B. E., Viglione, A., & Byrd, A. (2016). *ERDC/CHL CHETN-X-1 A Bayesian Analysis of the Flood Frequency Concept*. Vicksburg, MS: U.S. Army Engineer Research and Development Center, [Coastal and Hydraulics Laboratory].
- Smith, E. (2005). *Bayesian Modelling of Extreme Rainfall Data*. Newcastle, NSW: University of Newcastle.
- Stedinger, J. R. (1982). Confidence Intervals For Design Events. *Journal of Hydraulic Engineering*, 13-27.
- Stedinger, J. R. (1983). Design Events With Specified Flood Risk. *Water Resources Research*, 511-522.
- Stedinger, J. R., & Cohn, T. A. (1986). Flood frequency analysis with historical and paleoflood information. *Water Resources Research*, 22(5).
- Stephenson, A., & Ribatet, M. (2006). *A User's Guide to the evdbayes Package (Version 1.1)*. Newcastle, NSW: Macquarie University.
- ter Braak, C. J., & Vrugt, J. A. (2008). Differential Evolution Markov Chain with snooker updater and fewer chains. *Statistics and Computing*, 435-446.
- U.S. Geological Survey. (1982). *Guidelines for Determining Flood Flow Frequency Bulletin 17B*.
- U.S. Geological Survey. (2018). *Guidelines for Determining Flood Flow Frequency Bulletin 17C*. <https://doi.org/10.3133/tm4B5>.
- Viglione, A., Merz, R., Salinas, J. L., & Bloschl, G. (2013). Flood frequency hydrology: 3. A Bayesian analysis. *Water Resources Research*, 49(2). Retrieved from doi:10.1029/2011WR010782
- Wagner, D. M., Krieger, J. D., & Veilleux, A. G. (2016). *Methods for estimating annual exceedance probability discharges for streams in Arkansas, based on data through water year 2013*. U.S. Geological Survey. Reston: U.S. Geological Survey. doi:<http://dx.doi.org/10.3133/sir20165081>